# Tungsten bronzes as indicating potentiometric electrodes

by

Paul Balser Hahn

A Dissertation Submitted to the

Graduate Faculty in Partial Fulfillment of

The Requirements for the Degree of

DOCTOR OF PHILOSOPHY

Department: Chemistry
Major: Analytical Chemistry

Approved:

Signature was redacted for privacy.

In Charge of Major Work

Signature was redacted for privacy.

For the Major Department

Signature was redacted for privacy.

For the Graduate College

Iowa State University
Ames, Iowa

1973

TABLE OF CONTENTS


| | Page |
|---|---|
| INTRODUCTION | 1 |
| THE TUNGSTEN BRONZES | 3 |
| EXPERIMENTAL | 13 |
| Materials and Apparatus | 13 |
| Procedures | 16 |
| Dissolved oxygen measurement | 16 |
| Chelometric titrations | 18 |
| Metal ion response | 21 |
| Voltammetric studies | 21 |
| RESULTS AND DISCUSSION | 22 |
| Potentiometric Response of Cubic $Na_xWO_3$ to Dissolved Oxygen | 22 |
| Application of the $Na_xWO_3$ Electrode to the Determination of Dissolved Oxygen | 33 |
| Response of Other Tungsten Bronzes to Dissolved Oxygen | 44 |
| Application of the $Na_xWO_3$ Electrode in Chelometric Titrations | 47 |
| Mechanism of Response | 64 |
| CONCLUSION | 88 |
| Future Studies | 90 |
| LITERATURE CITED | 92 |
| ACKNOWLEDGMENTS | 97 |

# INTRODUCTION

The recent discovery that the metal tungsten bronzes are extremely versatile potentiometric-indicating electrodes for following acid-base and redox titrations and for determining the concentration of certain reducible metals initiated this study into the possible further uses of tungsten bronze electrodes in analytical chemistry.

These investigations led to two significant discoveries: the ability of sodium tungsten bronze to act as a potentiometric-selective electrode for dissolved oxygen in basic solution and as a potentiometric-indicating electrode for following chelometric titrations of a large number of metals with EDTA in basic solution. These characteristics were found to be unique to the cubic sodium tungsten bronzes among the highly conducting alkali metal tungsten bronzes. Significant effort was directed toward demonstrating the analytical applicability of these discoveries.

The mechanism for the response of the sodium tungsten bronze to dissolved oxygen and in the chelometric titrations was not at all obvious. The extremely large response to oxygen (120 mV/decade instead of the expected 15 or 30 mV/decade) and the ability to perform chelometric titrations of nonreducible metals such as calcium made it impossible to explain the response on the basis of simple redox reactions. An adsorption mechanism involving the adsorption and displacement of hydroxide ions at the electrode surface was first proposed on the basis of a number of early observations. Subsequent observations however, which included voltammetric studies of several tungsten bronze electrodes, provided extremely strong evidence of a mixed-potential mechanism for the response of the sodium

tungsten bronze electrode in basic solution. The mixed potential established at the sodium tungsten bronze electrode was found to be the result of the spontaneous oxidation of the electrode surface to tungstate by oxygen or other oxidizing agents. The oxygen response, the response in chelometric titrations and a number of other intriguing observations are explained by the mixed-potential mechanism.

## THE TUNGSTEN BRONZES

The tungsten bronzes, due to their many unique and interesting properties, have been the object of considerable physical and chemical studies in the past four decades. They are nonstoichiometric metal-like oxides containing tungsten and at least one other metallic element located at a different site in the crystal lattice than the tungsten atom. The tungsten bronzes are not considered to be mixed oxides with the second metal replacing a portion of the tungsten atoms but rather a solid solution of tungstic oxide and the second metal which occupies vacant interstices between interlocking $WO_3$ octahedra. When only one other metal is present the general formula is represented by $M_xWO_3$ in which $0<x<1$. Tungsten bronzes containing the alkali and alkaline earth metals, lanthanum and other rare earths, aluminum, cobalt, nickel, copper, zinc, gallium, silver, cadmium, indium, thallium, tin, lead, thorium, and uranium have been reported (1-3). The concentration of the second metal is continuously variable within definite ranges depending on its ionic radius, its location in the crystal lattice and the overall structure of the bronze. In addition to the metal tungsten bronzes, hydrogen and ammonium tungsten bronzes have also been reported (4,5).

The first tungsten bronze reported was that of sodium, prepared by Wöhler (6) in 1823 by passing dry hydrogen over a molten mixture of $Na_2WO_4$ and $WO_3$ producing golden yellow crystals with a metallic appearance. Potassium tungsten bronze was first prepared by Laurent (7) in 1838 by the reduction of a $K_2WO_4$-$WO_3$ melt with hydrogen. First mention of the synthesis of similar compounds containing lithium and rubidium was made in the

early 1900's. Hallopeau (8) and Brunner (9) obtained dark blue crystals of $Li_xWO_3$ by reducing paratungstate melts ($Li_2WO_4$-$WO_3$) by electrolysis or with tin metal, and Schaefer (10) prepared $Rb_xWO_3$ by reducing a $Rb_2CO_3$-$H_2WO_4$ melt with a hydrogen-methane gas mixture. Tungsten bronzes containing metals other than the alkali metals and more than one other metal have only recently been prepared and characterized.

For many years it was thought that these oxide bronzes were unique to tungsten. However, investigations since the late 1940's have shown it possible to prepare analogous bronzes of molybdenum, vanadium, niobium, tantalum, titanium and rhenium having properties similar to those of the tungsten bronzes. Several excellent review articles on the oxide bronzes may be found in the recent literature (1-3).

Tungsten bronzes have been prepared by three methods; vapor phase reaction of a metal vapor and $WO_3$ vapor, chemical reduction in a molten mixture containing a salt of the secondary metal and tungstic oxide or electrolytic reduction at a platinum, tungsten or other electrode in a similar melt.

The vapor phase reaction is limited to metals appreciably volatile at high temperatures. Excellent single crystals of $Tl_xWO_3$ were prepared by Sienko (11), and Straumanis and Hsu (12) reported the production of $Li_xWO_3$ using this technique.

A number of investigators have prepared bronzes in the form of a powder or small single crystals using a variety of chemical reductants. Tungsten metal has been widely used in a molten mixture of $WO_3$ and the metal tungstate or oxide to produce $Na_xWO_3$ (13-16) and a number of rare earth tungsten bronzes (17,18). A typical reaction may be represented by

equation 1.

$$3xNa_2WO_4 + (6-4x)WO_3 + xW \text{ ----> } 6Na_xWO_3 \quad (1)$$

Tungsten dioxide has also been widely used as the reducing agent for the production of alkali metal bronzes from $M_2O$-$WO_3$ melts (19), for the production of $Pb_xWO_3$ from $PbCO_3$-$WO_3$ and $PbWO_4$-$WO_3$ melts (20), and for the production of a number of alkali and alkaline earth and other tungsten bronzes from a metal halide-$WO_3$ melt (21).

$$xMCl_2 + xWO_2 + WO_3 \text{ ----> } M_xWO_3 + xWO_2Cl_2 \quad (2)$$

Other reducing agents have included hydrogen for the production of tetragonal $K_xWO_3$ from $K_2O$-$WO_3$ melts and hexagonal $Rb_xWO_3$ from $Rb_2O$-$WO_3$ melts (19,22) and cubic sodium bronzes from $Na_2WO_4$-$WO_3$ melts (23), Sn and Zn metals for the production of alkali metal bronzes from similar melts (19) and alkali azides for the production of alkali metal bronzes from $WO_3$ melts at pressures of 100-3000 atm (24).

In the production of the tungsten bronzes by chemical reduction the reaction generally proceeds at temperatures of 500-1000°C for periods of time ranging from a few minutes to several days. Oxygen must be excluded to avoid competing reactions and the reduction is performed either in a vacuum or under an inert atmosphere (argon). The final composition of the bronze (x value) can be adjusted by varying the molar ratios of $WO_3$ and the secondary metal oxide or tungstate. Such reactions are generally far from complete and the relationship between melt composition and final bronze composition is at best very empirical.

The third and perhaps the most useful method of tungsten bronze

production is by electrolytic reduction in melts similar to those described above. The primary advantage of the electrolytic method is that large single crystals may be grown. Currents in the range of a few tenths of a milliampere to several amperes with voltages up to 6 volts have been employed to form and deposit the bronze at metal cathodes with the evolution of oxygen at the anode (11,19,25-30). As in the case of preparation by chemical reduction, melts are maintained at temperatures of 500-1000°C and the final bronze composition is a function of the melt composition. Electrolyses have been carried out for periods of time ranging from a few hours to several days.

Only recently has the electrochemistry of this bronze preparative technique been investigated. Fredlein and Damjanovic (31) studied the deposition and dissolution of $Na_2WO_4$-$WO_3$ melts and established from voltammetric curves that dissolution was not the simple reverse of deposition. They further established that the composition of the bronze was constant if deposited at a constant potential but that during dissolution, the ratio of Na and W dissolution rates changed. Meites et al. (32) studied the voltammetric behavior of Na, Li and K tungstate and polytungstate melts at Pt electrodes. From similar studies, Whittingham and Huggins (33) proposed the following electrochemical reactions for the production of $M_xWO_3$ from tungstate-tungstic oxide melts:

Anode reaction:

$$W_2O_7^{2-} \text{-----} > 2WO_3 + 2e^- + \tfrac{1}{2}O_2 \qquad (3)$$

Cathode reaction:

$$W_2O_7^{2-} + xe^- \text{ -----> } WO_4^{2-} + WO_3^{x-} \quad (4)$$

Overall reaction (alkali metal):

$$2\left(\frac{2-x}{xy}\right) M_2WO_4 \cdot yWO_3 \text{ -----> } 2\left(\frac{2-x-xy}{xy}\right) M_2WO_4 + \frac{4}{x} M_xWO_3 + O_2 \quad (5)$$

After preparation the bronzes are generally washed with boiling water or alkali hydroxide solutions to remove tungstates and tungstic oxide. It is also possible to alter the secondary metal content (x value) of such bronzes after they have been prepared. This was demonstrated by de Jong (34) as early as 1932 when he prepared tetragonal "blue Na-W bronze" by reducing cubic $Na_xWO_3$ with $H_2$ or Zn. Straumanis (13) also found it possible to remove sodium from $Na_xWO_3$ with $I_2$ vapor at 800°C. More recently, McNeill (15) and McNeill and Conroy (16) prepared cubic $Na_xWO_3$ ($x = 0.363, 0.291, 0.234$) by mixing finely divided stoichiometric amounts of $Na_{0.693}WO_3$ and $WO_3$ for the desired final sodium concentration and heating in a vacuum at 920°C for 9 days.

The characterization of the tungsten bronzes in terms of stoichiometry and crystal structure, chemical properties, and electrical and magnetic properties has been directed primarily toward the alkali metal bronzes with the major emphasis on the sodium compounds. In the early 1930's de Jong (34,35) and Hagg (36,37) established on the basis of X-ray measurements that the sodium tungsten bronzes could exist in the cubic perovskite structure with W at the center of the cube, the oxygen atoms arranged octahedrally at the face centers and the sodium atoms occupying a fraction of the interstitial sites at the cube corners. They also noted the characteristic color change of the sodium tungsten bronzes from gold

through orange red and violet to blue as the sodium content decreased. Hagg was the first to demonstrate that the various cubic sodium bronzes were not separate compounds but a continuous series of solid solutions of variable composition with an extended homogeneity range. He determined the lattice constants of these compounds and was the first to observe the contraction of the lattice with decreasing sodium content. De Jong also demonstrated a tetragonal structure for a low concentration sodium tungsten bronze.

The sodium tungsten bronzes are now known to exist in the cubic structure for x values from approximately 0.3 to nearly 1.0 (16,19). Brown and Banks (38) determined the relationship between the sodium concentration and the cubic lattice constant to be $a(\text{Å}) = 0.0819x + 3.7846$ by X-ray measurements coupled with chemical analysis. This linear relationship was later confirmed by Reuland and Voigt (39) using neutron activation analysis. The crystal structure of $Na_xWO_3$ decreases in symmetry as the sodium content decreases passing through two tetragonal phases ($0.05<x<0.4$) to the monoclinic structure of $WO_3$ itself (1,19,40,41).

The other alkali metal tungsten bronzes follow similar phase transitions as the x value varies. $Li_xWO_3$ is observed to have similar structures as its sodium analog, existing in the cubic form for $0.1<x<0.4$ and a tetragonal form for $0.05<x<0.3$ (19,29). Potassium bronzes may exist in the cubic form for $x \approx 0.9$ (24), the tetragonal form for $0.40<x<0.57$ (1,19) and in a hexagonal form for x, approximately 0.3 (19, 42,43). Rubidium and cesium tungsten bronzes have only been observed in the hexagonal form with x approximately 0.3 (19,42,43).

Considerable interest in the bronzes has resulted from their

unusually low electrical resistivities typical of metals rather than metal oxides. Resistivities of various tungsten bronzes have been determined by a number of investigators and are summarized by Dickens and Whittingham (1), Sienko (44) and Shanks et al. (45). Resistivities for a number of alkali tungsten bronzes (cubic sodium and lithium, tetragonal potassium and sodium) were found to range from about 20 $\mu$ ohm cm for x values of 0.9 to approximately 400 $\mu$ ohm cm for x values approaching 0.3 (45). The resistivities of the bronzes rise linearly with temperature indicating metal-like conduction and appear to be more a function of x value rather than the alkali metal or the crystal structure. At lower alkali metal concentration ($x<0.25$) the resistivity of the tungsten bronzes is very much larger and they are semiconductors.

Measurements of the Hall and Seebeck effects in the highly conducting bronzes has confirmed that one free electron exists per alkali metal atom (two for alkaline earth, three for rare earth) in the bronze lattice and that the carrier mobility is comparable to that of free electrons in the conduction band of typical metals (1,44-47). Magnetic measurements on the cubic alkali metal tungsten bronzes has shown only a small temperature-independent paramagnetism showing the absence of two isolated spin states for tungsten (48). The old theory of the tungsten bronzes being solid solutions containing tungsten in two oxidation states $W^{VI}O_3$ and $MW^{V}O_3$) has thus given way to the theory that they are solutions of M in a $WO_3$ matrix with the ionized secondary metal providing the free electrons which are located in a delocalized conduction band (1).

Three models have been proposed concerning the origin of the conduction band. Mackintosh (49) and Fuchs (50) considered that the conduction

band results from direct overlap of the alkali metal 3p orbitals while Sienko (44) proposed that the band results only from W-W bonding via direct overlap of the W 5d($t_{2g}$) orbitals. Two observations placed serious doubt on the Mackintosh-Fuchs model (1). Nuclear magnetic resonance measurements showed no significant 3p character of the conduction band, and $ReO_3$ which is isoelectric with $Na_{1.0}WO_3$ exhibits metallic conductivity without any alkali metal present. The third model, proposed by Goodenough and coworkers (51-53), refines that of Sienko by mixing oxygen p$\pi$ orbitals with tungsten $t_{2g}$ orbitals. This model was based on the observation that $Sr_2MgReO_6$, a compound with the necessary symmetry for Re($t_{2g}$) overlap but not for Re($t_{2g}$)-O(p$\pi$) overlap, showed only semiconducting properties.

The tungsten bronzes are insoluble in water and are extremely resistant toward acids developing an insoluble surface film of tungstic acid. $Na_xWO_3$ is insoluble in basic solution in the absence of oxidizing agents but dissolves slowly with the formation of tungstate in the presence of oxygen and rapidly in the presence of sodium peroxide (12,13). Ammoniacal silver nitrate also oxidizes $Na_xWO_3$ with the spontaneous plating of metallic silver and the formation of $WO_4^{2-}$. Other tungsten bronzes including $Li_xWO_3$ and mixed $Li_xNa_yWO_3$ appear much more resistant toward oxidation. They are not attacked by hot, concentrated base in the presence of oxygen (54).

Much of the practical interest in the tungsten bronzes has been concerned with their catalytic activity in gas phase reactions and their electrocatalytic activity as electrodes in aqueous solution. The sodium tungsten bronzes have been demonstrated to catalyze the decomposition of formic acid at high temperature (14), the ortho-para hydrogen conversion and hydrogen-deuterium exchange in the gas phase (55). Their catalytic

activity for the dehydration of certain alcohols however, was shown to be very small (56). As electrodes in electrolytic cells the sodium tungsten bronzes were found to catalyze the evolution of hydrogen in acid solution (57), the oxidation of carbon monoxide and reformer gas (78% $H_2$, 2% CO, 20% $CO_2$) in acid electrolyte fuel cells (58), and the reduction of oxygen in acid solution (59-70).

In the past decade there has been considerable interest in the ability of the bronzes to catalyze the reduction of oxygen, perhaps to serve as an economically feasible oxygen electrode in fuel cells. Their high conductivity, resistance to attack, and low cost compared to the noble metal catalysts were certainly in their favor. Early studies by Damjanovic, Sepa and Bockris (59,60) showed $Na_xWO_3$ to be almost as good as platinum (the best catalyst known) for catalyzing the reduction of $O_2$ in acid solution. More recent investigations however, have demonstrated this catalytic activity to be due to trace platinum impurities incorporated in the bronzes during their preparation by electrolysis on Pt cathodes (62,64-66,68,70). Bockris and McHardy (70) have quantitatively evaluated the influence of Pt and other dopants on the catalytic effect of the sodium tungsten bronzes and proposed models for the increased activity.

The tungsten and other transition metal bronzes have been found to act as potentiometric-indicating electrodes for a number of electroactive species. Koksharov and Ust-Kachkinsev found the cubic sodium tungsten bronzes (71) and the strontium niobium bronzes (72) to have linear potentiometric response to pH over a wide interval (pH 0-14) with slopes of response ($\Delta E/\Delta pH$) of 58 mV for $Na_xWO_3$ and 40-50 mV for the strontium niobium bronze. They demonstrated the utility of these electrodes for

acid-base titrations in both aqueous and alcoholic solution and in the presence of oxidizing ($MnO_4^{2-}$) and reducing (Fe(II)) agents which appeared to have little effect on the potential developed at the bronze electrode. The same authors found only minimal pH response for tetragonal $Na_xWO_3$ (71) and for copper and silver vanadium bronzes (73). Wechter et al. (74) recently demonstrated the pH response of the cubic $Na_xWO_3$ electrode and the ability to perform acid-base titrations in aqueous and non aqueous systems.

The inability of the bronzes to respond to oxidizing and reducing agents has, however, been discredited by two groups of investigators. Weser and Pungor (75) demonstrated that cubic $Na_xWO_3$ and $ReO_3$ electrodes exhibited a potentiometric response similar to that of platinum for the Fe(II)-Fe(III) and the ferro-ferricyanide redox couples in acid solution. Wechter et al. (74) showed the $Na_xWO_3$ electrode to respond to both the Fe(II)-Fe(III) and the Ce(IV)-Ce(III) redox couples by titrating Fe(II) with Ce(IV) in acid solution. In this titration the bronze electrode response was found to lag slightly behind that of a platinum electrode affording the opportunity to directly obtain an excellent first derivative titration curve if the potential between a bronze and Pt electrode is monitored.

Wechter et al. also demonstrated the ability of the $Na_xWO_3$ electrode to function as a potentiometric-indicating electrode for a number of easily reducible metals in acid solution. Nernstian response was found for Ag(I) (60 mV/decade), Hg(II) and Cu(II) (30 mV/decade) for concentrations ranging from $10^{-1}$ to nearly $10^{-7}$M.

# EXPERIMENTAL

## Materials and Apparatus

Crystals of the alkali metal tungsten bronzes, $M_xWO_3$, used for electrodes were grown by the electrolysis of a melt of the metal tungstate ($M_2WO_4$) and tungstic oxide ($WO_3$) (26,27). After preparation they were washed with dilute NaOH and deionized water to remove any tungstate or tungstic oxide adhering to the surface. The metal content or the x value of the bronzes had been previously determined by activation analysis, the measurement of lattice parameters (39,76,77), or by estimation on the basis of the electrolytic melt composition during preparation.

Individual electrodes were prepared from pieces either cut with a diamond saw or chipped from larger single crystals of bronze. The crystals which were cut had smooth flat surfaces, while those chipped from the parent crystal had jagged uneven surfaces. One series of sodium tungsten bronzes was annealed at 650°C in an argon atmosphere for several days and cooled at a rate of 50°C/hr to achieve a greater degree of homogeneity.

The electrodes themselves were prepared by cementing the crystals to glass tubing with epoxy compound and making electrical contact through a mercury pool to a copper wire (Figure 1). The electrical resistance of each electrode was checked with an ohmmeter; those exhibiting a resistance greater than 1-2 ohms were not used. The exposed surface areas of the bronze electrodes were estimated to vary between 0.05 and 0.2 $cm^2$. Table 1 lists the characteristics of the tungsten bronze electrodes used in this investigation.

All solutions used in this study were prepared from reagent grade

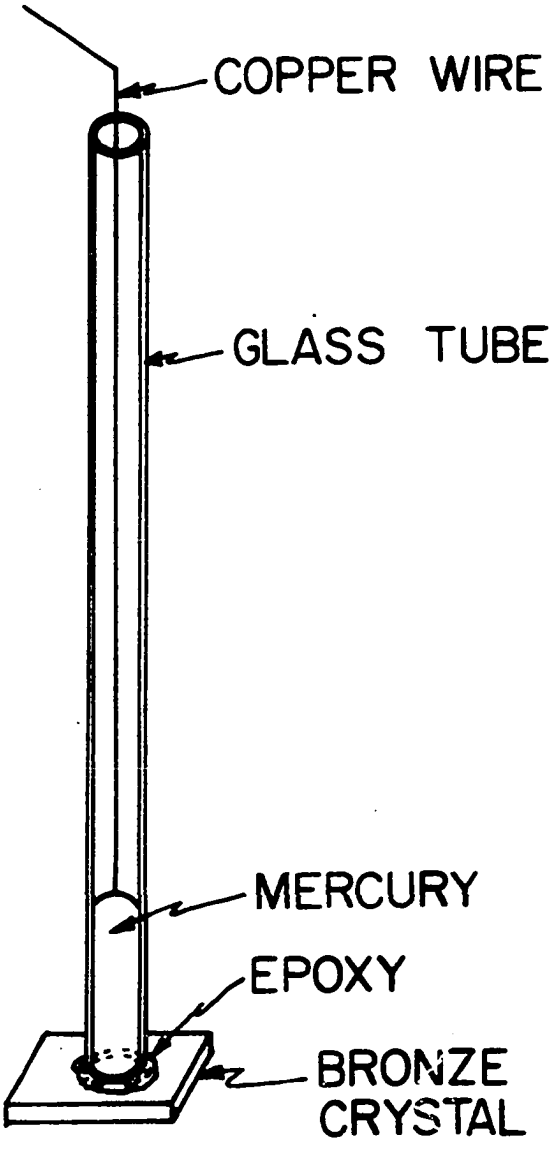


Figure 1. The tungsten bronze electrode

Table 1. Characteristics of the tungsten bronze electrodes

| Electrode | x value | Crystal structure | Remarks |
|---|---|---|---|
| $Na_xWO_3$ | 0.507 | cubic | chipped |
| $Na_xWO_3$ | 0.626 | cubic | chipped |
| $Na_xWO_3$ | 0.65 | cubic | cut (4x4x2mm), annealed |
| $Na_xWO_3$ | 0.718 | cubic | chipped |
| $Na_xWO_3$ | 0.81 | cubic | chipped |
| $Na_xWO_3$ | 0.907 | cubic | chipped |
| $Li_xWO_3$ | 0.35 | cubic | chipped |
| $K_xWO_3$ | 0.3 | hexagonal | chipped |
| $K_xWO_3$ | 0.5 | tetragonal | chipped |
| $Rb_xWO_3$ | 0.3 | hexagonal | chipped |
| $Cs_xWO_3$ | 0.3 | hexagonal | chipped |

chemicals and deionized water; no attempt was made to prepare carbonate-free basic solutions. Gases used for oxygen equilibration were dry 99.995% nitrogen and 99.6% oxygen, Matheson "Zero" grade air, and specific oxygen-nitrogen gas mixtures (10.12, 3.27, 0.99, 0.35 and 0.10% $O_2$ by volume) prepared and analyzed ($\pm$ 2 relative percent) by Matheson Gas Products.

Potentiometric measurements were made with Beckman Zeromatic SS-3 or H-5 pH meters or a Keithley Model 640 vibrating capacitor electrometer. The output from these was fed into a Sargent Model MR recorder to monitor electrode response as a function of time. All potential measurements

were made vs. a Beckman saturated calomel reference electrode. Voltammetric studies of the tungsten bronze electrodes were performed with a Leeds and Northrup Electro-Chemograph Model E polaragraph. A large surface area saturated calomel electrode (78) was used as the reference electrode in these studies.

## Procedures

### Dissolved oxygen measurement

The potentiometric response to dissolved oxygen was determined in pH 9.2 (0.0246M $Na_2B_4O_7$, 0.0018M NaOH), pH 10.5 (0.0172M $Na_2B_4O_7$, 0.031M NaOH), and pH 12.0 (0.161M KCl, 0.0387M NaOH, 0.5mM EDTA) buffer solutions (79) and in 0.1M KOH-1.0mM EDTA.

Three separate techniques were employed to establish or independently measure the concentration of dissolved oxygen in these solutions. The first was by mixing varying volumes of nitrogen-saturated and oxygen-saturated solutions and calculating the relative oxygen concentration on the basis of the volumes, assuming no loss of dissolved gases upon mixing.

In the second, air and nitrogen were purged into solution at varying rates and the dissolved oxygen was determined voltammetrically with a rotating platinum disc electrode (80). In this method the dissolved oxygen concentration was calculated from the observed diffusion limited current for the $2H_2O + O_2 + 4e^- \longrightarrow 4OH^-$ reaction (Equation 6).

$$C = \frac{i_l}{0.62\, n\, F(\pi r^2)\, D^{2/3} \omega^{1/2} \nu^{-1/6}} \qquad (6)$$

In this equation C is the concentration in moles/liter, $i_l$ the limiting

current in mA, n the number of electrons involved in the redox reaction, $\pi r^2$ the area of the electrode (0.470 $cm^2$), D the diffusion coefficient for $O_2$ in aqueous solution (2.6 X $10^{-5}$ $cm^2$/sec) (81), $\omega$ the angular velocity of the rotating electrode (168 radians/sec), and $\nu$ the kinematic viscosity of the solution (0.01002 poise) (79).

The third technique made use of the pre-mixed $N_2$-$O_2$ gases described above to establish the oxygen concentration. This technique was used in most of the experiments because it was much easier than the other two and provided much better stability in oxygen concentration over long periods of time.

The oxygen concentrations in the solutions may be calculated assuming Henry's Law. The effect of KOH on the solubility of oxygen has been determined by Davis et al. (82) who found the relation

$$\log s = \log 1.26 \times 10^{-3} - 0.1746\ M \qquad (7)$$

between the solubility of oxygen, s, in moles per liter and the KOH concentration, M, also in moles per liter at 25°C. Calculated values of the oxygen concentrations in the solution used in most of the measurements, 0.1M KOH - 1mM EDTA, are given in Table 2. The effect of 0.1M KOH is to reduce the solubility from that in pure water by about 4%. Except for the oxygen and air there is an uncertainty of ±2% in these values based on the analyses provided with the gas mixtures.

All potentiometric measurements were performed in a rapidly stirred solution after the electrode was allowed to equilibrate for 2-10 minutes. When the equilibrating gases were used the temperature of the solution was controlled within a few tenths of a degree with a constant temperature bath.

Table 2. Calculated oxygen concentrations in 0.1M KOH-1mM EDTA at 25°C as a function of equilibrating gas

| Equilibrating gas volume % $O_2$ | $O_2$ Concentration M | ppm |
|---|---|---|
| 100 ($O_2$) | $1.21 \times 10^{-3}$ | 38.7 |
| 20.9 (air) | $2.53 \times 10^{-4}$ | 8.10 |
| 10.12 | $1.23 \times 10^{-4}$ | 3.94 |
| 3.27 | $3.96 \times 10^{-5}$ | 1.27 |
| 0.99 | $1.20 \times 10^{-5}$ | 0.384 |
| 0.35 | $4.24 \times 10^{-6}$ | 0.136 |
| 0.10 | $1.21 \times 10^{-6}$ | 0.039 |

The potentiometric response to dissolved oxygen was also determined in several flow-through systems having the basic design illustrated in Figure 2. The sample solution equilibrated with one of the gas mixtures, and the deoxygenated KOH-EDTA reagent solution were simultaneously introduced into a mixing chamber and allowed to flow sequentially past the bronze and saturated calomel reference electrodes. The sample solution was introduced by gravity at a rate of 2-5 times that of the reagent solution which was introduced either by gravity or under 1-2 $lb/in^2$ nitrogen pressure.

Chelometric titrations

Chelometric titrations were performed with $10^{-1}$, $10^{-2}$, or $10^{-3}$M disodium EDTA solutions in either 1M $NH_4OH$ or a pH 10 buffer solution

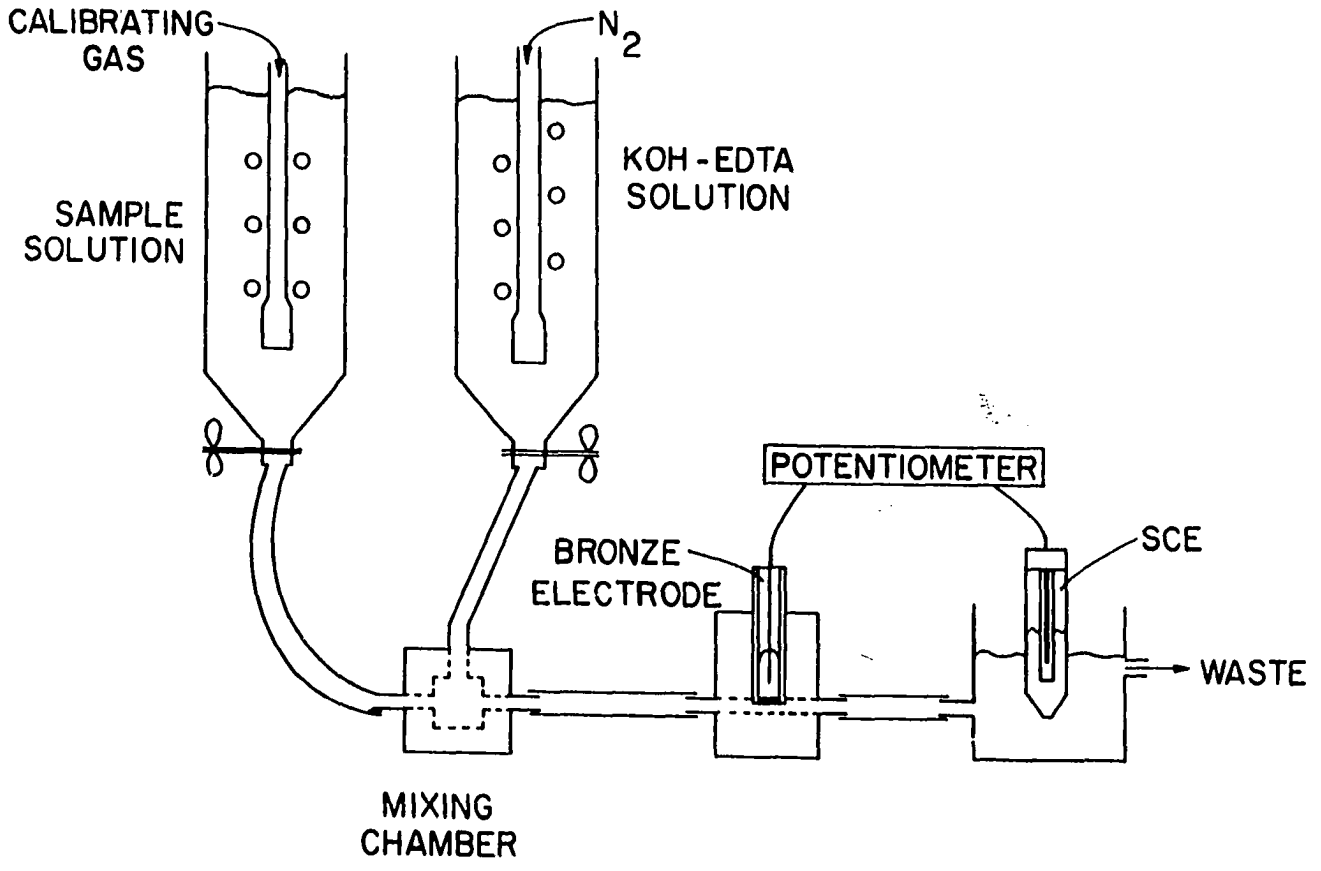


Figure 2. Flow-through system for dissolved oxygen analysis

(0.16M $NH_4OH$, 0.025M $NH_4Cl$). The metal solutions used in the quantitative determinations (Mg, Zn, Cu, and Fe) were made by dissolving a precisely weighed quantity of metal in a minimum volume of 6N $HNO_3$ and diluting to 0.1M with deionized water. The EDTA solutions used in the quantitative measurements were standardized potentiometrically using a $Na_{0.65}WO_3$ electrode against a calcium solution prepared by dissolving dried $CaCO_3$ in a minimum of $HNO_3$. The other metal solutions, used primarily to determine the general shapes of the titration curves, were made by dissolving the appropriate reagent grade chemical in deionized water.

All titrations were performed in 100-150 ml of solution which was stirred magnetically. The potential between the bronze and SCE electrodes was monitored as a function of the titrant volume. Equivalence points in the quantitative measurements were determined by the second derivative method.

The simultaneous titration of $Ca^{2+}$ and $Mg^{2+}$ was performed by first adjusting the pH to greater than 13 with 8M NaOH to precipitate $Mg(OH)_2$ and titrating for the $Ca^{2+}$ end point. The precipitate was then dissolved with 6M HCl, the solution buffered to pH 10 and titrated to the $Ca^{2+}$ + $Mg^{2+}$ end point.

In the reverse titrations, excess EDTA was added to the solution containing the metal ion and the excess EDTA was titrated with a 0.1M $CaCl_2$ solution.

The Fe(III) titration differed from the others in that it was performed in acid solution (pH 2-3).

Metal ion response

The potentiometric response of the various bronze electrodes to a number of metals was determined in 1M $NH_4OH$ solution. In these measurements 5 µl to 10 ml aliquots of the 0.01 or 0.1M metal solution were diluted to 100-200 ml establishing formal concentrations in the range of $10^{-6}$ to $10^{-2}$M. As in the case of the chelometric titrations all solutions were stirred magnetically.

Voltammetric studies

Voltammetric curves were obtained for the bronze electrodes using an assembly to rotate the electrode at a speed of 300 rpm. The voltage between the bronze electrode and the large area SCE electrode was scanned at a rate of 0.200 V/min. Voltage scans were generally carried out in both directions (+ to - and - to +) for each individual situation to check for significant differences in the polarization curves. The current was monitored in the -50 µA (anodic) to +50 µA (cathodic) range as a function of potential. As described earlier, the oxygen concentrations of the solutions were established by purging nitrogen, oxygen or one of the premixed gas mixtures into the system.

## RESULTS AND DISCUSSION

### Potentiometric Response of Cubic $Na_xWO_3$ to Dissolved Oxygen

Cubic sodium tungsten bronze $0.5<x<0.9$ was found to have a remarkable potentiometric response to dissolved oxygen in basic solution (pH>12). Potential shifts as large as 500-550 mV were observed upon transferring $Na_xWO_3$ electrodes between oxygen-saturated and oxygen-free (nitrogen-saturated) solutions. Figure 3 illustrates this response in 0.1M KOH-1mM EDTA for several x values as a function of time after transfer. The potentiometric response to dissolved oxygen was found to be Nernstian-like over a concentration range of approximately two orders of magnitude from $P_{O_2} = 0.209$, $C_{O_2} = 8.3$ ppm (air saturation) to $P_{O_2} = 0.0035$, $C_{O_2} = 0.14$ ppm or lower. Analytically useful response extended from oxygen saturation ($C_{O_2} = 39$ ppm) to $P_{O_2} = 0.001$ atm (0.04 ppm). The slopes of potential-log $C_{O_2}$ plots at 25°C, Figures 4-6, are extremely large at pH 12-13, ranging from 90 to more than 150 mV/decade. Figure 4 illustrates the response of two $Na_{0.63}WO_3$ and two $Na_{0.81}WO_3$ electrodes to dissolved oxygen in a pH 12 solution as determined using the dilution technique. Figure 5 illustrates the response of a $Na_{0.71}WO_3$ electrode at pH 12.0, 10.5 and 9.2 as a function of oxygen concentration measured independently by voltammetry. A typical response curve for an annealed flat-surfaced crystal ($x = 0.65$) in 0.1M KOH-1mM EDTA using the premixed gases to establish the $O_2$ concentration is shown in Figure 6.

A series of time response curves for a $Na_{0.65}WO_3$ electrode at different oxygen concentrations is shown in Figure 7. In this study the electrode was transferred from an air saturated KOH solution into one of

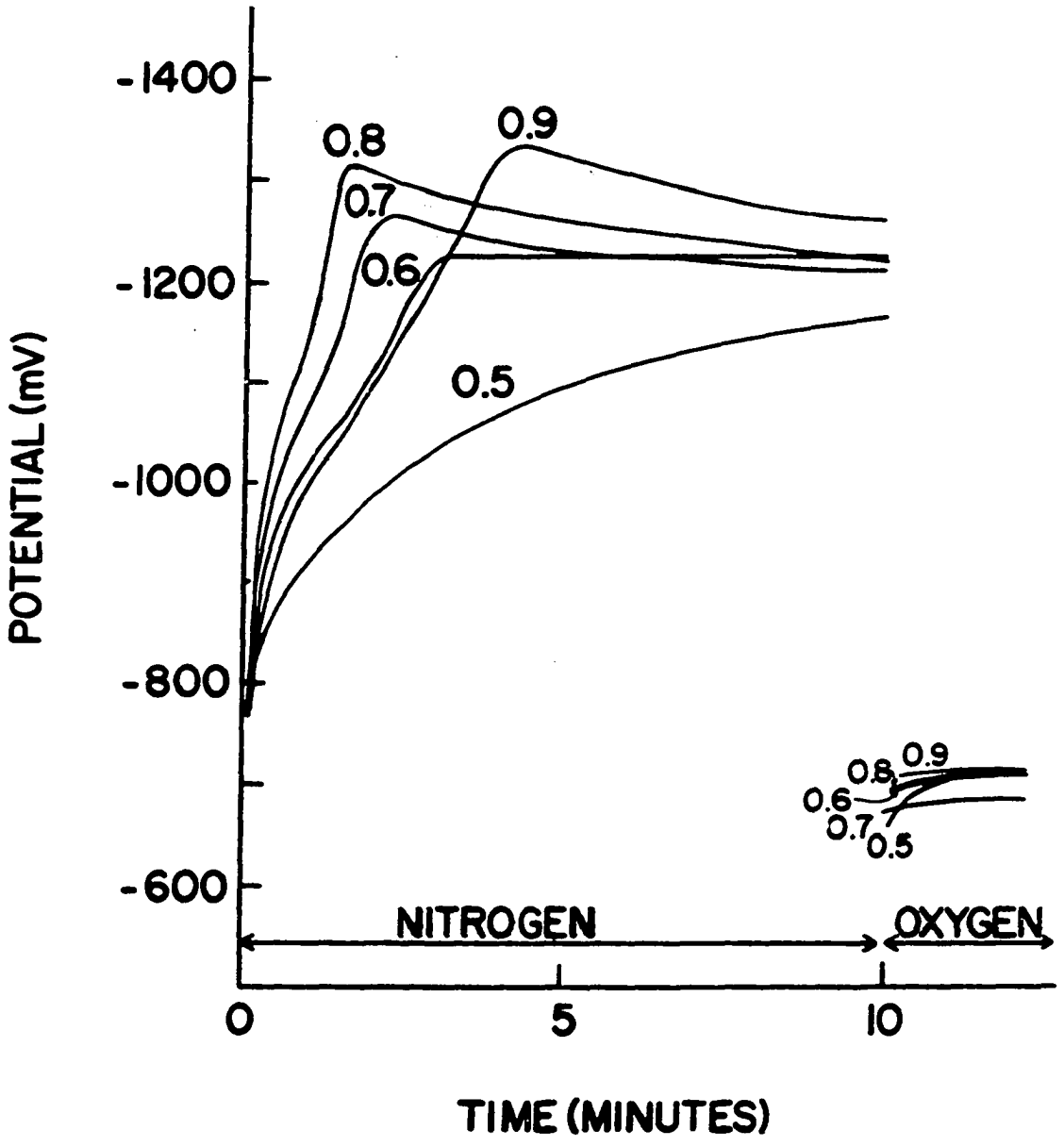


Figure 3. Time response of $Na_xWO_3$ electrodes in nitrogen and oxygen-saturated 0.1M KOH-1mM EDTA solutions as a function of x value

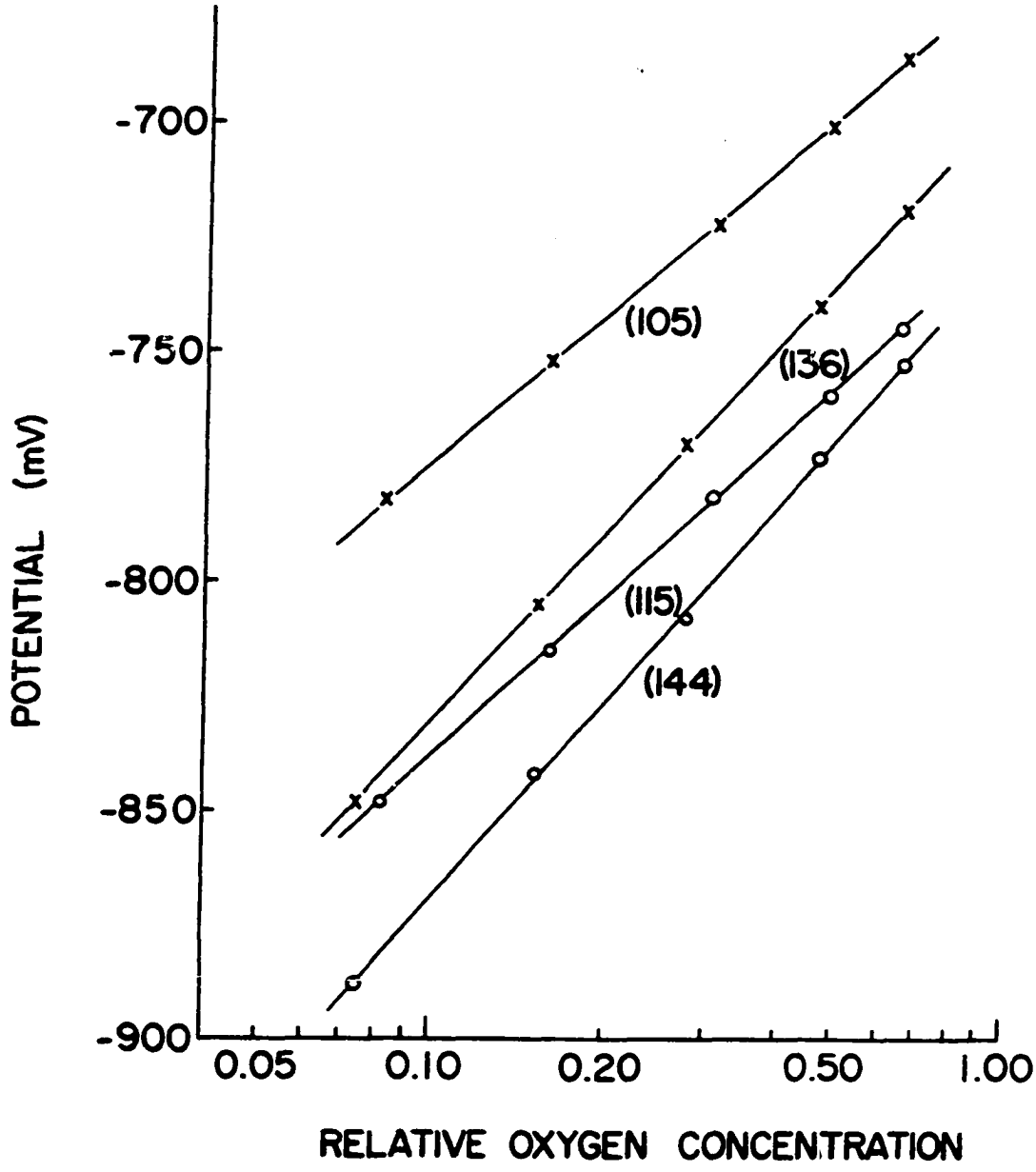


Figure 4. Oxygen response at pH-12 by dilution technique. Values in parentheses are slopes in mV/decade. Concentration relative to saturation with pure $O_2$

(x) $Na_{0.63}WO_3$ electrodes (o) $Na_{0.81}WO_3$ electrodes

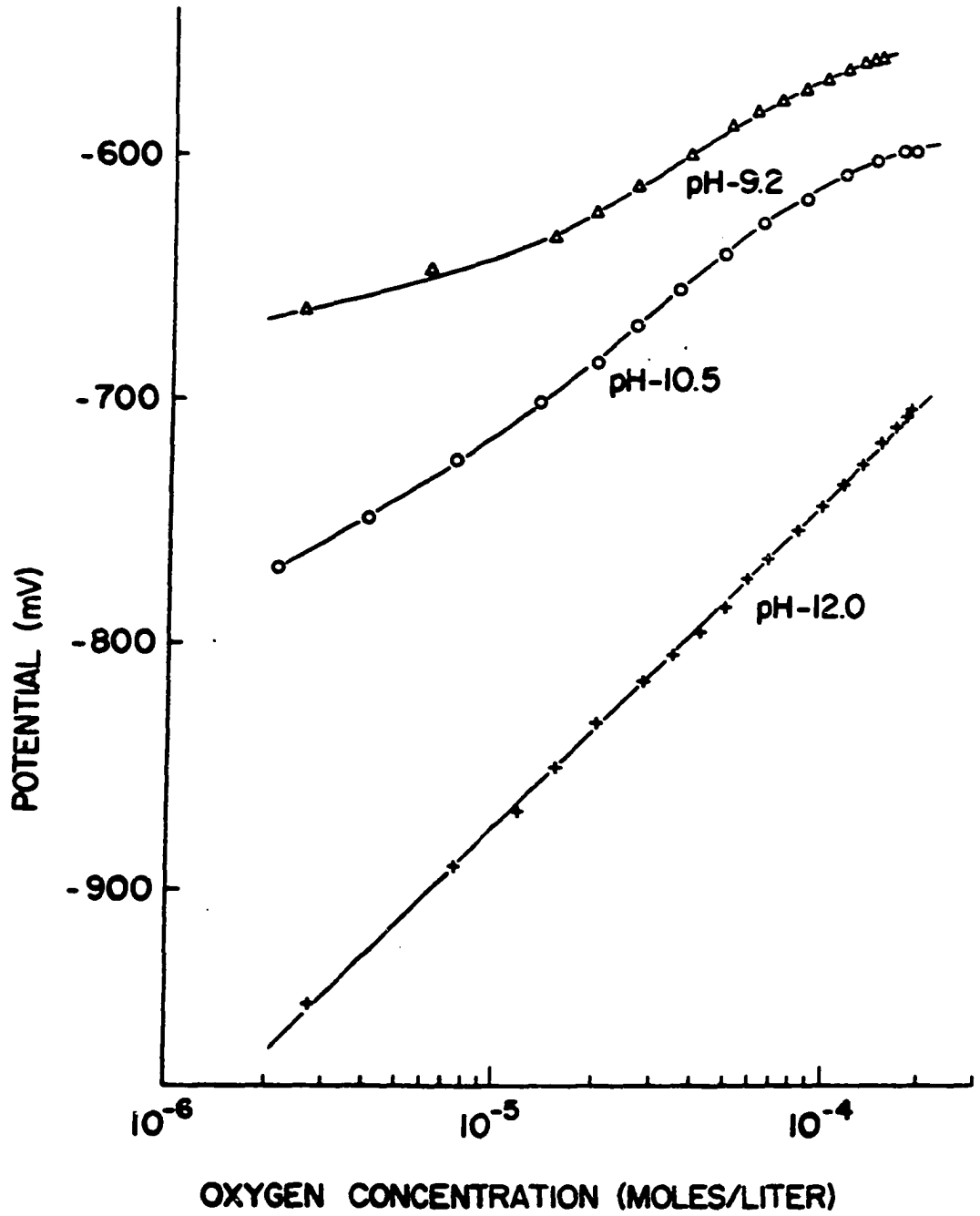


Figure 5. Oxygen response of the $Na_{0.71}WO_3$ electrode at several pH values

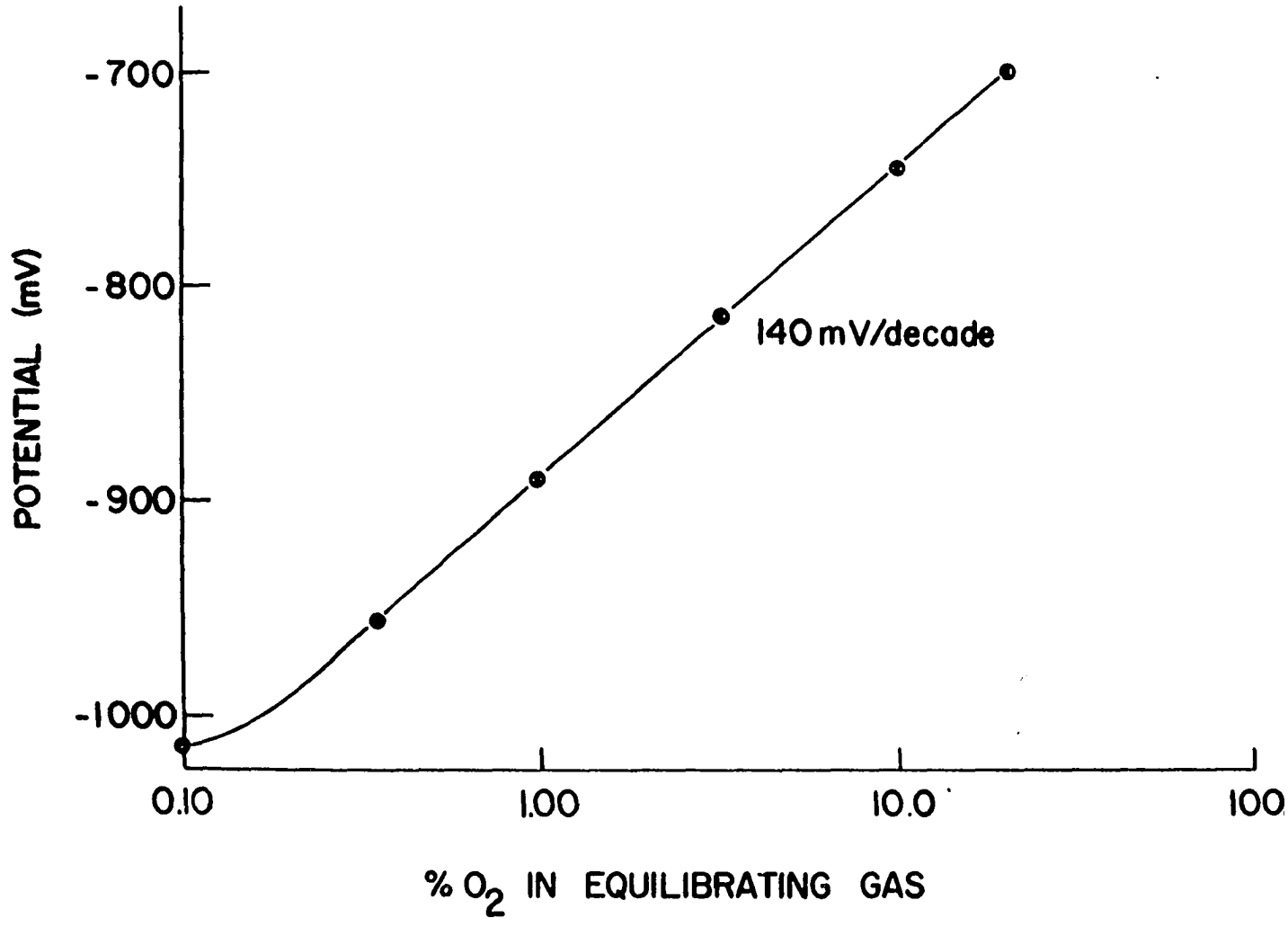


Figure 6. Oxygen response of $Na_{0.65}WO_3$ electrode in 0.1M KOH-1mM EDTA using $N_2$-$O_2$ mixtures

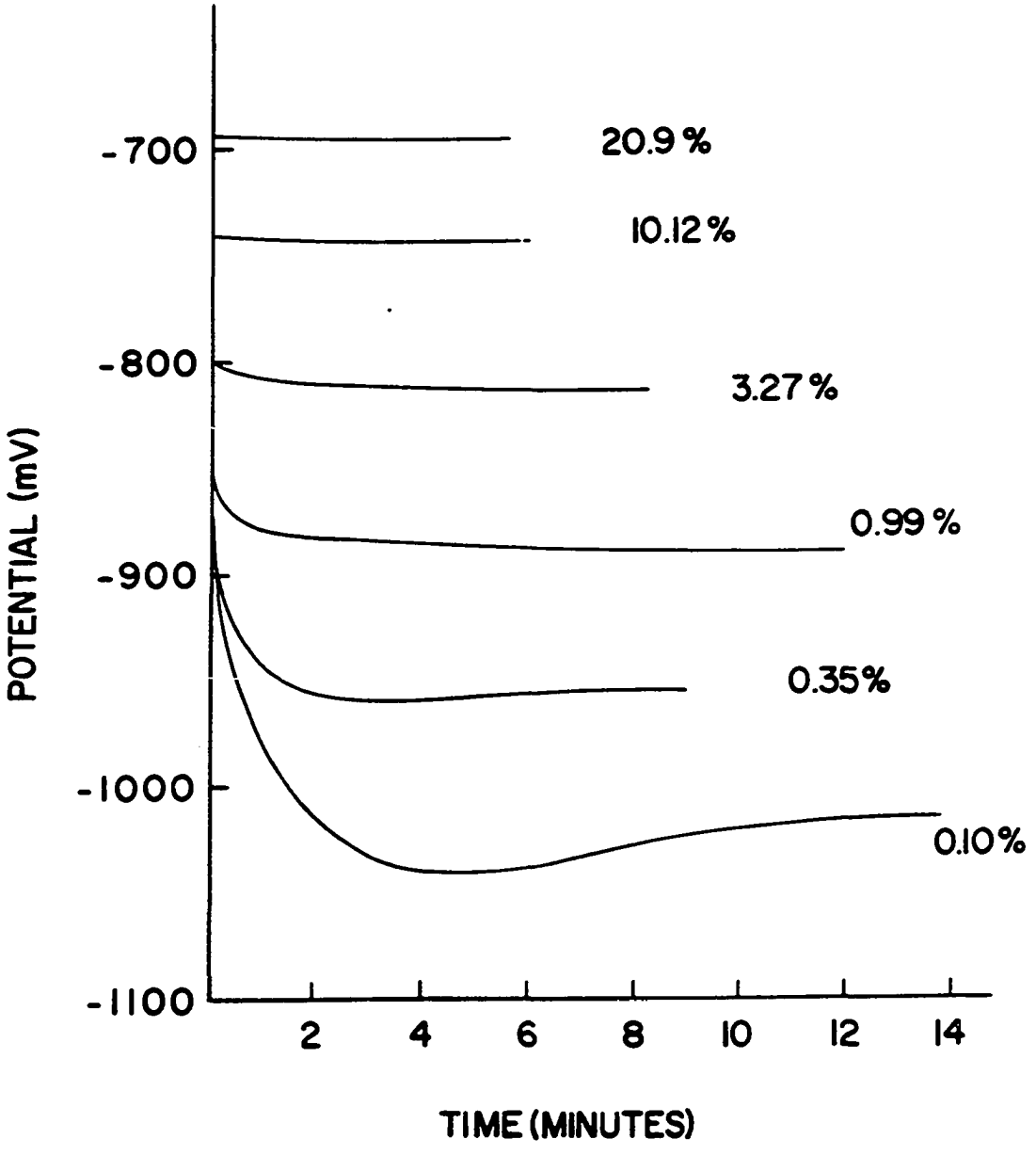


Figure 7. Time response of $Na_{0.65}WO_3$ electrode

lower $O_2$ concentration equilibrated with one of the premixed $N_2$-$O_2$ gases. At the higher $O_2$ concentrations ($P_{O_2}$ >0.01 atm) a stable potential was reached in 2-3 minutes but at lower concentration significantly longer time was required and a minimum was observed before the equilibrium potential was reached. Consistent and rapid stirring was found to be an essential factor both in maintaining a stable potential at a given $O_2$ concentration and in obtaining linear potential vs. log-C calibration plots. The bronze electrode potential in unstirred solutions drifted in a negative direction, and in very dilute oxygen solutions the potential stabilized at a value corresponding to a completely deoxygenated system indicating a depletion of oxygen in the vicinity of the electrode surface.

Variations in the slopes of the response curves and the potential established in an air-saturated solution (referred to as the "air potential") were found to be considerable. These variations were apparent not only between cubic sodium tungsten bronzes of differing x values but also between electrodes cut or chipped from the same parent crystal. In fact, the day-to-day response of a given electrode could exhibit variations as wide as those between electrodes of different x values. As an example, a $Na_{0.65}WO_3$ electrode exhibited response slopes of 163, 116, 131 and 105 mV/decade over a three day period. The corresponding potentials in air-saturated solution were 641, 701, 702 and 678 mV. These variations are considered to be due to changes in the bronze surface characteristics from repeated contact with the basic solutions. Visible etching and pitting of the electrode surface was generally encountered after prolonged use.

Somewhat less electrode to electrode variability was encountered

with a series of electrodes which had been annealed at 650°C in an argon atmosphere to insure homogeneity and cut with flat regular surfaces. A comparison between these and a series of non annealed crystals with irregular surfaces is shown in Table 3. The only apparent difference

Table 3. Comparison of electrode variability

| | Annealed, flat surface | Not annealed, irregular surface |
|---|---|---|
| x value | 0.65 | 0.63 |
| No. of electrodes | 16 | 8 |
| No. of observations | 20 | 15 |
| Average air potential (mV) | -695 ± 22[a] | -712 ± 42 |
| Average slope (mV/decade) | 120 ± 13 | 124 ± 14 |

[a]One standard deviation

in this comparison was the significantly lower variability of the air potential for the annealed, flat-surfaced electrodes. The annealed, flat-surfaced electrodes, moreover, were found to respond more rapidly to a change in $O_2$ concentration and Nernstian-like response generally extended to lower oxygen concentration.

Sodium tungsten bronzes having x values in the range 0.60-0.70 appeared to show the best response to dissolved oxygen. Electrodes of lower x value (0.5) usually responded extremely slowly and for those of higher x value (0.8) the calibration plots were often nonlinear.

The addition of EDTA at a concentration of 0.5 to 1mM was found to be necessary to complex traces of easily reducible metals which interfere with the oxygen response. Without the EDTA, the response would hardly extend to 1 ppm dissolved oxygen. Figure 8 shows the response of a $Na_{0.62}WO_3$ electrode when transferred between $O_2$-saturated and $O_2$-free 0.1M KOH solutions, illustrating the effect of EDTA at a concentration of 1mM. The EDTA extended the potentiometric range approximately 200 mV which corresponds to a factor of nearly 40 in oxygen concentration.

The temperature coefficient, dE/dT, for an annealed flat-surface $Na_{0.65}WO_3$ electrode in 0.1M KOH-1mM EDTA at $P_{O_2}$ = 0.0327 atm ($3.96 \times 10^{-5}$M dissolved $O_2$) was found to be -7.04 mV/°C over a temperature range of 3-35°C (Figure 9). Only a small portion (-0.98 mV/°C) of this temperature coefficient may be attributed to the change in oxygen solubility as a function of temperature. This value was estimated from the expression

$$\frac{0.1984T}{n}\left(\frac{d \log a_i}{dT}\right)$$

in which T is the temperature, n a constant depending on the slope of potentiometric response, and $a_i$ the activity of the dissolved oxygen (83). Based on the observed 120 mV/decade oxygen response 0.5 was chosen for n. The value for $d(\log a_i)/dT$ was calculated from oxygen solubilities at 20°C and 30°C, 43.39 and 35.88 ppm respectively (84).

Analytically useful dissolved oxygen response was limited to strongly basic solution. At pH 10.5 or less, the response deteriorated and the potential-log C relationship became nonlinear (Figure 5). In acid solution (0.1M $HClO_4$) only minimal response was observed (20-30 mV/decade) for 0.01 atm$<P_{O_2}<$1 atm. Potassium hydroxide solutions appeared superior

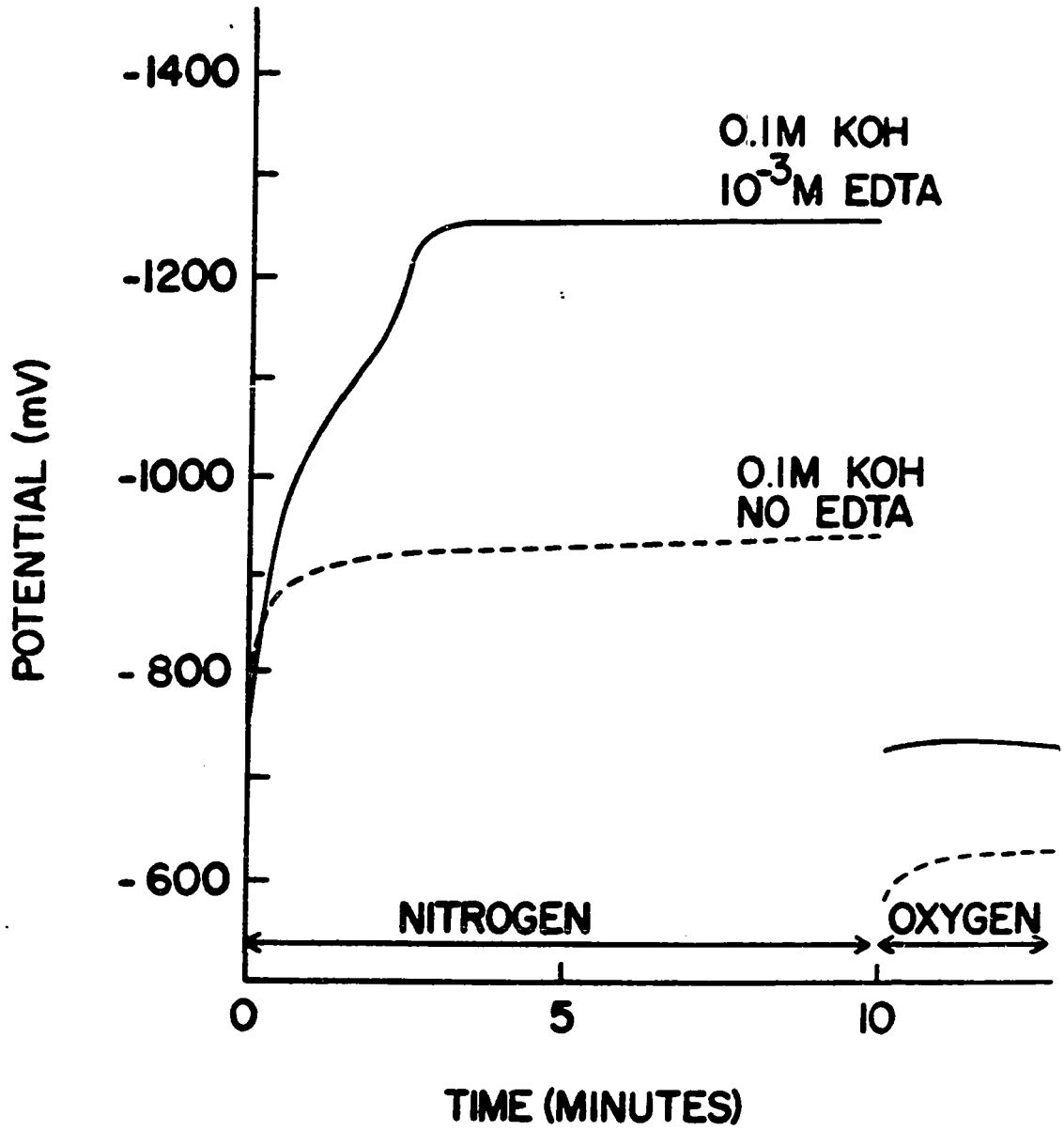


Figure 8. Effect of EDTA on the response of $Na_{0.63}WO_3$ electrode in nitrogen and oxygen-saturated 0.1M KOH solution

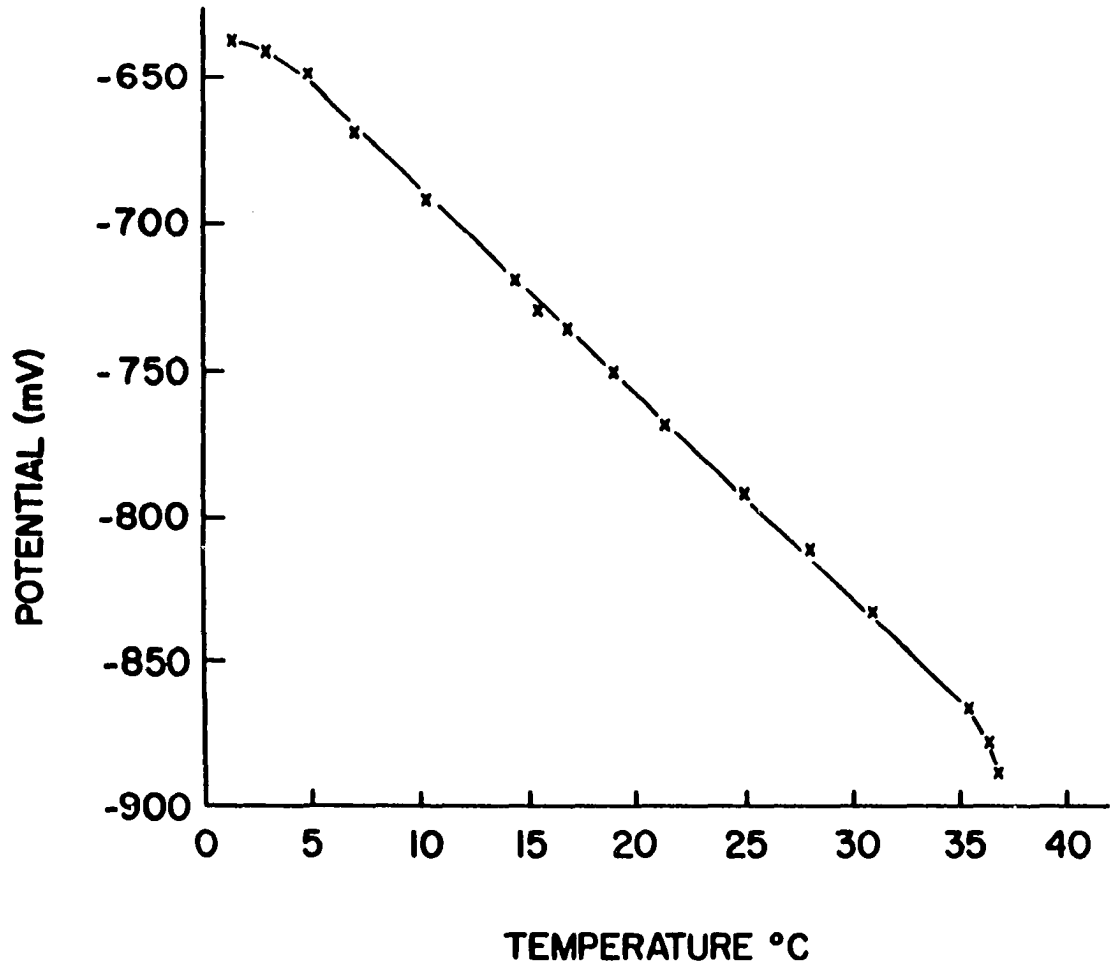


Figure 9. Effect of temperature on response of $Na_{0.65}WO_3$ electrode

to both NaOH and LiOH. The electrode response in NaOH was often found to be sluggish and the linear dependence did not extend to as low oxygen concentrations as in KOH. In LiOH little response to dissolved oxygen was found for electrodes having x values of 0.6 or less (compare Figures 3 and 10).

## Application of the $Na_xWO_3$ Electrode to the Determination of Dissolved Oxygen

The cubic sodium tungsten bronze electrode was found to perform very well as a selective-potentiometric electrode for the determination of dissolved oxygen in basic solution. The results of 20 series of analyses using 16 annealed, flat-surface $Na_{0.65}WO_3$ electrodes are presented in Table 4. For each series the electrode potentials were measured in 0.1M KOH-1mM EDTA saturated sequentially with the $N_2$-$O_2$ gas mixtures listed in Table 2. The potentials established in air-saturated and 0.99% saturated solutions were used to provide a two-point calibration of the form, log C = m(mV) + constant, from which the partial $O_2$ pressures of the other four gases were determined.

Analyses at 10.12 and 3.27% oxygen partial pressure exhibited no systematic error and had relative standard deviations of approximately ±5%. Analyses at 0.35 and 0.10% appeared to be systematically low with deviations of 14 and 21% from the reported value and relative standard deviations of similar magnitude. Significant improvement in accuracy in this lower concentration range was achieved when calibrations were made at the same order of magnitude as the unknown. Also presented in Table 4 are the results of the analyses performed on the 0.35% $O_2$ gas mixture when the two-point calibration was done with the 0.99 and 0.10% $O_2$ gas mixtures.

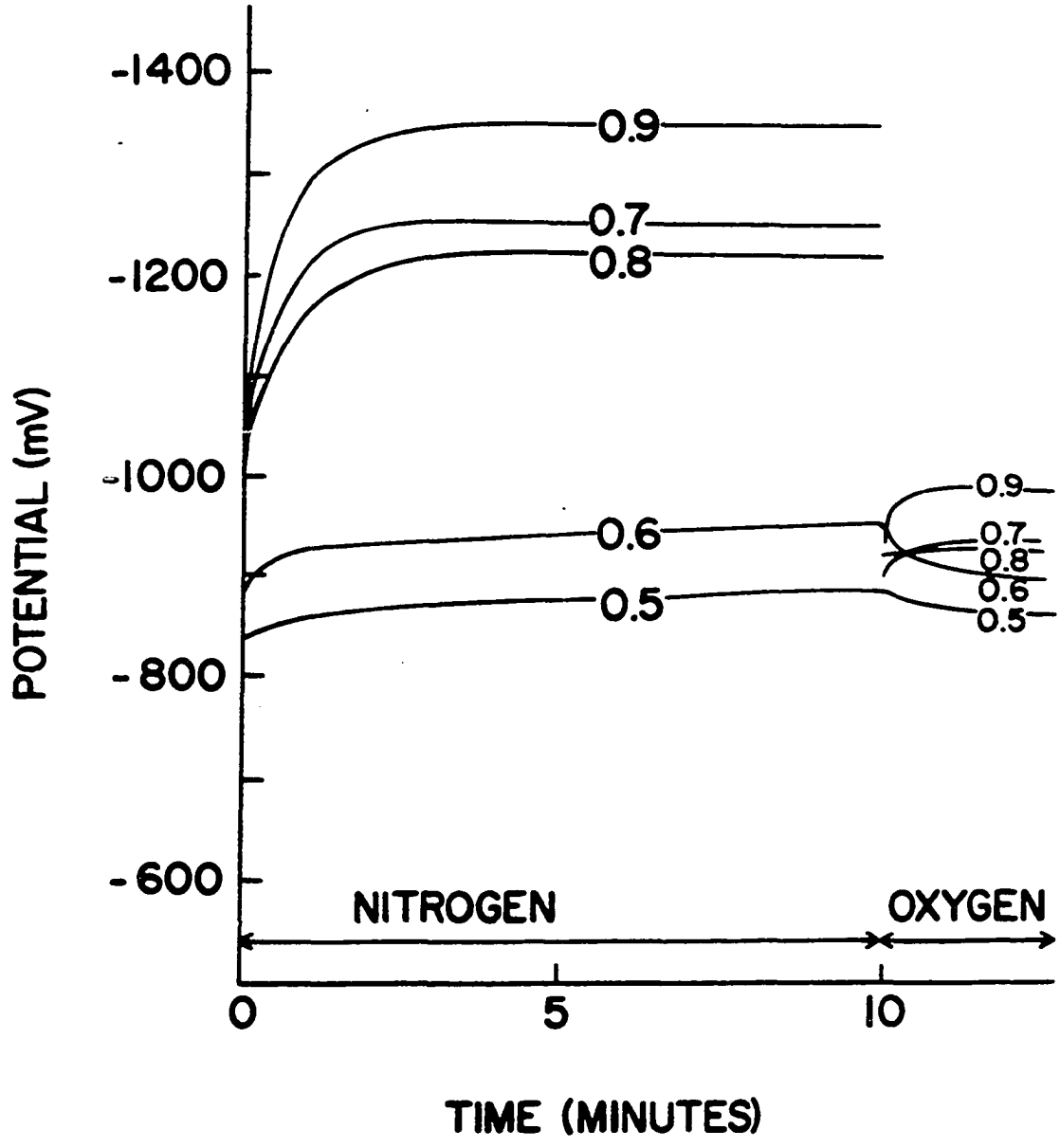


Figure 10. Time response of $Na_xWO_3$ electrodes in nitrogen and oxygen-saturated 0.1M LiOH-1mM EDTA solutions as a function of x value

Table 4. Results of oxygen determinations using the $Na_{0.65}WO_3$ electrode

| Electrode | Date | Air potential (mV) | Slope (mV/decade) | Measured $O_2$ partial pressure (% $O_2$ saturated) | | | | |
|---|---|---|---|---|---|---|---|---|
| | | | | 10.12[a] | 3.27[a] | 0.35[a] | 0.10[a] | 0.35[b] |
| 680 | 7/26 | -689 | 119 | 9.76 | 3.40 | 0.295 | 0.068 | 0.351 |
| 681 | 7/26 | -689 | 105 | 9.54 | 3.21 | 0.306 | 0.087 | 0.328 |
| 681 | 7/27 | -718 | 116 | 9.81 | 3.55 | 0.295 | 0.081 | 0.327 |
| 682 | 7/26 | -690 | 118 | 9.95 | 3.30 | 0.286 | 0.072 | 0.335 |
| 683 | 7/26 | -705 | 110 | 10.07 | 3.06 | 0.283 | 0.106 | 0.305 |
| 685 | 7/26 | -678 | 118 | 10.91 | 3.22 | 0.317 | 0.092 | 0.330 |
| 686 | 7/27 | -700 | 123 | 10.91 | 3.22 | 0.281 | 0.072 | 0.329 |
| 690 | 8/03 | -698 | 116 | 10.05 | 3.73 | 0.397 | 0.061 | 0.469 |
| 690 | 8/03 | -708 | 126 | 10.80 | 3.50 | 0.303 | 0.064 | 0.367 |
| 690 | 8/04 | -711 | 117 | 9.85 | 3.27 | 0.255[c] | 0.029[c] | - |

[a]Calibration at 20.9 and 0.99% $O_2$ partial pressure

[b]Calibration at 0.99 and 0.10% $O_2$ partial pressure

[c]Result discarded from statistical analysis

Table 4. (Continued)

| Electrode | Date | Air potential (mV) | Slope (mV/decade) | Measured $O_2$ partial pressure (% $O_2$ saturated) | | | | |
|---|---|---|---|---|---|---|---|---|
| | | | | 10.12[a] | 3.27[a] | 0.35[a] | 0.10[a] | 0.35[b] |
| 691 | 8/04 | -717 | 159 | 9.65 | 3.05 | 0.384 | 0.108 | 0.371 |
| 691 | 8/08 | -664 | 131 | 9.76 | 3.25 | 0.253 | 0.067 | 0.310 |
| 692 | 8/08 | -622 | 96 | 9.81 | 3.12 | 0.323 | 0.077 | 0.363 |
| 693 | 8/07 | -695 | 133 | 9.88 | 3.36 | 0.283 | 0.086 | 0.305 |
| 694 | 8/07 | -678 | 128 | 9.84 | 3.24 | 0.258 | 0.065 | 0.319 |
| 695 | 8/07 | -712 | 111 | 9.55 | 3.04 | 0.425[c] | 0.272[c] | - |
| 696 | 8/07 | -717 | 123 | 10.73 | 3.69 | 0.298 | 0.065 | 0.361 |
| 697 | 8/07 | -700 | 108 | 9.86 | 3.23 | 0.273 | 0.084 | 0.308 |
| 698 | 8/08 | -696 | 112 | 10.26 | 3.50 | 0.249 | 0.053 | 0.335 |
| 699 | 8/07 | -707 | 119 | 10.14 | 3.40 | 0.325 | 0.103 | 0.321 |
| Average | | -694.7 | 119.5 | 10.056 | 3.317 | 0.301 | 0.078 | 0.341 |
| 1 std. deviation | | ±22.3 | ±12.9 | ±0.439 | ±0.199 | ±0.039 | ±0.016 | ±0.038 |
| | | | | (4.4%) | (6.0%) | (13.1%) | (20.7%) | (11.3%) |

The systematic error was reduced from 14 to 2.5 per cent but the precision of analysis was not significantly improved.

The wide variation in response slopes between electrodes had little or no bearing on the success of an oxygen determination; results were similar for electrodes 691 and 692 with slopes of 159 and 96 mV/decade as well as for electrodes having intermediate values. The variability of the response of a given electrode over a period of time, however, could cause considerable analytical error if the electrode was not calibrated soon after sample measurement. The effects of temperature variation and stirring have already been discussed, and a successful analysis would also depend upon the control of these variables.

Excellent oxygen response was also obtained in both tap water and lake water when adjusted to 0.1M in KOH and 1mM in EDTA (Figure 11). The impurities normally found in such samples are not expected to cause any problems in the determination of dissolved oxygen. Calcium and Fe(III) at concentrations below that of the EDTA (1mM) cause little interference in the oxygen response. The only effect noted was a slight shift in potential in the positive direction (Figures 12 and 13). The oxygen calibration curves remained linear for 0.001 atm$<P_{O_2}<$0.10 atm. At calcium concentrations in excess of that of the EDTA however, an excessive positive shift was noted and the calibration curve lost its linearity. This shift is not considered to be due to the calcium ion itself but to the reaction of calcium with the EDTA thereby decreasing its concentration to a level insufficient to adequately chelate traces of reducible metals which cause the shift. Increasing the EDTA concentration above that of the $Ca^{2+}$ should eliminate this problem. Copper(II) and silver(I) were found to

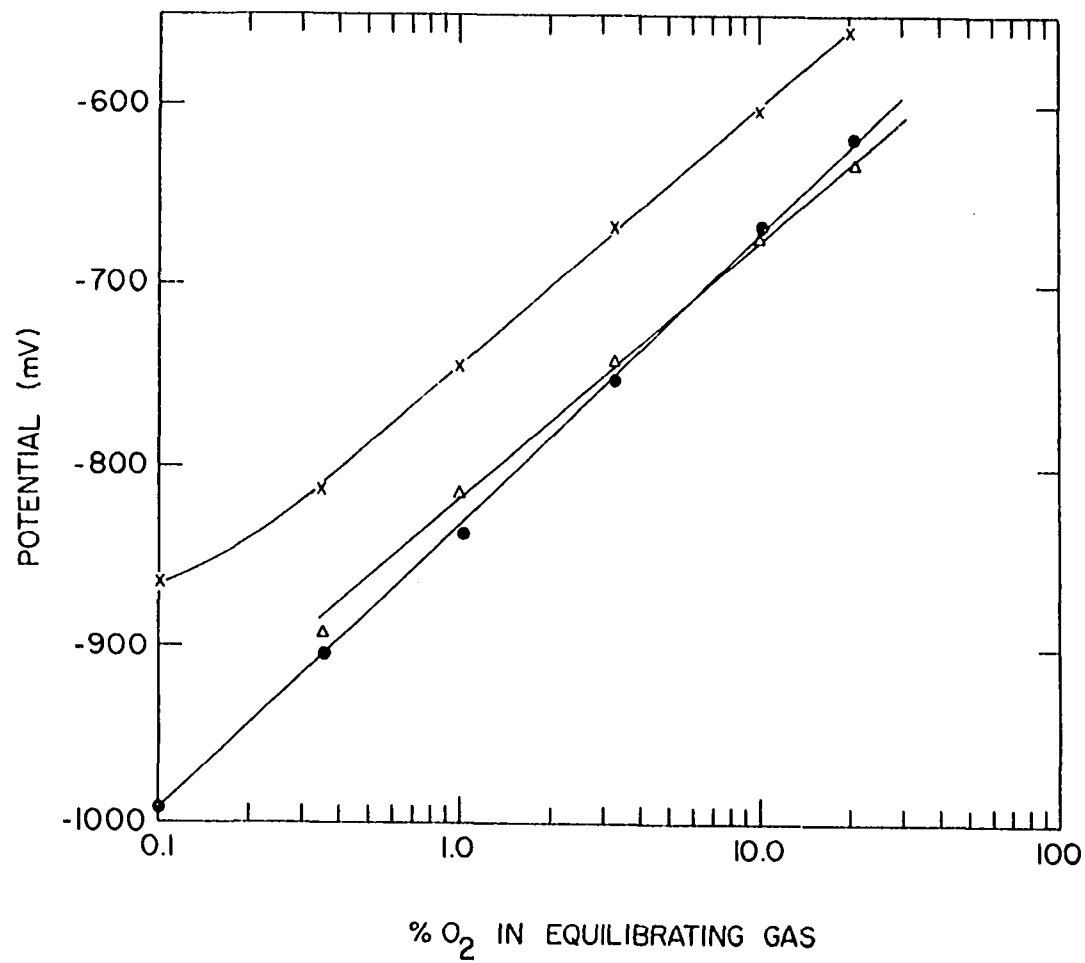


**Figure 11.** Oxygen response in tap (Δ) and lake (x) (●) water when adjusted to 0.1M KOH-1mM EDTA

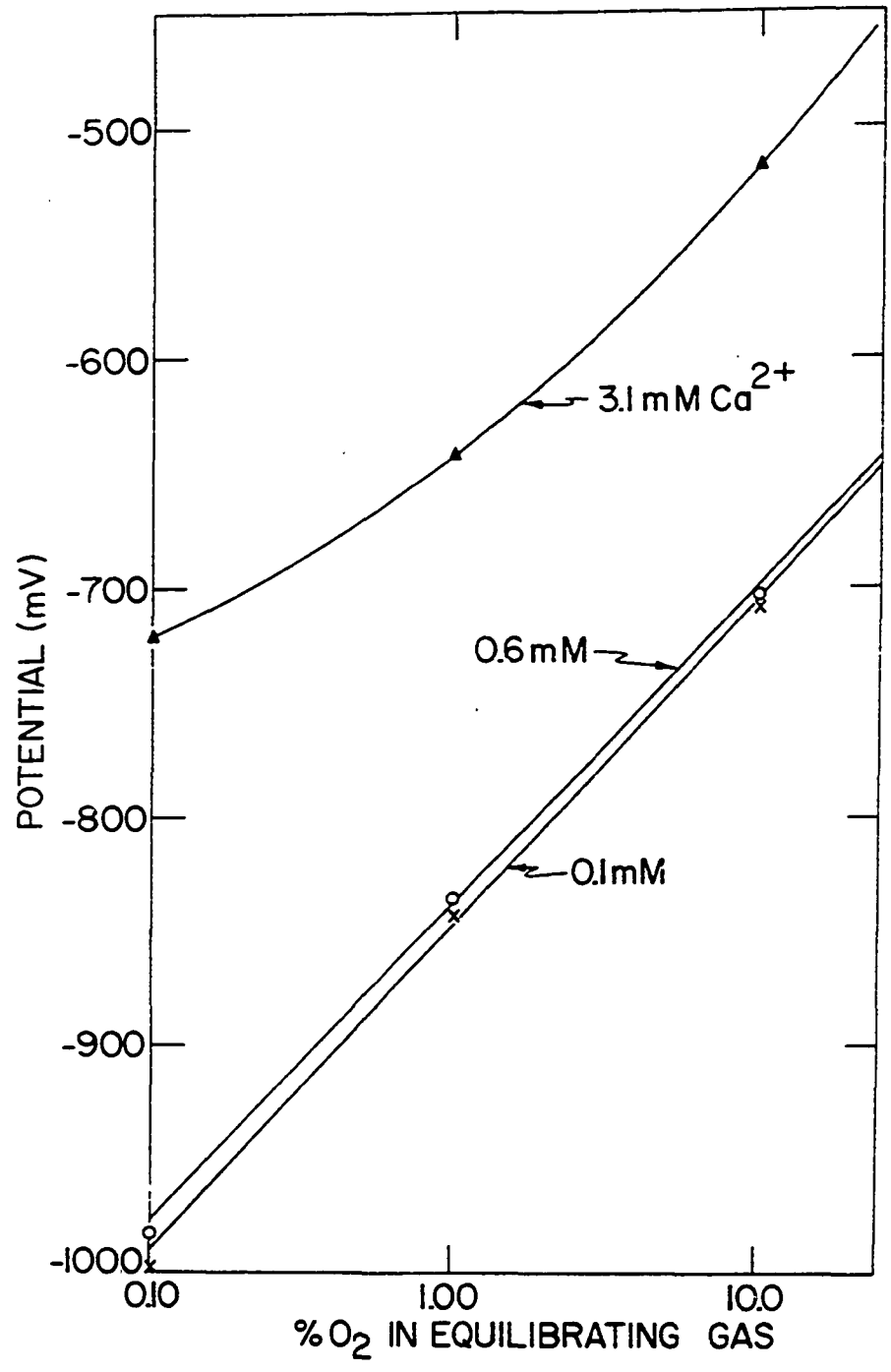


Figure 12. Effect of $Ca^{2+}$ on the oxygen response of the $Na_{0.65}WO_3$ electrode in 0.1M KOH-1mM EDTA

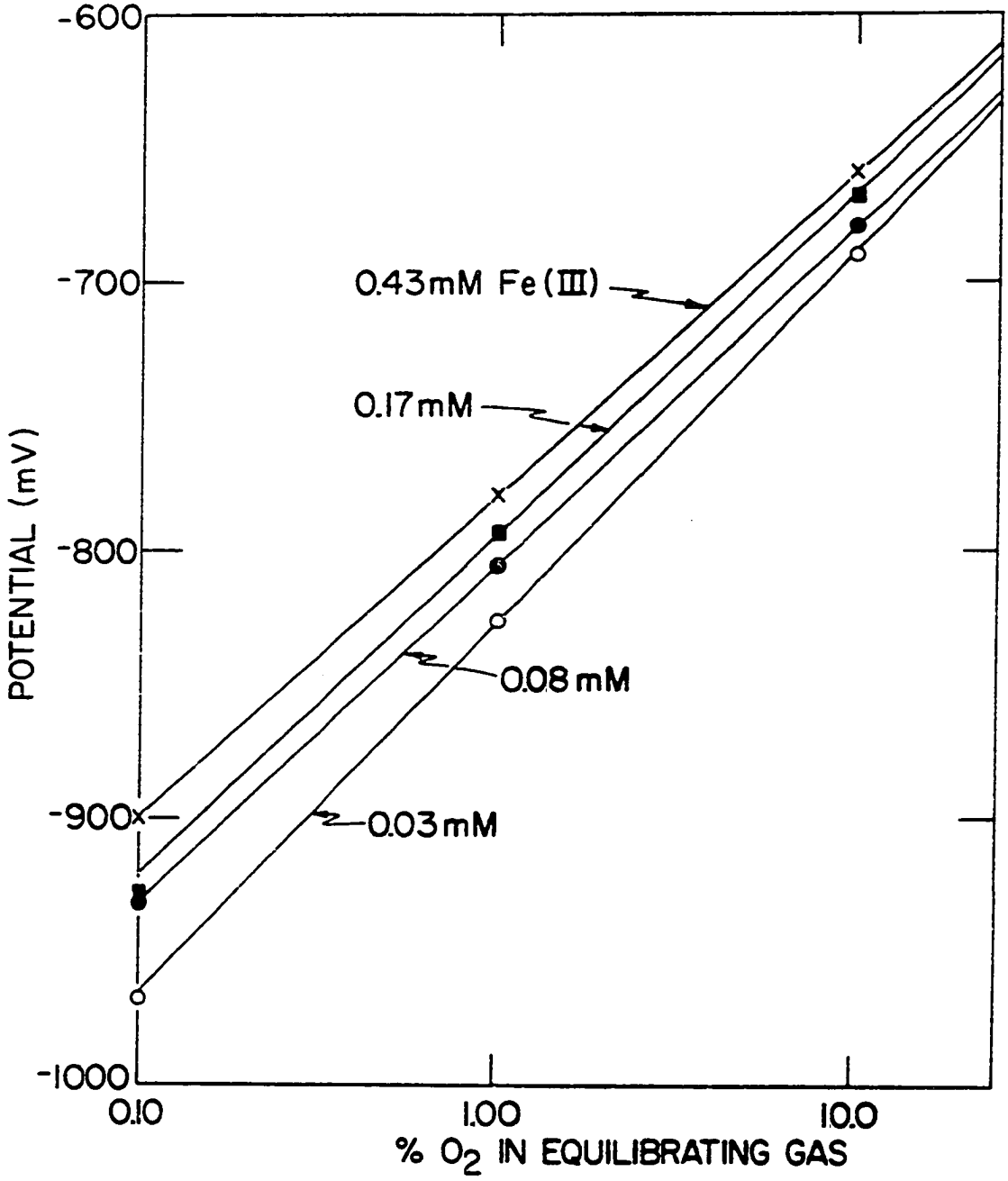


Figure 13. Effect of Fe(III) on the oxygen response of the $Na_{0.65}WO_3$ electrode in 0.1M KOH-1mM EDTA

interfere much more seriously (Figures 14 and 15). As little as 0.03mM Cu(II) caused enough positive potential shift to destroy the linearity of response below $P_{O_2}$ = 0.01 atm. The oxygen response above $P_{O_2}$ = 0.01 atm however, was not seriously affected at copper concentrations below 0.02mM. Trace silver (0.008mM) resulted in very large positive potential shifts and non-linear response and actually enhanced the oxygen response from approximately 120 mV/decade to 160-220 mV/decade. Visible deposits of metallic silver were observed on the $Na_xWO_3$ electrode, and the radical change in oxygen response is attributed to the subsequent change in the electrode surface characteristics.

The application of the $Na_xWO_3$ electrode for the determination of dissolved oxygen in a flow-through system was demonstrated using several modifications of the apparatus shown in Figure 2. System specifications are listed in Table 5 and the dissolved oxygen responses are illustrated in Figure 16. Linear calibration curves with slopes between 100-130 mV/decade were generally realized for 0.01 atm$<P_{O_2}<$0.209 atm. The $10^3$ cm/min linear flow past the bronze electrode appeared to provide sufficient agitation to establish a potential representative of the oxygen concentration. Attempts to measure dissolved oxygen below $P_{O_2}$ = 0.01 atm however, were generally unsuccessful, probably due to the diffusion of atmospheric oxygen into the system. Improved system design should correct this limitation.

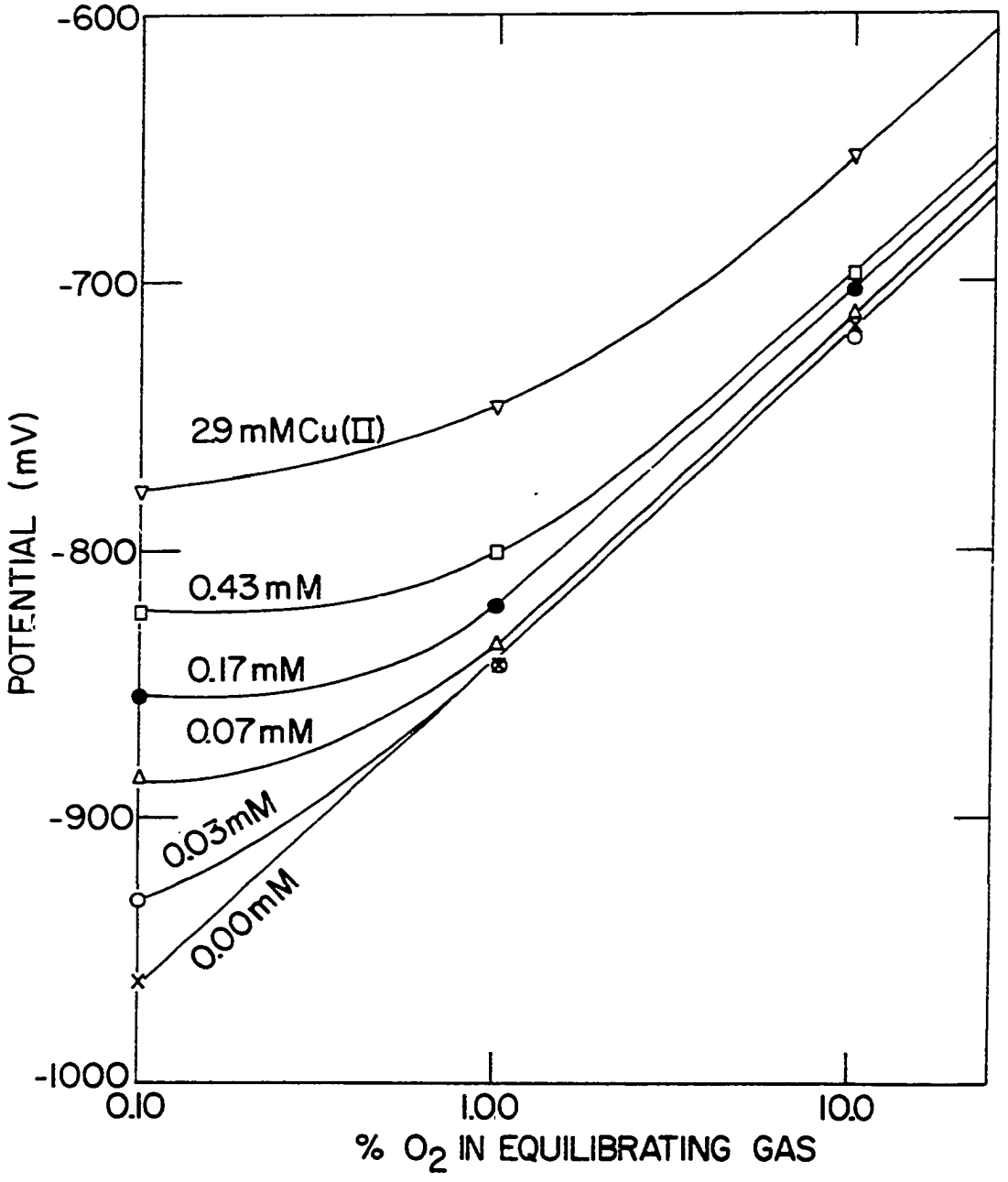


Figure 14. Effect of Cu(II) on the oxygen response of the $Na_{0.65}WO_3$ in 0.1M KOH-1mM EDTA

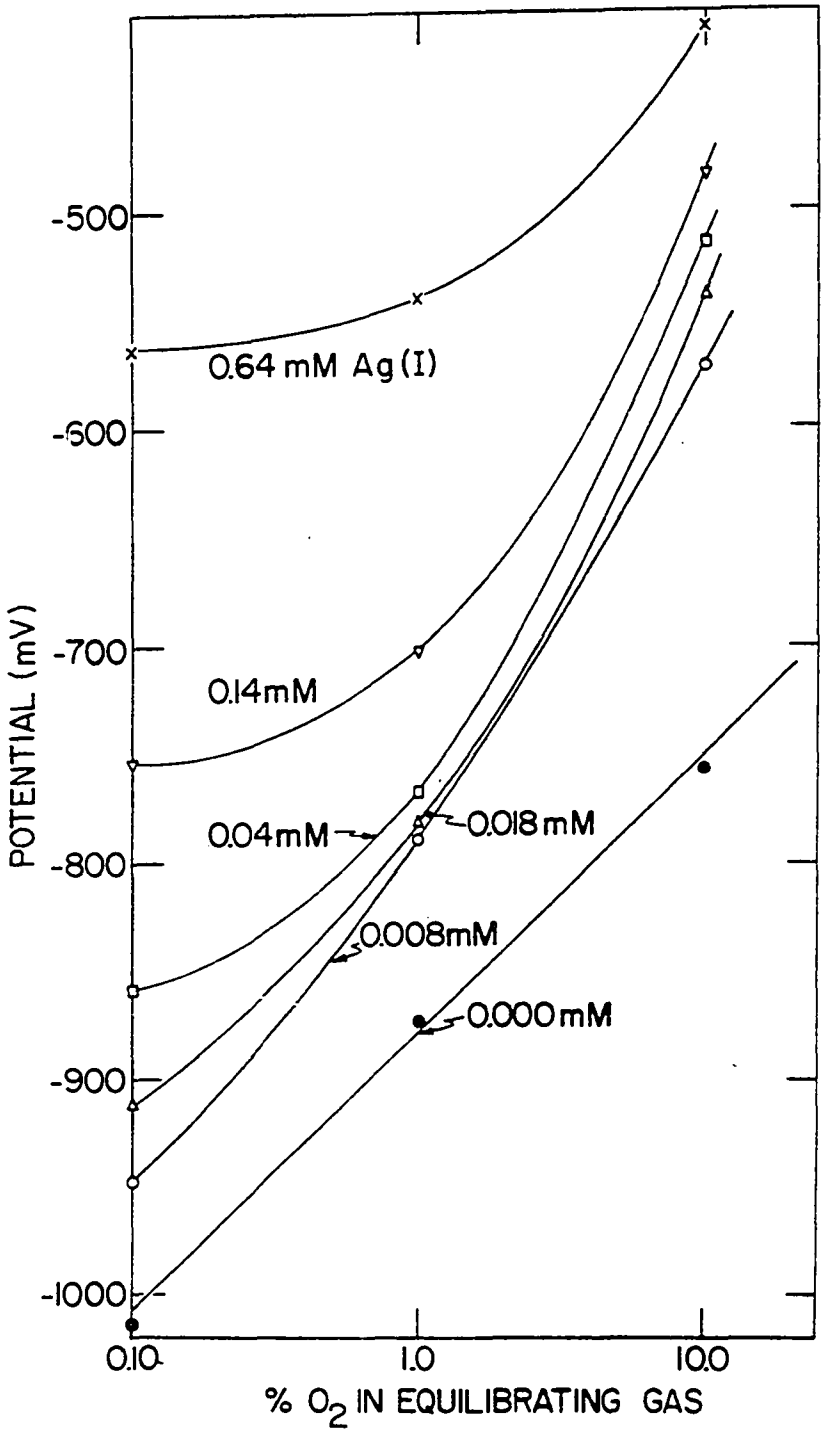


Figure 15. Effect of Ag(I) on the oxygen response of the $Na_{0.65}WO_3$ in 0.1M KOH-1mM EDTA

Table 5. Flow-through system specifications

| System | Reagent | Flow rate (ml/min) Reagent | Flow rate (ml/min) Sample | Mixing chamber volume (ml) | Linear flow past electrode (cm/min) |
|---|---|---|---|---|---|
| I | 1M KOH 10mM EDTA | 10[a] | 20 | 30 | $10^3$ |
| II | 1M KOH 10mM EDTA | 10[a] | 20 | 10 | $10^3$ |
| III | 0.5M KOH 5mM EDTA | 13[b] | 47 | 1 | $10^3$ |

[a]Gravity feed

[b]Pressure feed

## Response of Other Tungsten Bronzes to Dissolved Oxygen

The excellent oxygen response appears quite unique to the cubic sodium tungsten bronzes. The dissolved oxygen responses of a number of other highly conducting alkali metal tungsten bronzes in 0.1M KOH-1mM EDTA are presented in Figure 17. Little or no response was observed for the hexagonal potassium and rubidium tungsten bronzes. The response of cubic lithium bronze was marginal (≈30 mV/decade) while significant responses were observed for tetragonal potassium bronze, ($K_{0.5}WO_3$), (≈70 mV/decade) and hexagonal cesium bronze (≈80 mV/decade). These responses were much inferior to that of the cubic sodium tungsten bronze. They were extremely slow, much less reproducible, and exhibited nonlinear potential-log C relationships.

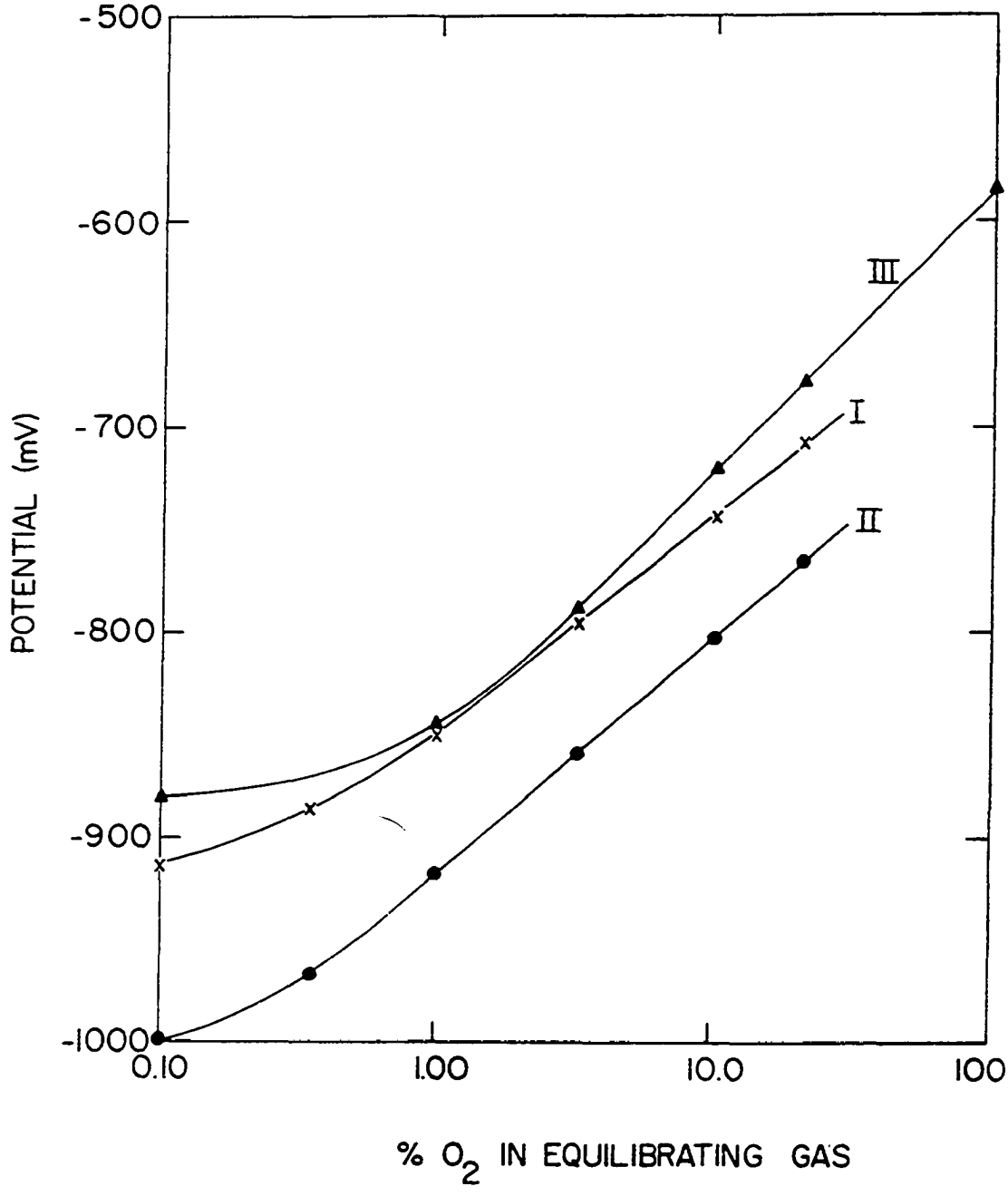


Figure 16. Oxygen response in flow-through systems. See Table 5

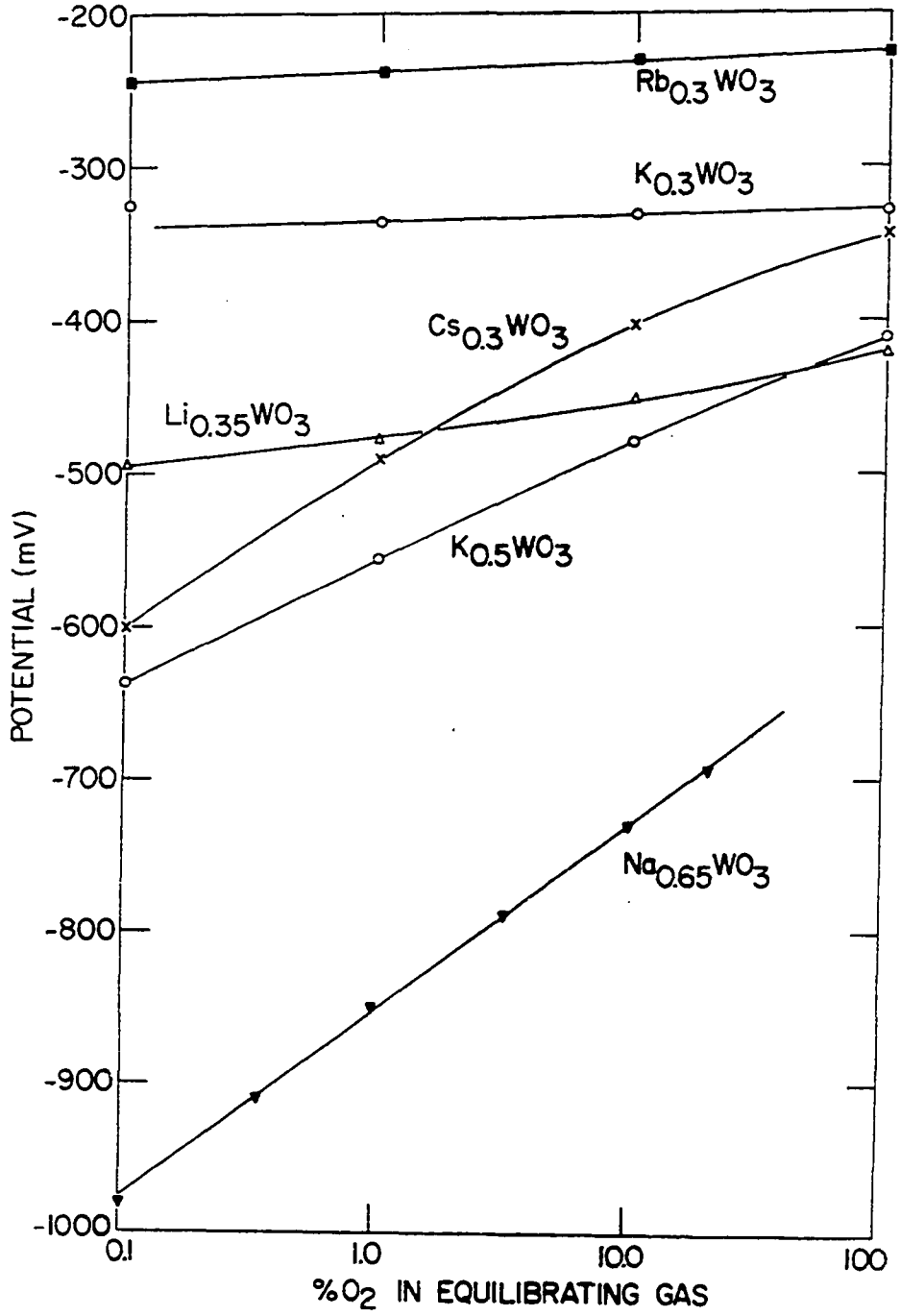


Figure 17. Oxygen response of the hexagonal $M_{0.3}WO_3$, cubic $Li_{0.35}WO_3$, tetragonal $K_{0.5}WO_3$ and cubic $Na_{0.65}WO_3$ electrodes in 0.1M KOH-1mM EDTA

## Application of the $Na_xWO_3$ Electrode in Chelometric Titrations

The large negative potential shift observed for the $Na_xWO_3$ electrode when EDTA was added to 0.1M KOH (Figure 8) suggested the possibility of using the electrode to potentiometrically detect the end point in metal-EDTA titrations in basic solution. Titrations involving a number of metals with high metal-EDTA stability constants were performed in 0.1 to 1M $NH_4OH$ (pH 10-11) and potentiometrically followed with a $Na_{0.65}WO_3$ electrode. Ammonium hydroxide was chosen as the titration medium over an alkali metal hydroxide in view of the increased solubility of a number of metal salts.

Direct titrations of Ca and Mg at pH 10 (0.16M $NH_4OH$-0.03M $NH_4Cl$) are shown in Figures 18 and 19. End point-potential shifts of -50 to -100 mV were realized when 2.5 millimoles of metal were titrated with 0.1M EDTA. Analytically useful curves were obtained for as little as 0.01 millimole of metal when titrated with $10^{-3}$M EDTA. It was also found possible to accurately determine both calcium and magnesium in a mixture by titrating for Ca at pH 13 where Mg was precipitated as the hydroxide and then titrating for Ca + Mg at pH 10 where Mg is soluble. Figure 20 illustrates this titration curve. Excellent titration curves were also obtained for Ni(II), Mn(II), Cu(II), Cd(II) and Co(II) in ammoniacal solution (Figures 21-23).

Back titrations of excess EDTA with calcium gave extremely good potentiometric end points when monitored with a $Na_{0.65}WO_3$ electrode (Figures 22-25). Reverse titrations involving Zn(II) and Pb(II) exhibited significantly sharper potential breaks at the end point than the corres-

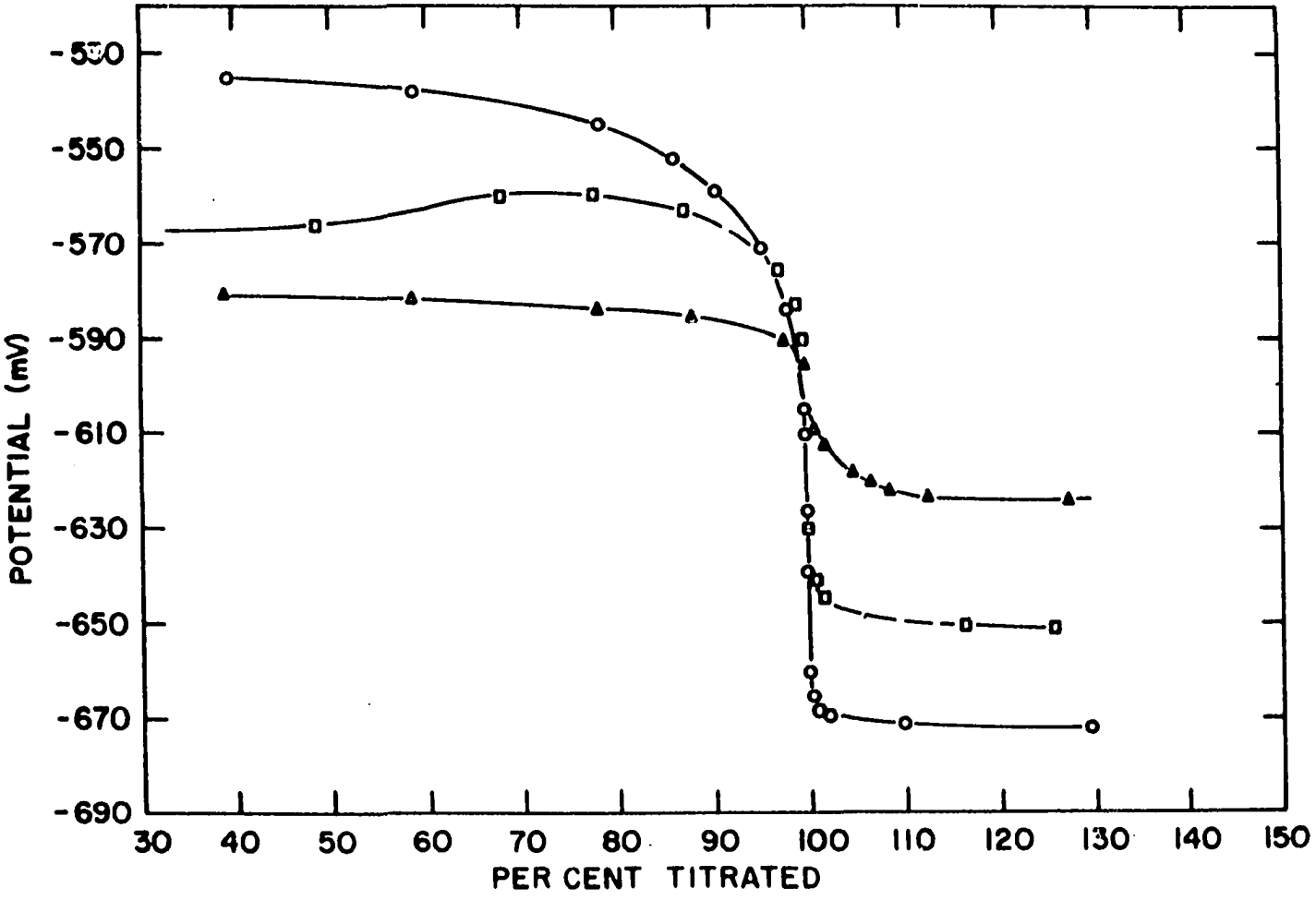


Figure 18. Calcium titrations with $Na_{0.65}WO_3$ electrode at pH 10. (O) 100 mg Ca(II) with $10^{-1}$M EDTA (□) 4.10 mg Ca(II) with $10^{-2}$M EDTA (Δ) 0.41 mg Ca(II) with $10^{-3}$M EDTA

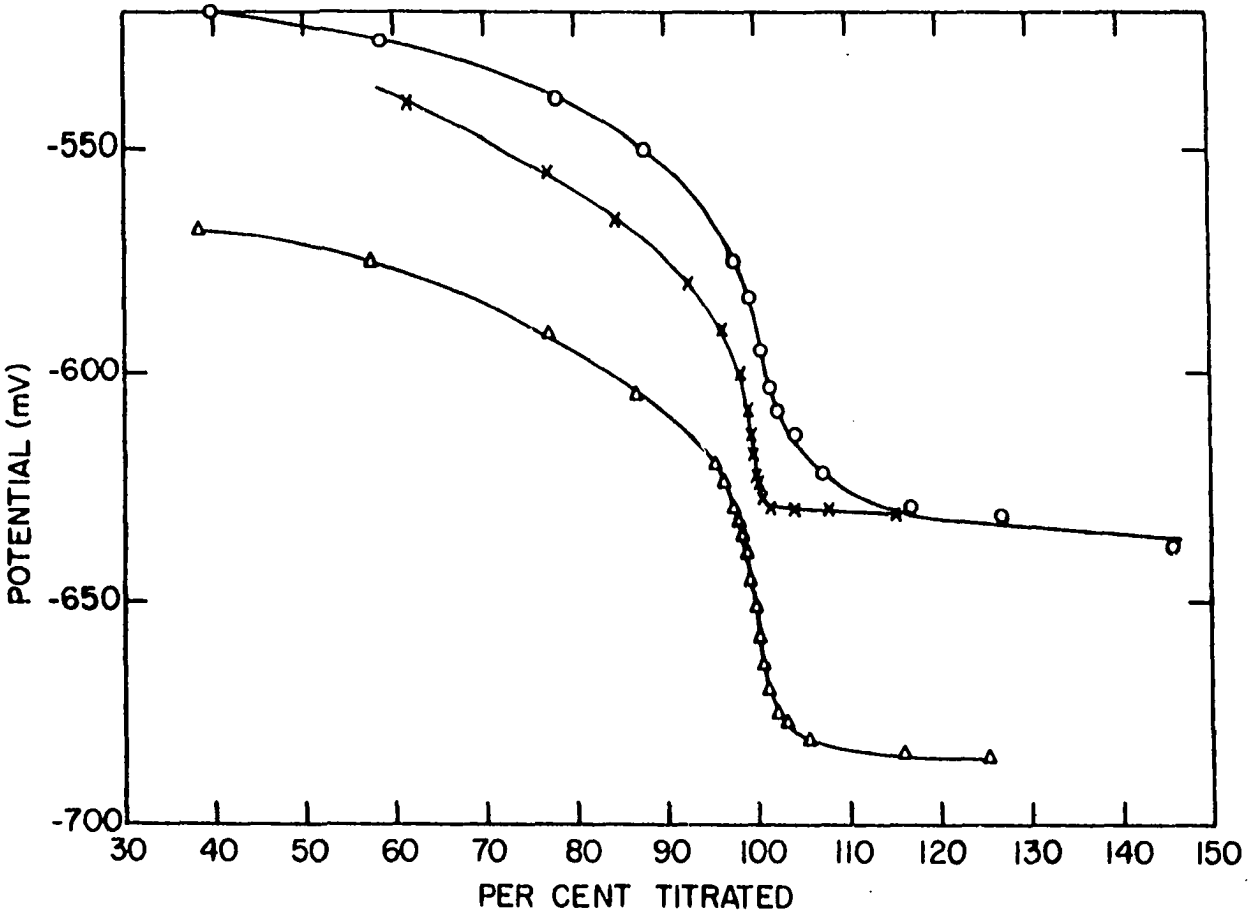


Figure 19. Magnesium titrations with $Na_{0.65}WO_3$ electrode at pH 10. (X) 62.52 mg Mg(II) with $10^{-1}$M EDTA (Δ) 2.50 mg Mg(II) with $10^{-2}$M EDTA (O) 0.25 mg Mg(II) with $10^{-3}$M EDTA

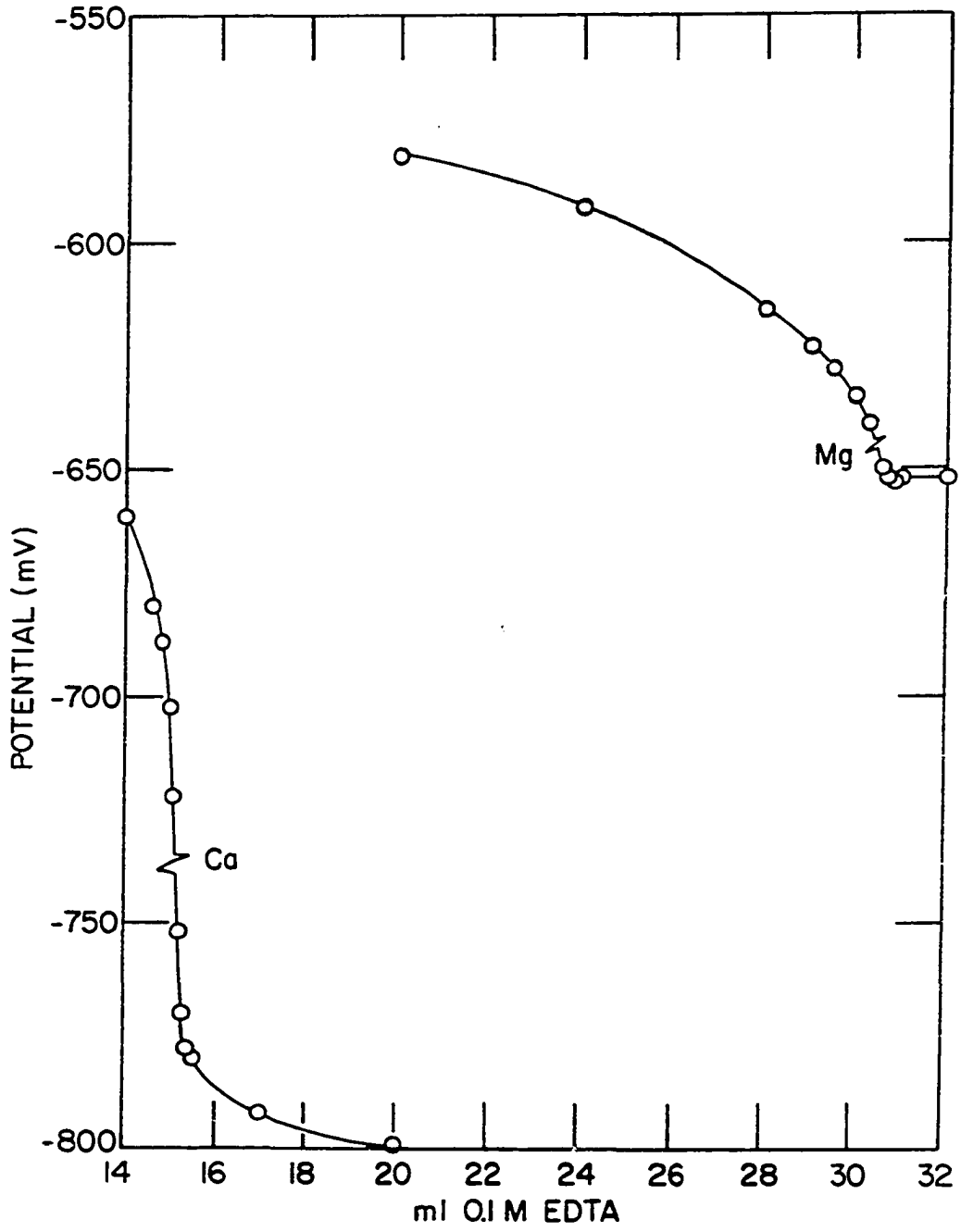


Figure 20. Simultaneous titration of calcium and magnesium

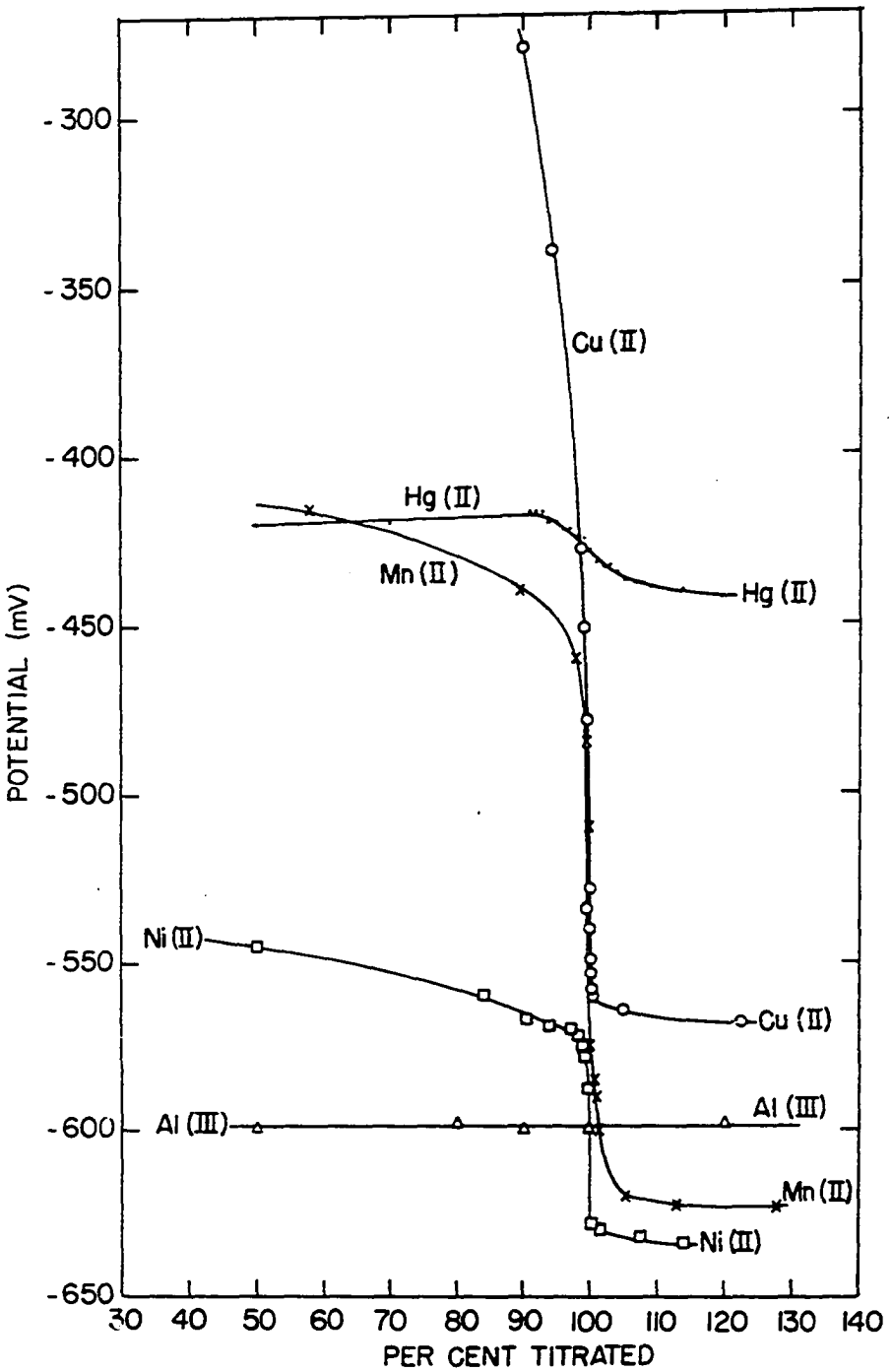


Figure 21. Titration of 1.0-2.5 millimoles of several metals with 0.1M EDTA electrode at pH 10

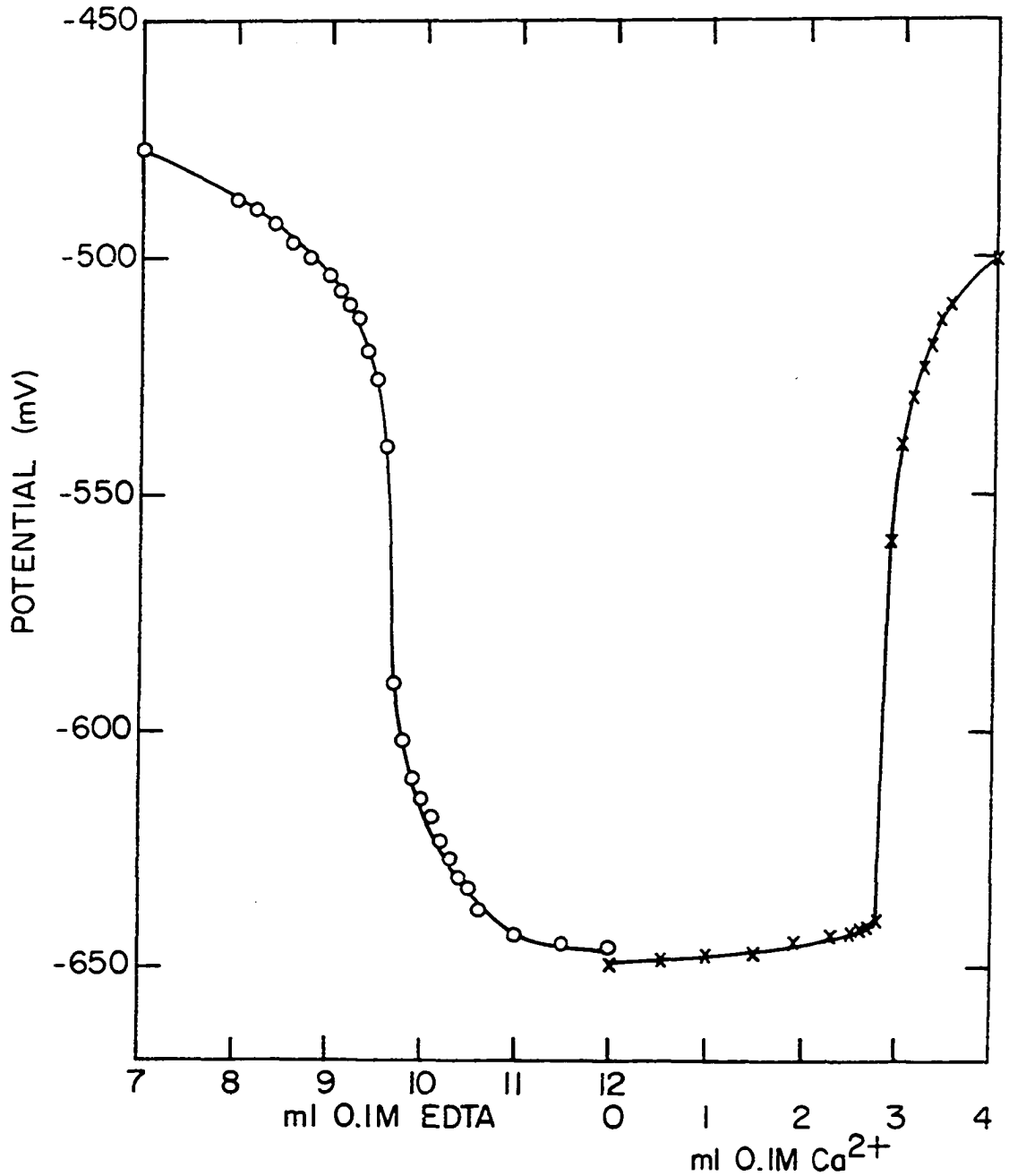


Figure 22. Direct and reverse titrations of Cd(II) in 1M $NH_4OH$

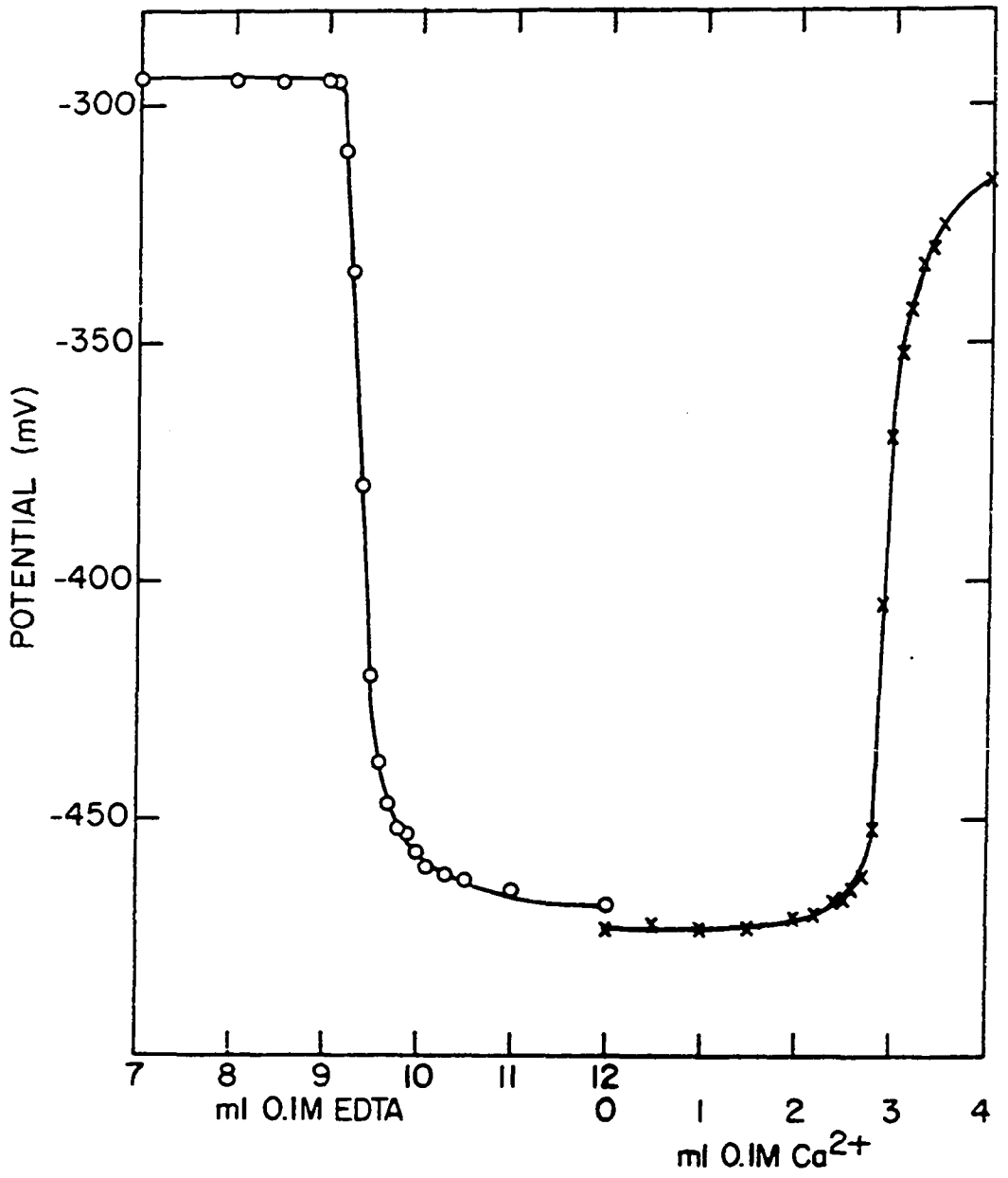


Figure 23. Direct and reverse titrations of Co(II) at pH 10

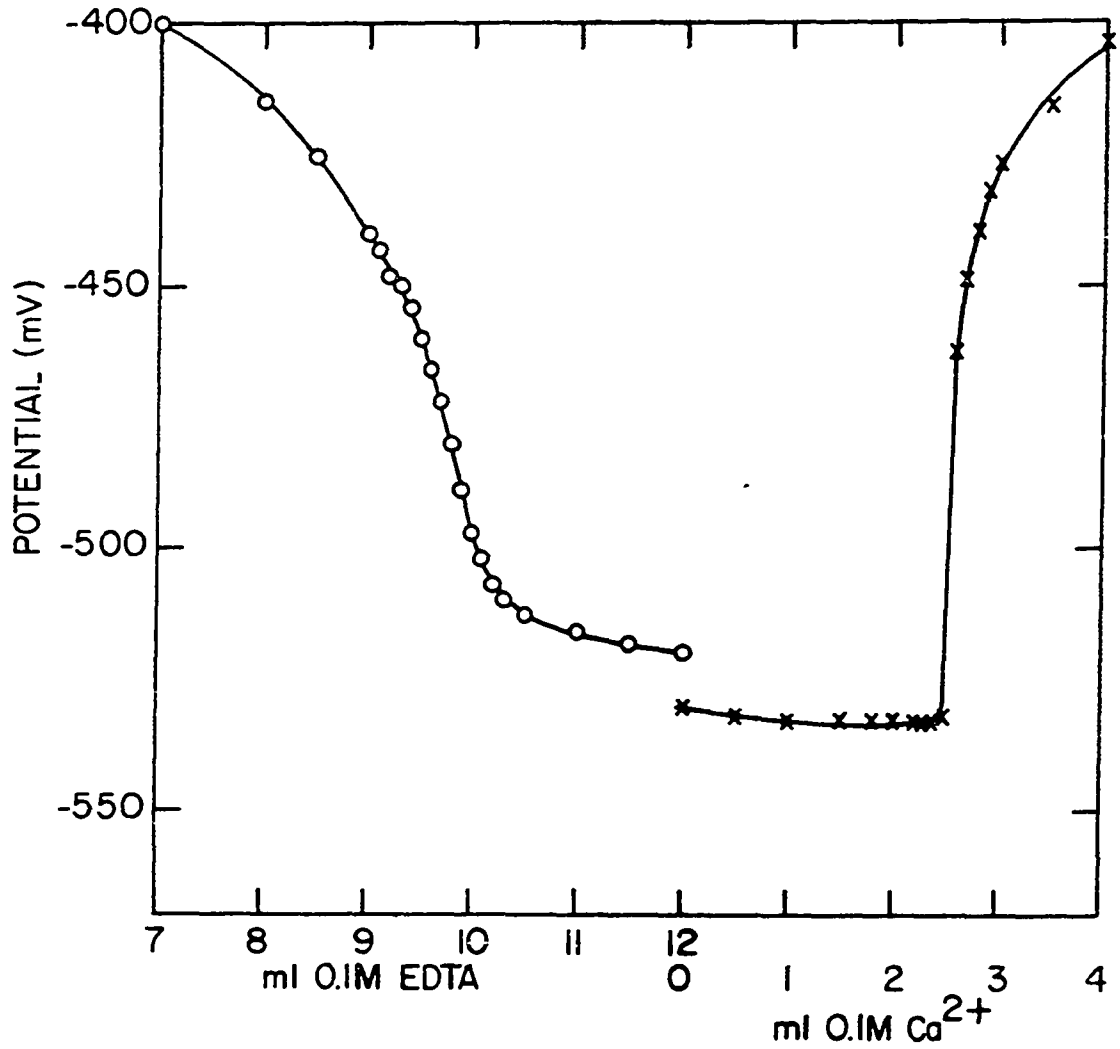


Figure 24. Direct and reverse titrations of Zn(II) at pH 10

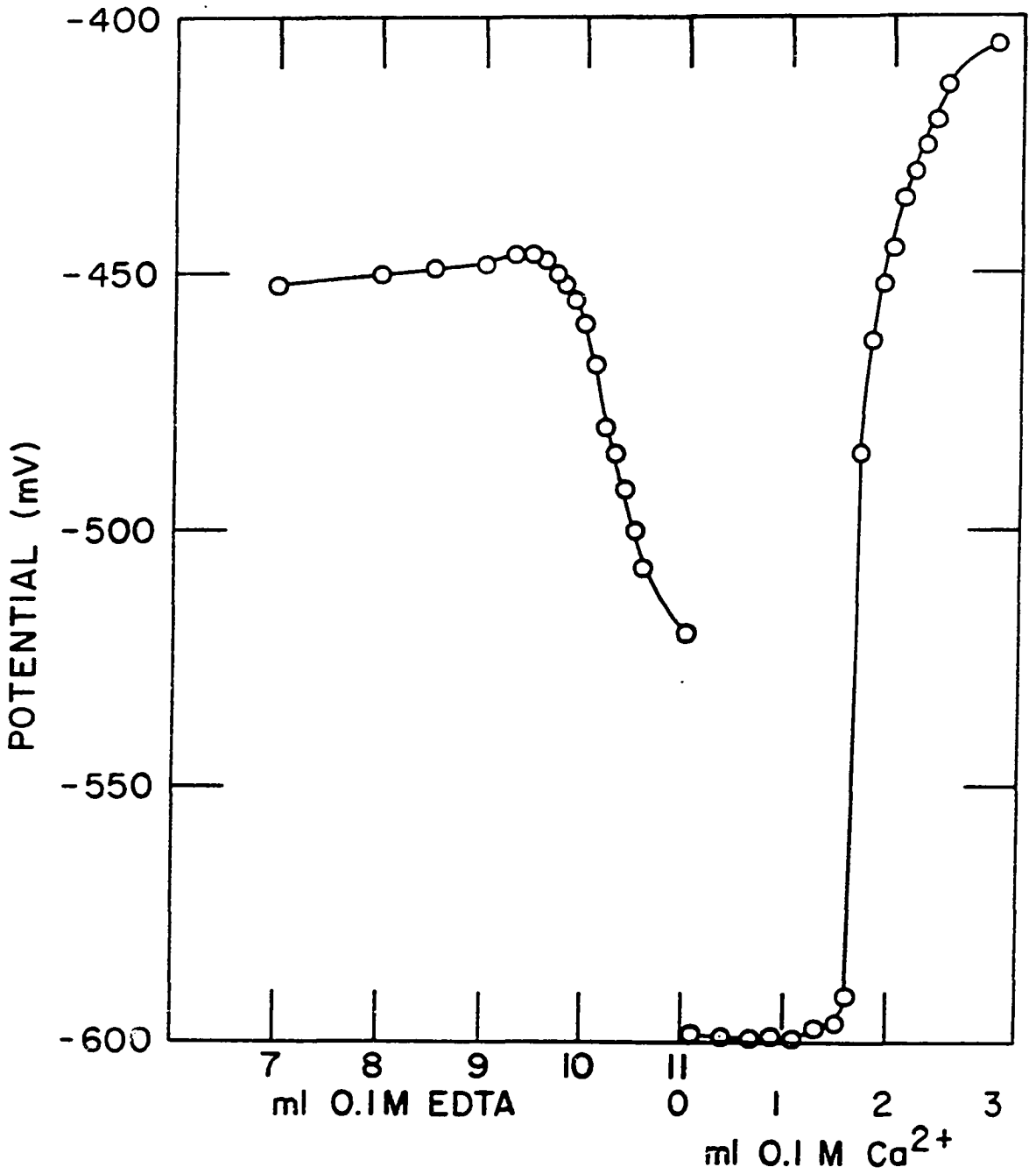


Figure 25. Direct and reverse titrations of Pb(II) in 1M $NH_4OH$

ponding direct titration. The poor end points in the direct titrations of these metals are probably a result of slow reactions between the EDTA and the $Pb(OH)_2$ precipitate or the strong $Zn(NH_3)_4^{2+}$ complex which exists before the equivalence point. Aluminum(III) is an extreme example. No potential shift was detected at the expected equivalence point in either the direct or indirect titration. The shift was observed at the first minute addition of EDTA indicating essentially no reaction between Al(III) and EDTA at pH 10.

The titration of Cu(II) was unique. An extremely large potential shift of 300-400 mV was observed at and near the equivalence point instead of the usual 50-150 mV shift experienced with the other metals. Subsequent investigations showed the potentiometric response of the $Na_{0.65}WO_3$ and other cubic sodium tungsten bronzes to Cu(II) to be extremely large (55-125 mV/decade) in ammoniacal solution (Figure 26). The Cu(II) response extended down to a formal concentration of $10^{-6}$M or lower suggesting that trace copper may act as a redox indicator in the titration of the other metals. A direct correlation was noted between the copper response of a given electrode and the size of the potential break in a calcium titration (Figure 27). Low x value $Na_xWO_3$ electrodes which exhibited the largest copper response (125 mV/decade) gave potential breaks of approximately 160-170 mV while higher x value electrodes with lower copper response (55-75 mV/decade) gave potential breaks of 130-135 mV in identical calcium titrations.

Further evidence that copper may be acting as a redox indicator in the chelometric titrations of other metals was demonstrated in the significantly larger potential breaks obtained when Cu(II) was added to the

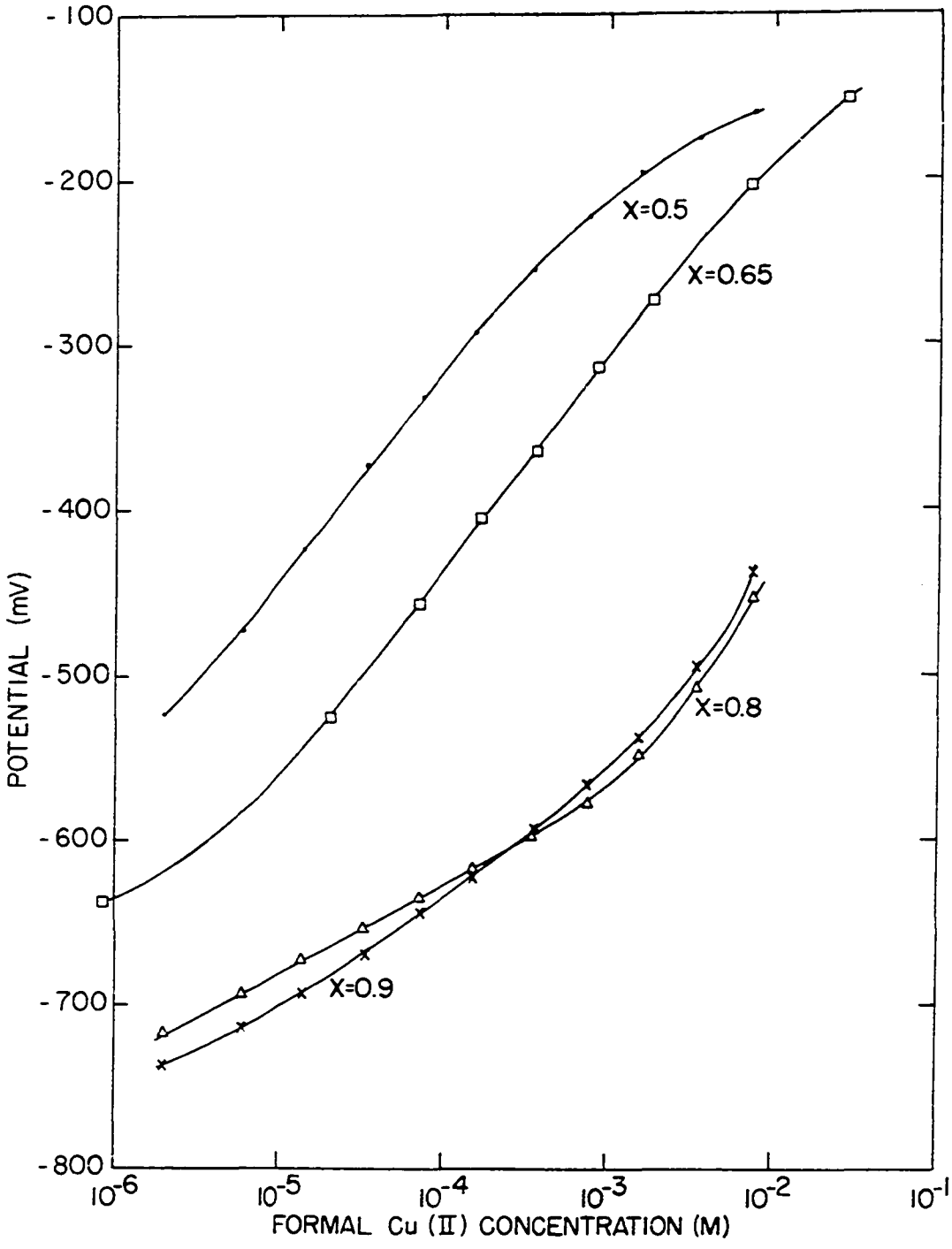


Figure 26. Potentiometric response of $Na_xWO_3$ electrodes to Cu(II) in 1M $NH_4OH$ as a function of x value

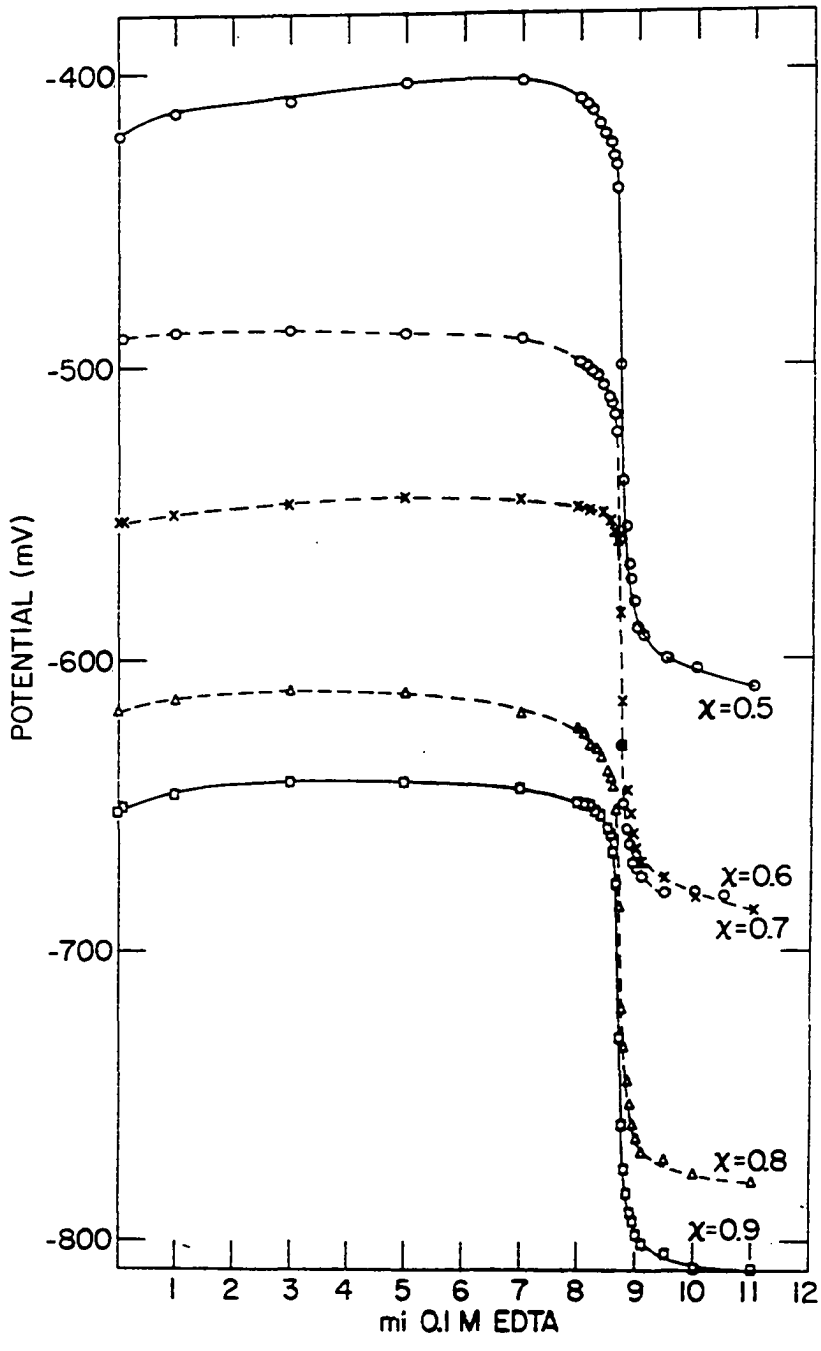


Figure 27. Titration of calcium in 1M $NH_4OH$ as a function of $Na_xWO_3$ electrode x value

titration mixture. Figure 28 presents curves for the titration of 1 millimole of $Ca^{2+}$ with 0.1M EDTA and 0.3 millimole of EDTA with 0.1M $Ca^{2+}$ at zero and 5 X $10^{-5}$M added copper concentrations. The additional copper was found to nearly double the potential break at the end point in such titrations.

If trace copper is acting as a redox indicator in these titrations, it is doing so at extremely low concentrations. A colorimetric method employing bathocuproine (85) was used to analyze the deionized water and the $CaCl_2$, $NH_4OH$ and EDTA reagents for copper. The EDTA was first wet ashed with nitric and perchloric acids. Results of these analyses gave an upper limit of 1 to 5 X $10^{-7}$M for the copper concentration in the titration solution.

As in the case of the oxygen response, the cubic sodium tungsten bronzes were found to perform significantly better than other alkali metal tungsten bronzes in chelometric titrations. Figure 29 illustrates potentiometric titrations of 1 millimole of $Ca^{2+}$ with 0.1M EDTA in 1M $NH_4OH$ using hexagonal Rb, K, and Cs, cubic Li, and tetragonal K tungsten bronze electrodes. These electrodes were also found to have a much lower response to Cu(II) (30-40 mV/decade) than the cubic sodium tungsten bronzes (Figure 30), consistent with the previously discussed correlation between the titration potential break and the Cu(II) response.

The unique properties of cubic $Na_xWO_3$ are further emphasized when compared to some common metals as indicating electrodes. Potentiometric titrations of calcium with EDTA using Pt, Cu and W as the indicating electrodes are illustrated in Figure 31. Potential breaks using these metals were much smaller, 10-30 mV, and generally much less sharp than the

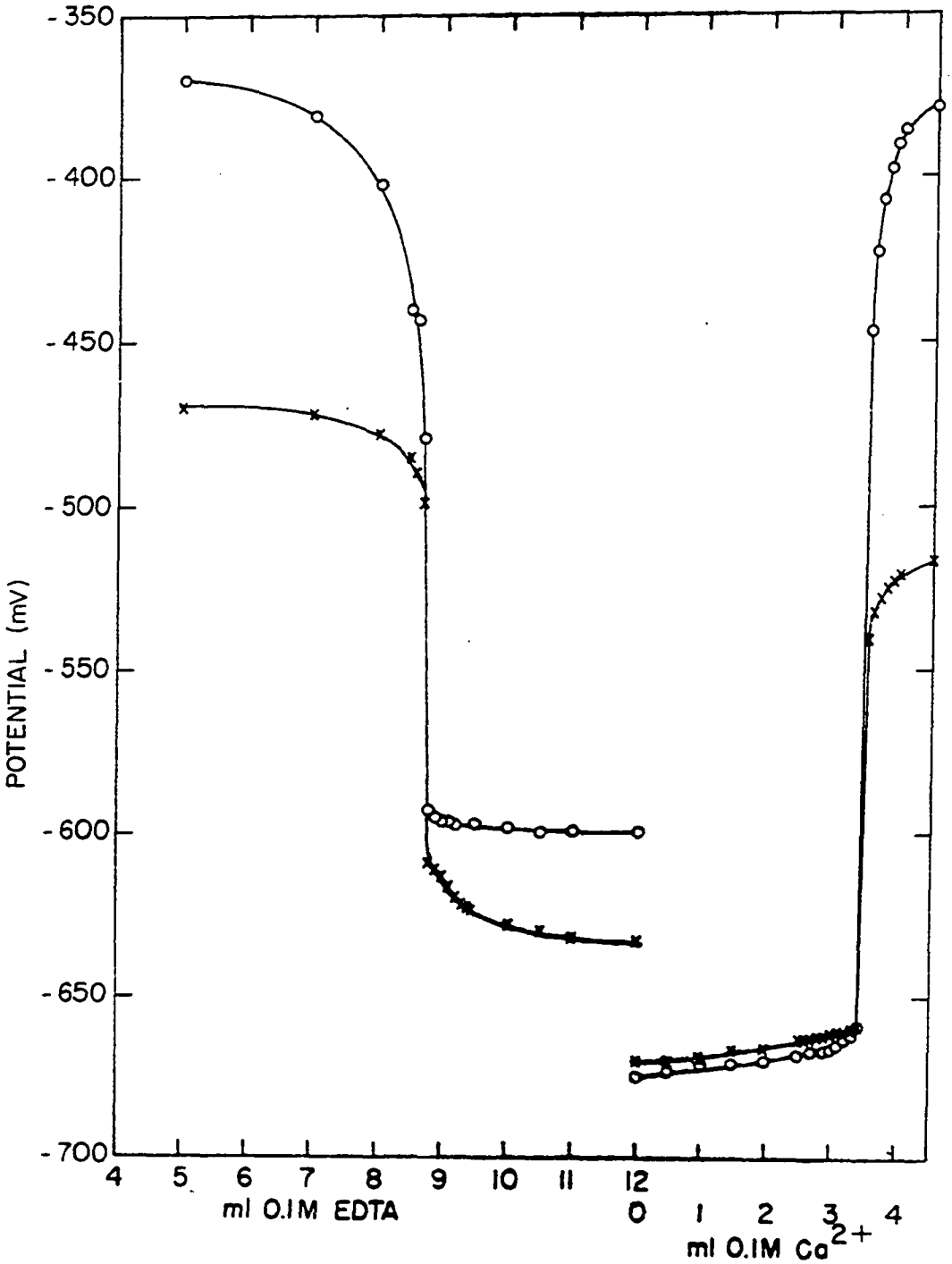


Figure 28. Titration of 1.0 millimole $Ca^{2+}$ with 0.1M EDTA and 0.3 millimole EDTA with 0.1M $Ca^{2+}$ at zero (x) and 5 X $10^{-5}$M (o) added Cu(II)

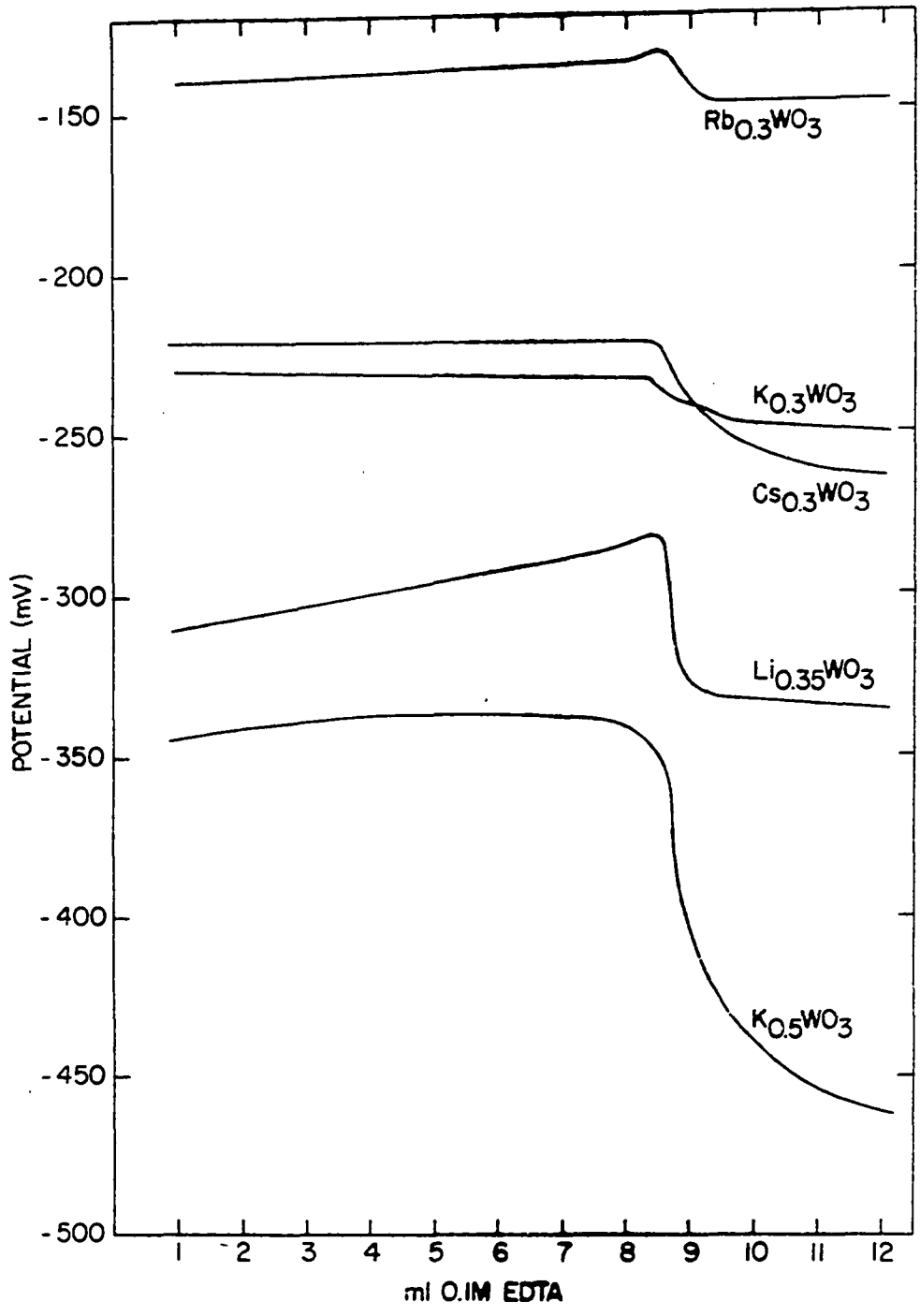


Figure 29. Titrations of 1.0 millimole $Ca^{2+}$ in 1M $NH_4OH$ using other alkali metal tungsten bronze electrodes

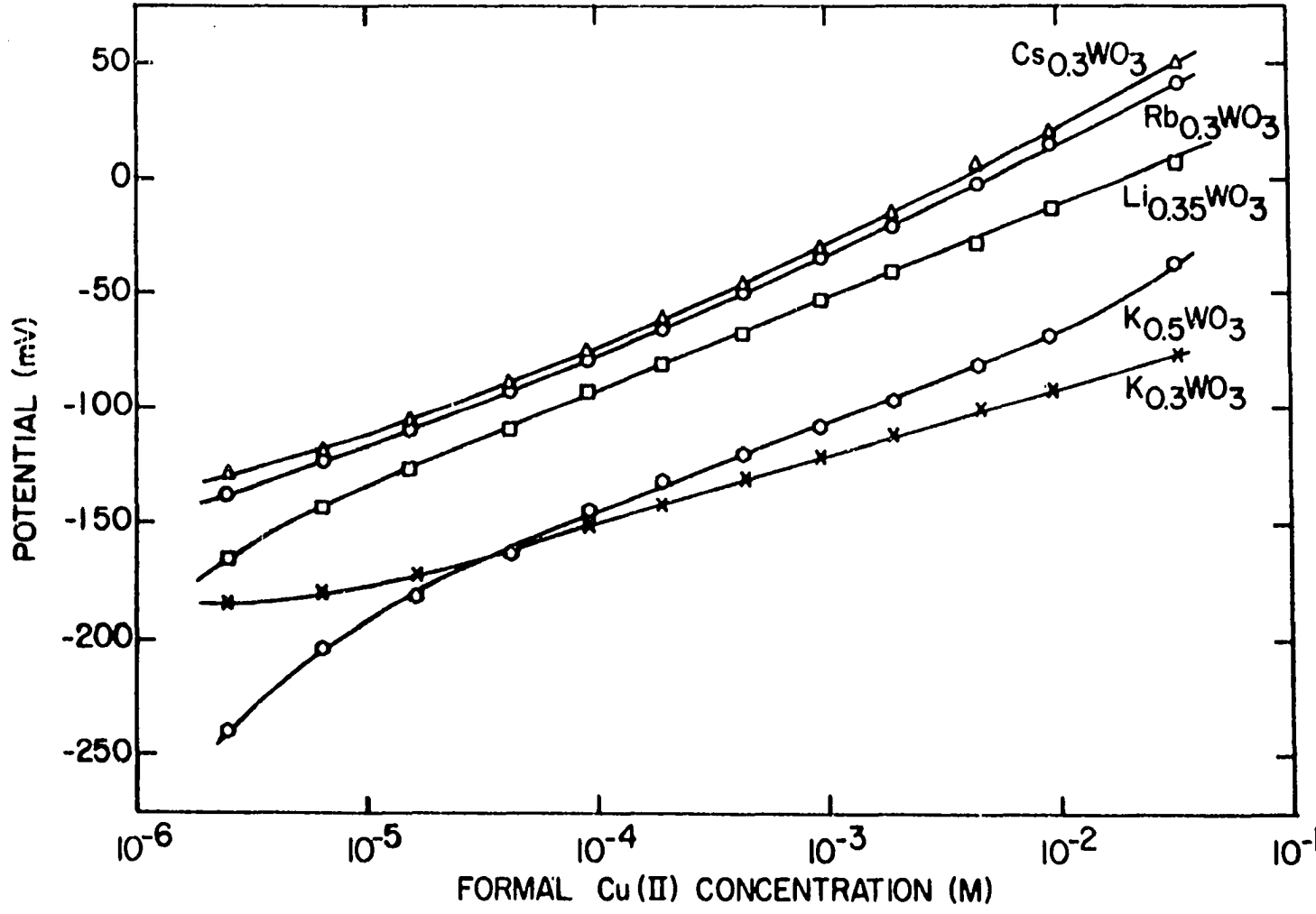


Figure 30. Potentiometric response of several alkali metal tungsten bronze electrodes to Cu(II) in 1M $NH_4OH$

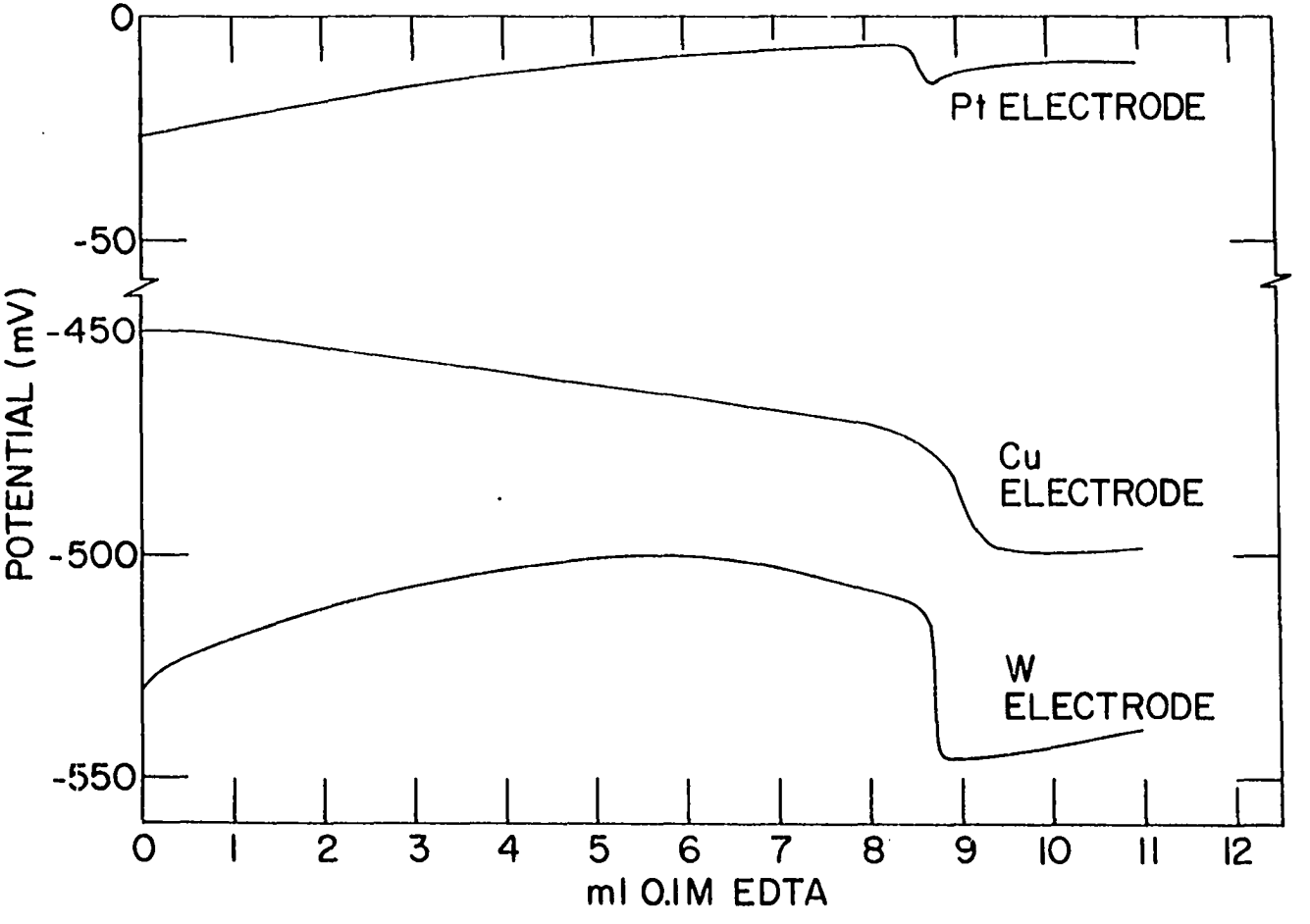


Figure 31. Titration of 1.0 millimole $Ca^{2+}$ in 1M $NH_4OH$ using Pt, Cu, and W electrodes

breaks obtained at the same concentration of reagents with $Na_xWO_3$.

In acid solution the response of the $Na_xWO_3$ electrode was typical of a highly conducting inert electrode. The titration of approximately 2.5 millimoles of Fe(III) with 0.1M EDTA at pH 2-3 is presented in Figure 32. The large potential change (at positive potential) reflects the change in the concentration ratio of the Fe(III)/Fe(II) redox couple and is much like that obtained with a platinum-indicating electrode (78).

Quantitative results from a number of titrations described in this section are presented in Table 6. All titrations were performed with an annealed, flat-surface cubic $Na_{0.65}WO_3$ indicating electrode and a SCE reference electrode. End points were determined by the second derivative method. Excellent agreement is seen between quantities taken and the measured value for even the most dilute titrations where 0.01 millimole of metal was titrated with $10^{-3}$M EDTA. Excellent results were also obtained for the simultaneous titration of Ca and Mg in a mixture and for Pb(II) by reverse titration.

## Mechanism of Response

The extremely large oxygen response (120 mV/decade) made it appear doubtful that simple oxygen redox reactions played a major role in the response. The reduction of $O_2$ to $OH^-$ or $H_2O$ requires four electrons per molecule predicting a 15 mV/decade response slope by the Nernst Equation while reactions yielding peroxide require two electrons predicting a 30 mV/decade slope. The poisoning of the oxygen response for low x value $Na_xWO_3$ electrodes in LiOH and the potential shifts experienced in EDTA titrations of nonreducible cations without any apparent redox

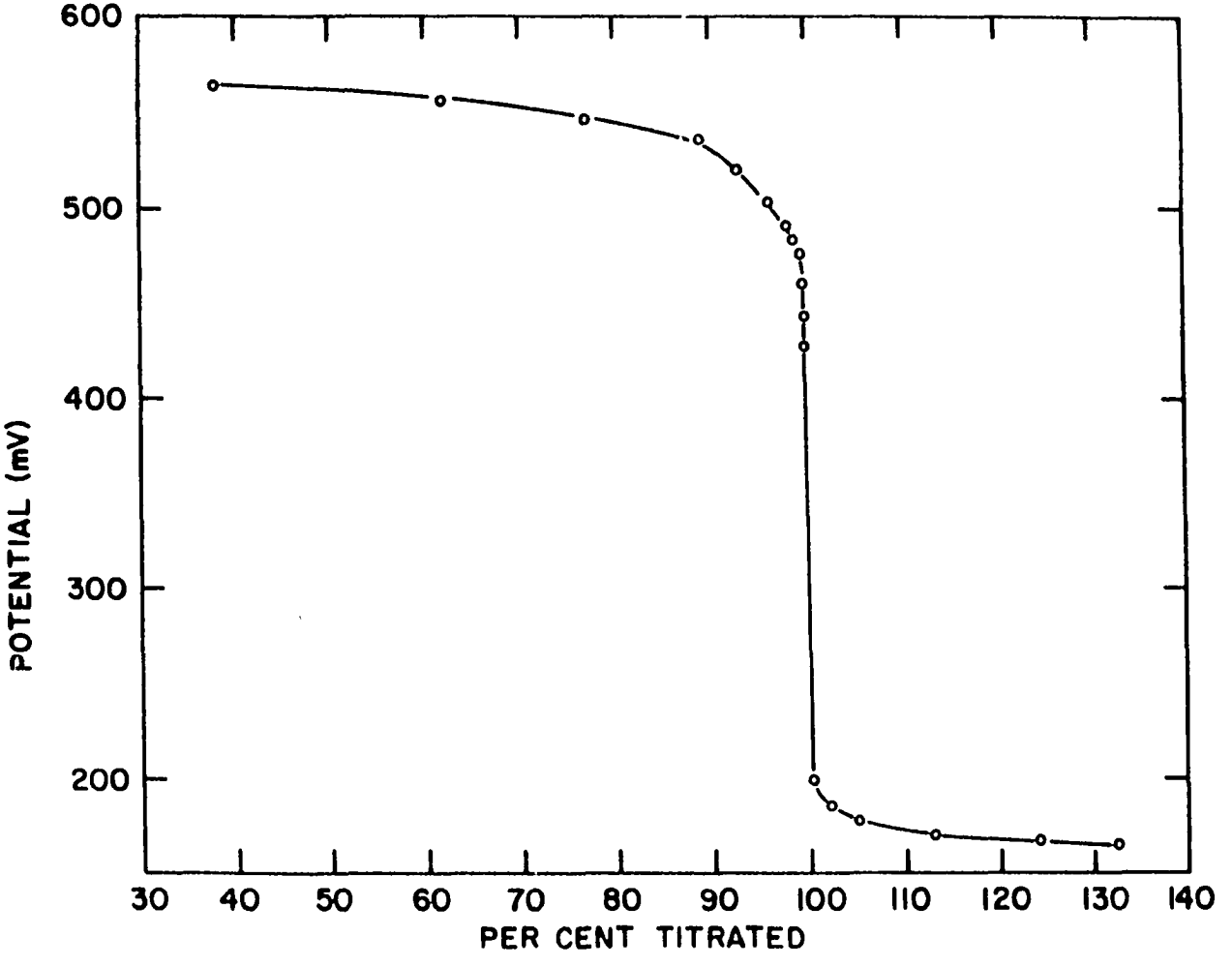


Figure 32. Titration of Fe(III) with 0.1M EDTA at pH 2-3 using the $Na_{0.65}WO_3$ electrode

Table 6. Results of metal-EDTA titrations

| Metal detected | Log $K_m$ (78) | pH | Approximate titrant (EDTA) concentration, M | Weight of metal titrated (mg) Taken | Found |
|---|---|---|---|---|---|
| Ca(II) | 10.7 | 10 | $10^{-1}$ | 100.4 | 100.4 |
| | | | $10^{-2}$ | 4.10 | 4.10 |
| | | | $10^{-3}$ | 0.41 | 0.41 |
| Mg(II) | 8.7 | 10 | $10^{-1}$ | 62.52 | 62.56 |
| | | | $10^{-2}$ | 2.50 | 2.50 |
| | | | $10^{-3}$ | 0.25 | 0.25 |
| Zn(II) | 16.7 | 10 | $10^{-1}$ | 162.3 | 161.1 |
| | | | $10^{-2}$ | 6.49 | 6.56 |
| Ca(II), Mg(II) | | 13,10 | $10^{-1}$ | 61.50, 37.53 | 61.39, 37.38 |
| Cu(II) | 18.8 | 10 | $10^{-1}$ | 146.9 | 146.5 |
| Pb(II) (back titration) | 18.0 | 10 | $10^{-1}$ (EDTA) $10^{-1}$ ($Ca^{2+}$) | 202 | 200 |
| Fe(III) | 25.1 | 3 | $10^{-1}$ | 143.1 | 143.3 |

indicator were also difficult to explain in terms of conventional oxidation reduction reactions.

Very early in the course of this investigation the correlation was made between the unique response of the $Na_xWO_3$ electrode and the presence of the hydroxide ion. The oxygen response deteriorated and chelometric titrations of nonreducible metals became unsuccessful at lower hydroxide concentration.

Consequently a mechanism was proposed in which the adsorption and desorption of hydroxide ions at the $Na_xWO_3$ surface played an important role in establishing the potential of the electrode. The pH response of the $Na_xWO_3$ electrode (Figure 33) could be explained on this basis where adsorbed hydroxide ions form a charged double layer at the electrode surface and establish the negative potential. Numerous parallel examples may be cited among the ion-selective potentiometric electrodes developed in recent years. These include the glass electrodes for measuring pH and alkali and alkaline earth metals, the solid state rare earth fluorine membrane electrodes for $F^-$, and mixed sulfide membrane electrodes for $S^{2-}$ and various cations, and the liquid and ion exchange resin membrane electrodes for anions and cations. The potentiometric response of these are all considered to arise from the specific adsorption of charged species at the electrode surface (86,87).

The oxygen response could be explained as follows: The strong adsorption of hydroxide ions in de-oxygenated 0.1M KOH establishes the large negative potential (-1200 mV or less). When $O_2$ molecules are introduced, they also are strongly adsorbed at the bronze surface, displacing the negatively charged $OH^-$ ions and resulting in a positive

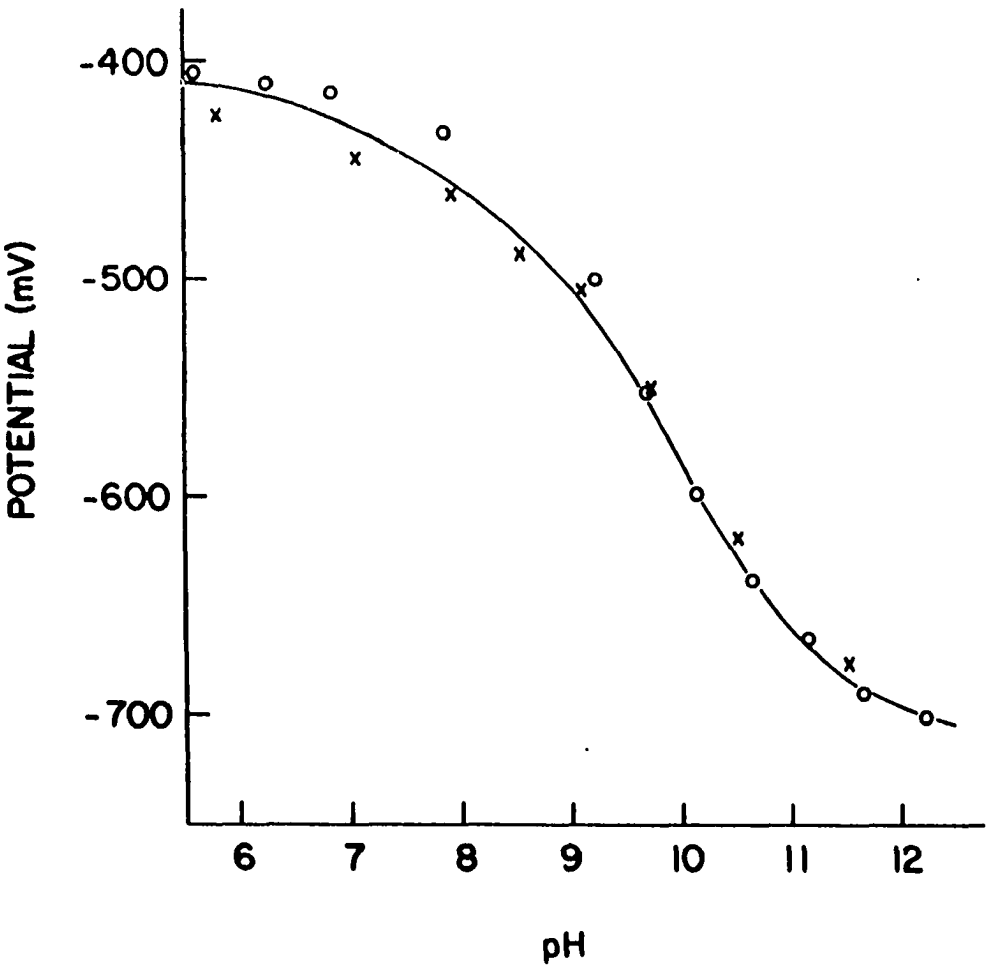


Figure 33. pH response of $Na_{0.65}WO_3$ electrode in air-saturated solution
(o) Increasing pH
(x) Decreasing pH

shift in electrode potential. The success of EDTA titrations in basic solution and the action of $Li^+$ on the oxygen response could similarly be explained if the positive ions act in a manner similar to the oxygen molecules in displacing adsorbed $OH^-$.

Subsequent observations and considerations however, place serious doubt on this adsorption mechanism. The potentiometric response to a number of species was determined in 1M $NH_4OH$ and appeared to be limited to only those species which are easily reduced in aqueous solution (Figure 34). Response slopes for Cu(II), Ag(I) and $Fe(CN)_6^{3-}$ were found to be unpredictably large (80-300 mV/decade) paralleling the response to dissolved oxygen in 0.1M KOH. Response to difficultly reducible metals, Cd(II), Zn(II), Ni(II), Ca(II), was extremely small and the success of chelometric titrations of these species could no longer be explained on the basis of displacement of adsorbed $OH^-$ ions as the cause of the substantial shift in potential. Further evidence that a redox reaction takes place at the $Na_xWO_3$ electrode in basic solution was seen during oxygen measurements in quiescent solutions when the electrode potential drifted in a negative direction indicating the depletion of dissolved oxygen in the vicinity of the electrode. This observation was consistent with those of other investigators (12,13) who demonstrated the slow dissolution of $Na_xWO_3$ in basic solution in the presence of oxygen and the rapid dissolution in the presence of very strong oxidizing agents such as sodium peroxide. The spontaneous plating of metallic silver from ammoniacal and 0.1M KOH-1mM EDTA solutions containing Ag(I) provided additional evidence of the ability of $Na_xWO_3$ to act as a reducing agent in basic solution.

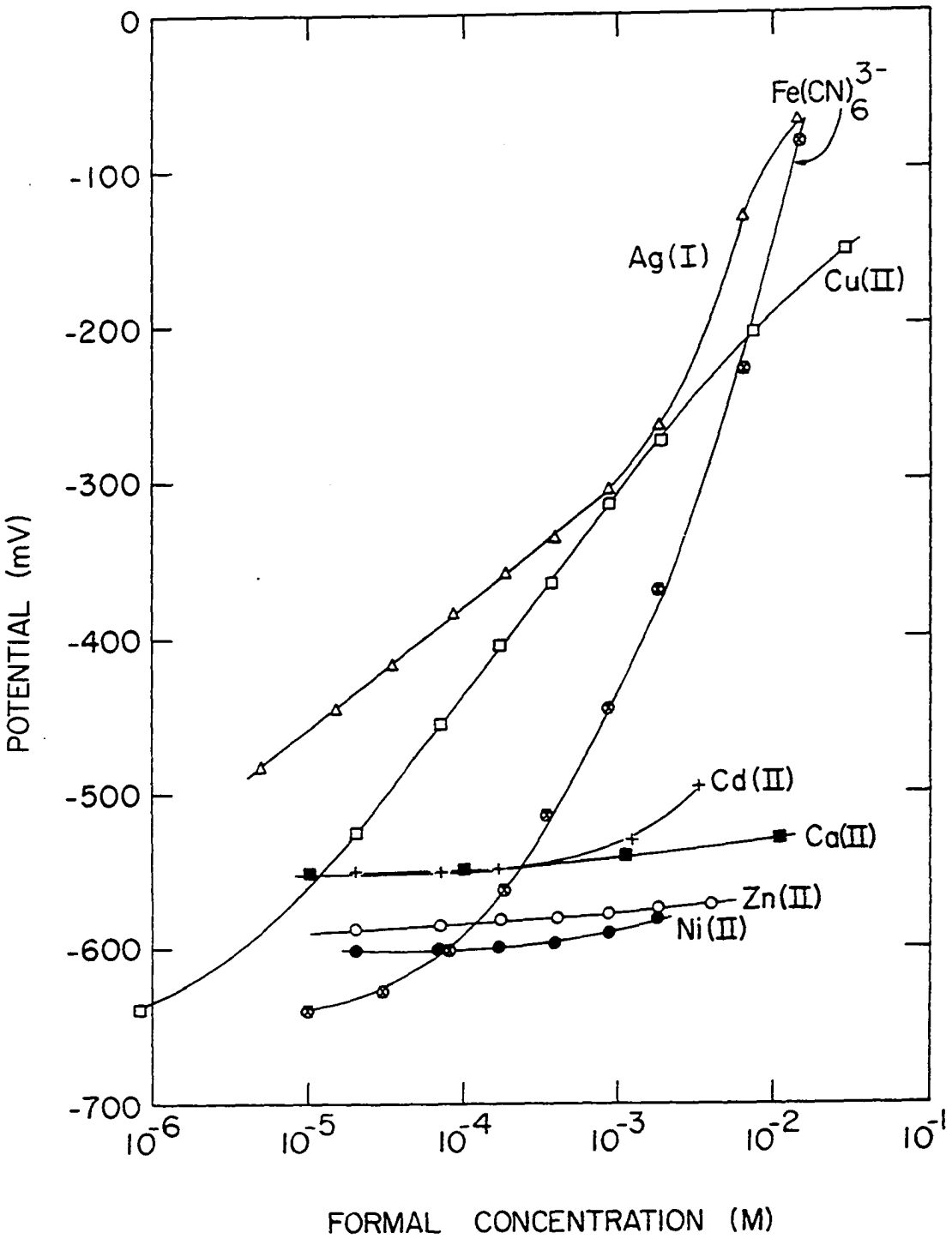


Figure 34. Potentiometric response of the $Na_{0.65}WO_3$ electrode to several species in 1M $NH_4OH$

Voltammetric measurements involving cubic $Na_xWO_3$ electrodes in 0.1M KOH-1mM EDTA demonstrated that both the reduction of dissolved oxygen and the oxidation of $Na_xWO_3$ were occurring in the same general potential range of the potentiometric oxygen response (-600 to -1200 mV *vs.* SCE). Figures 35 and 36 illustrate current *vs.* potential curves for $Na_xWO_3$ electrodes having x values of 0.65 and 0.79 in KOH solutions saturated with nitrogen, the 1%, 3.3% and 10% oxygen gas mixtures and pure oxygen.

In deoxygenated solution the voltammetric curves exhibited the expected cathodic wave for the reduction of $H_2O$ to $H_2$ at approximately -1.5 V *vs.* SCE much like that observed with platinum electrodes (81). Also observed however, was an anodic wave beginning at -1.0 to -1.2 V *vs.* SCE (the open circuit potential) and becoming extremely large at potentials more positive than -0.5 to -0.6 V *vs.* SCE. The anodic wave was attributed to the oxidation of the $Na_xWO_3$ electrode to $WO_4^{2-}$ (tungstate) for two reasons; the absence of other oxidizable species and the observation that dissolved oxygen (which establishes potentials between -0.6 and -1.2 V at the $Na_xWO_3$ electrode) is known to cause this reaction to take place (12,13). When oxygen was introduced into the 0.1M KOH-1mM EDTA solution, a cathodic wave representing the reduction of $O_2$ to $H_2O$ was observed in the same general potential range (-0.6 to -1.2 V) where the $Na_xWO_3$ oxidation takes place.

The potentiometric response of the $Na_xWO_3$ electrode to dissolved oxygen in basic solution must therefore be considered to arise from a mixed potential established by the spontaneous oxidation of the $Na_xWO_3$ electrode by dissolved oxygen.

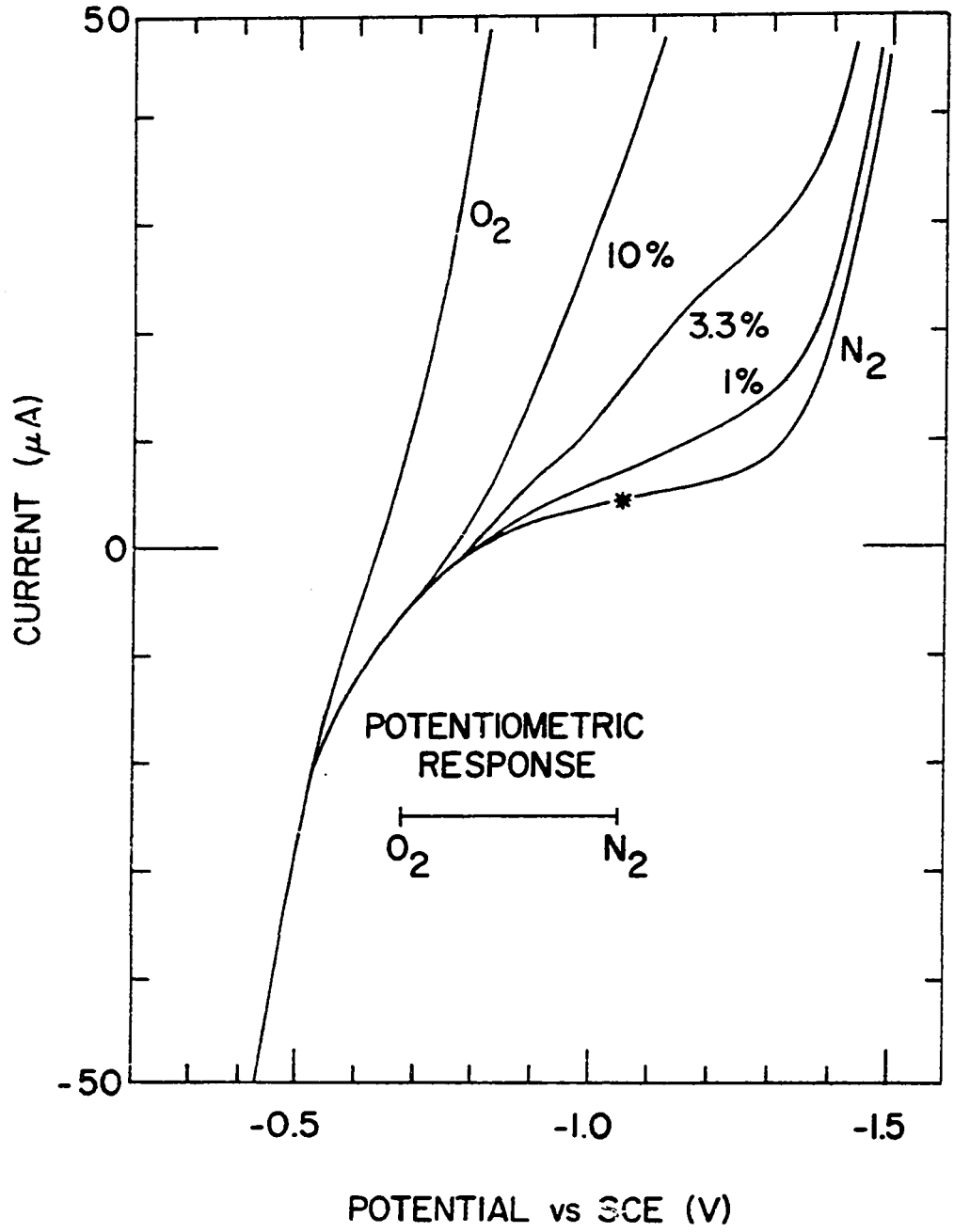


Figure 35. Voltammetric curves of $Na_{0.65}WO_3$ electrode in 0.1M KOH-1mM EDTA as a function of oxygen concentration. (*) Open circuit potential in $N_2$-saturated solution

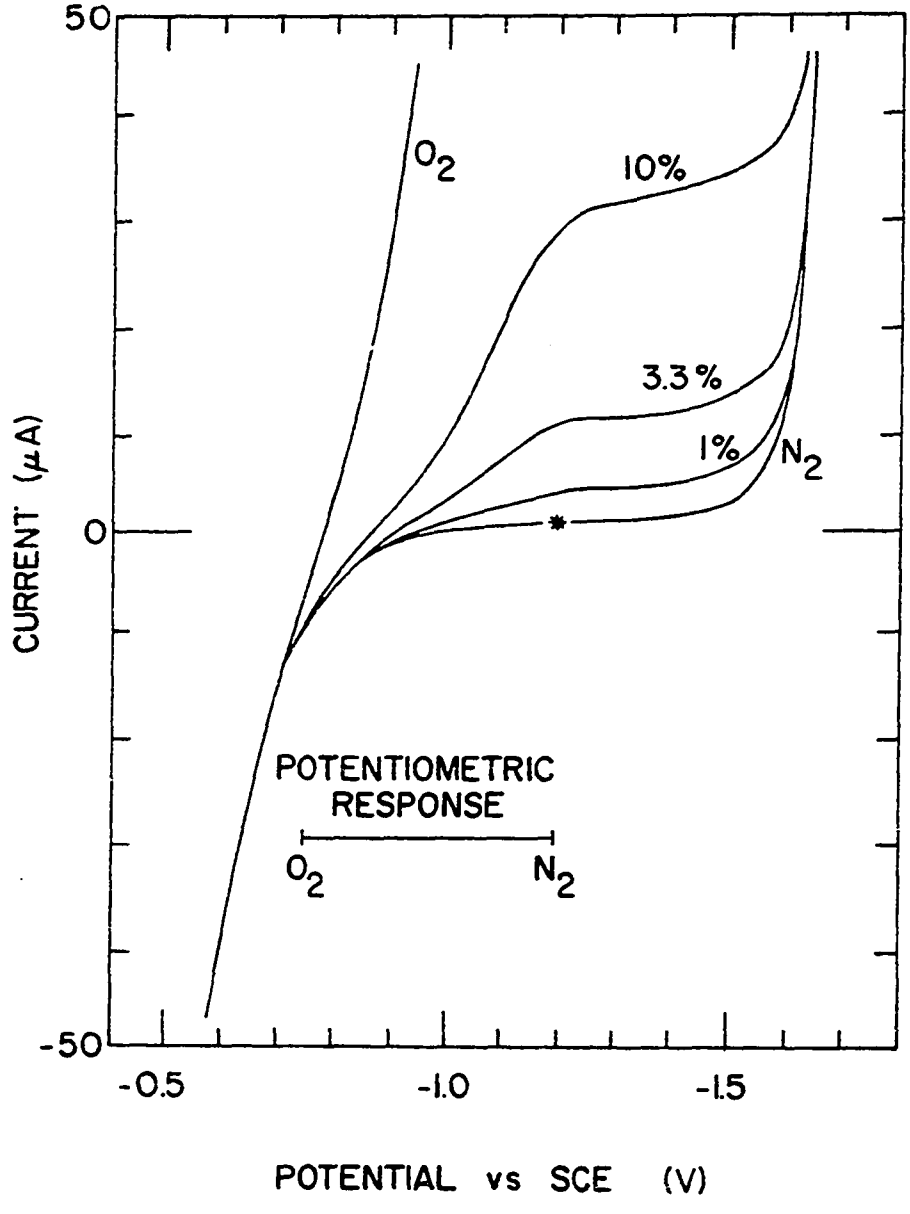


Figure 36. Voltammetric curves of $Na_{0.79}WO_3$ electrode in 0.1M KOH-1mM EDTA as a function of oxygen concentration. (*) Open circuit potential in $N_2$-saturated solution

Mixed potential phenomena have been discussed by a number of authors (88-93) and are considered to arise when a nonequilibrium state exists involving two or more different electrode processes. Such a state is connected with a spontaneous change at the electrode surface where simultaneous oxidation and reduction are occurring. The classic example is the reaction $Zn + 2H^+ \text{-----} > Zn^{2+} + H_2$ at a zinc electrode in acid solution which was first studied in terms of mixed potentials by Wagner and Traud (88).

The sum of the partial currents, $i_{cathodic} - i_{anodic}$, of such a reaction must be equal to zero and since the rate of each partial reaction is dependent on the electrode potential, the mixed potential satisfying the condition of zero net current is established. If the voltammetric polarization curves of cathodic and anodic processes can be individually determined the value of the mixed potential can be estimated schematically as shown in Figure 37. Represented in this figure are the anodic wave for the dissolution or oxidation of the $Na_{0.65}WO_3$ electrode in 0.1M KOH-1mM EDTA and a series of cathodic waves for the reduction of $O_2$ at different dissolved oxygen concentrations ($C_1 < C_2 < C_3 < C_4$). The anodic $Na_xWO_3$ wave was determined directly in nitrogen-saturated solution while the cathodic oxygen waves were estimated by subtracting the anodic wave from the corresponding total voltammetric waves in Figure 35. The condition of equal and opposite anodic and cathodic currents (zero net electrode current) to establish the mixed potential is represented by the vertical dashed lines for the various dissolved oxygen concentrations. The shift of the mixed potential toward positive potentials with increasing dissolved oxygen concentration is clearly illustrated.

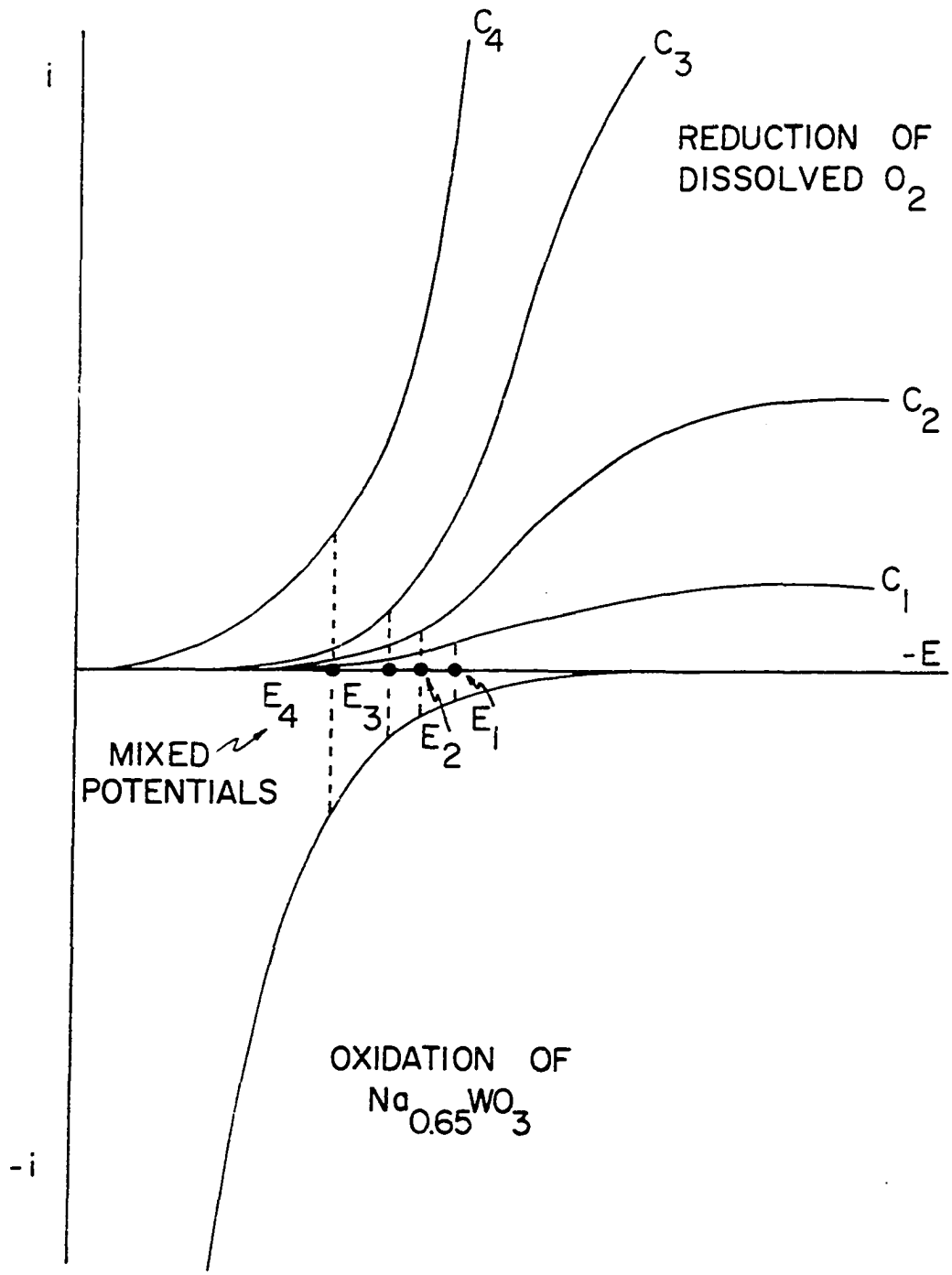


Figure 37. Schematic diagram illustrating the establishment of the mixed potential

The potentiometric response of the $Na_xWO_3$ electrode to Cu(II) and other oxidizing agents in ammoniacal solution can be similarly explained. The only prerequisite for such response would be that the cathodic wave for the oxidizing agent exist over the same potential range where the $Na_xWO_3$ anodic wave occurs. Figure 38 presents voltammetric curves for various Cu(II) concentrations in 1M $NH_4OH$. The similarity between these and the oxygen curves in 0.1M KOH (Figures 34 and 35) is apparent.

The extremely large potentiometric response slopes observed in the oxygen, Cu(II), and $Fe(CN)_6^{3-}$ measurements are not totally unexpected. Herbelin et al. (93) encountered similarly large potentiometric response slopes (125-250 mV/decade) for Ce(IV) and Fe(II) when working in a mixed-potential system involving the Ce(IV)/Ce(III) and Fe(III)/Fe(II) redox couples.

Response slopes as high as 250 to 300 mV/decade could in fact be anticipated for the $Na_xWO_3$ electrode by the mixed-potential mechanism under certain conditions. Figure 39 is a logarithmic plot of the anodic wave for the oxidation of the $Na_{0.65}WO_3$ electrode in 0.1M KOH-1mM EDTA showing a ten-fold increase in anodic current for a 285 mV shift in potential. If the cathodic wave for the reduction of an oxidizing agent were completely diffusion limited in this general potential region the cathodic current would be directly proportional to the concentration and independent of the electrode potential. A ten-fold increase in the oxidant concentration would result in a similar ten-fold increase in the cathodic partial current. To balance this increase in cathodic current a ten-fold increase in the anodic partial current would be required which, in turn, would result in a 285 mV shift in the mixed potential of the $Na_xWO_3$

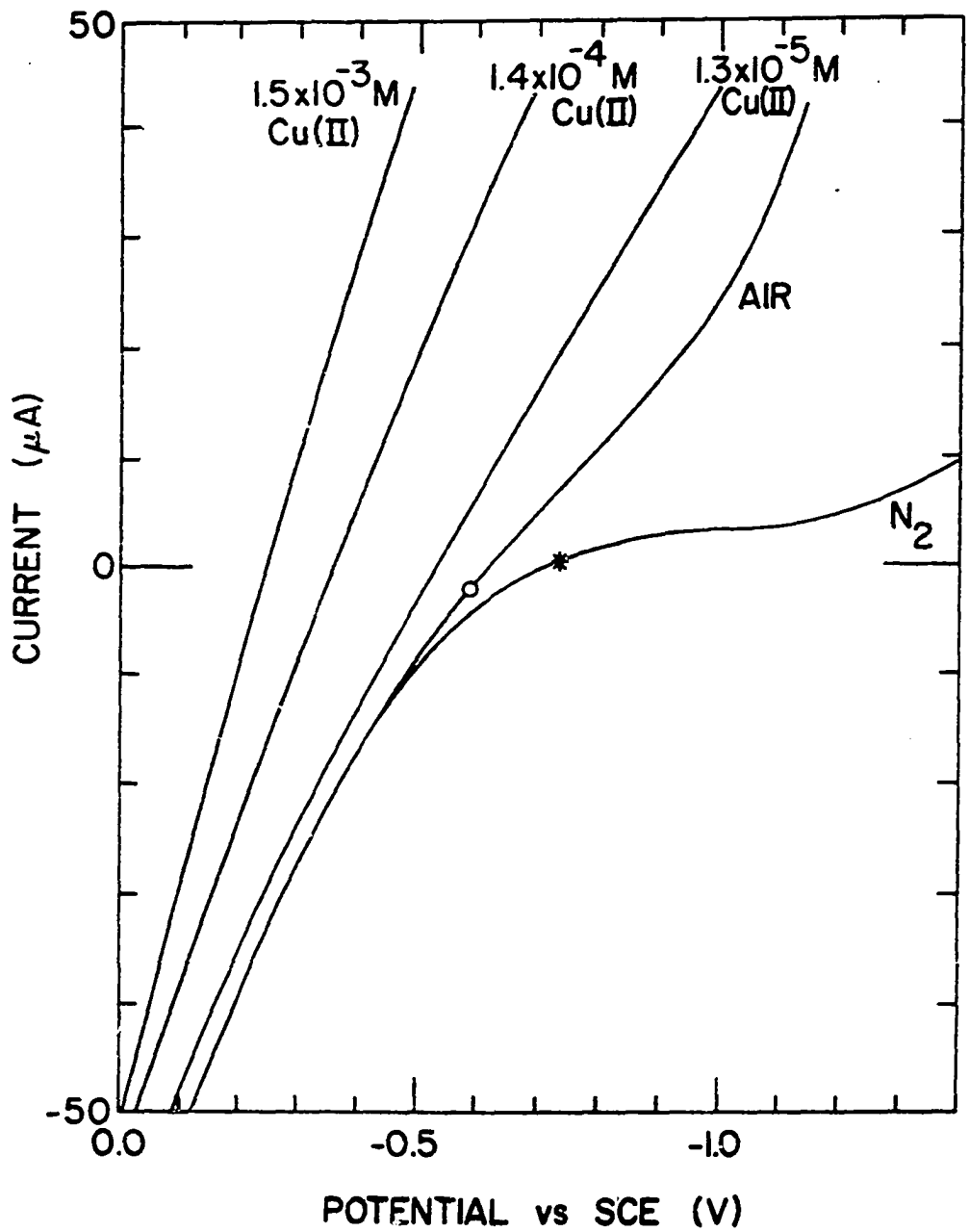


Figure 38. Voltammetric curves of $Na_{0.65}WO_3$ electrode in 1M $NH_4OH$ as a function of Cu(II) concentration

(o) (x) Open circuit potentials

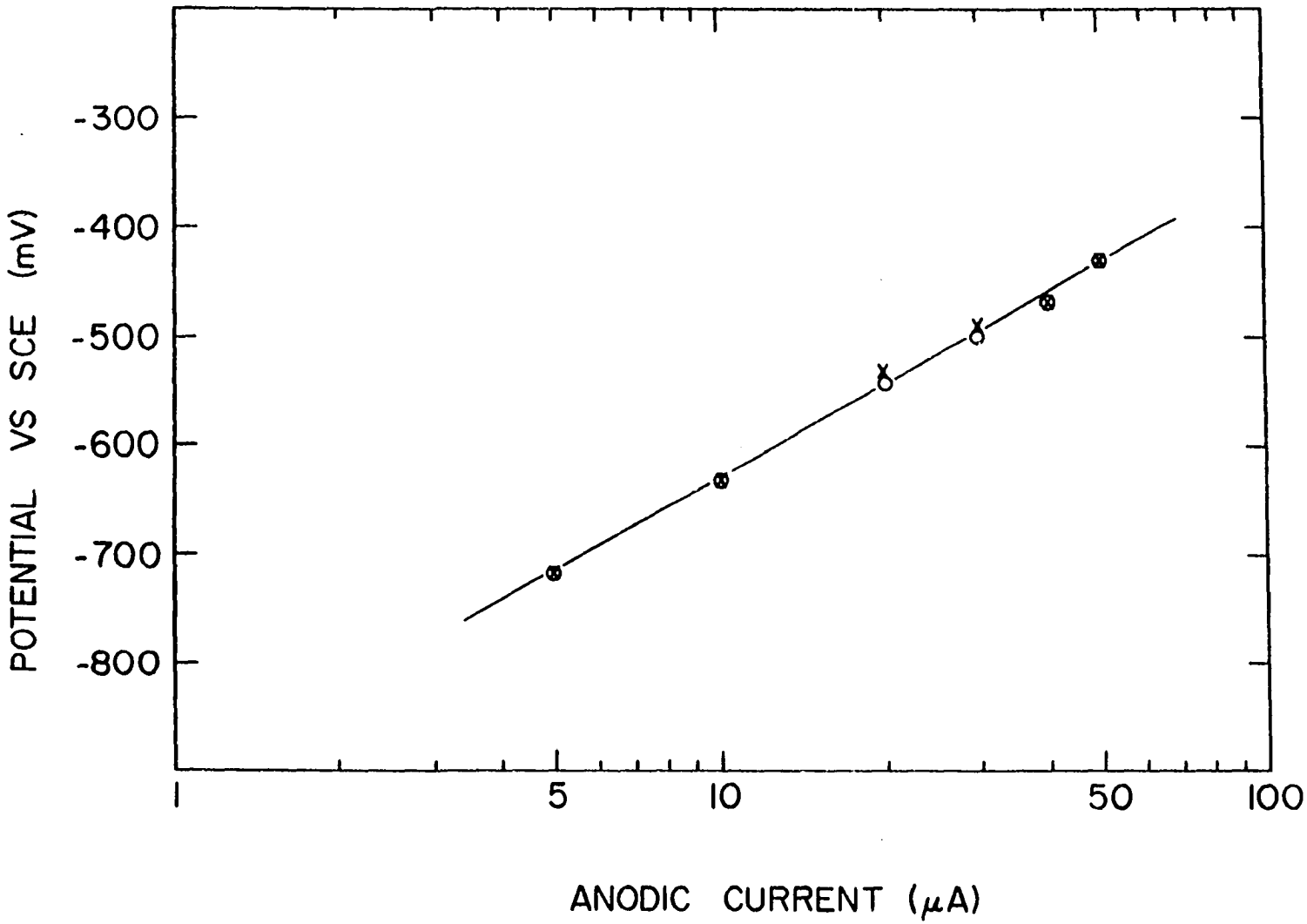


Figure 39. Anodic wave for the oxidation of the $Na_{0.65}WO_3$ electrode
(o) Positive to negative voltage scan (x) Negative to positive voltage scan

electrode. Such a situation may exist for ferricyanide in 1M $NH_4OH$ explaining the 300 mV/decade response slope observed at high $Fe(CN)_6^{3-}$ concentration (Figure 34).

The mixed-potential mechanism provides excellent explanations for several observations connected with the oxygen response of the $Na_xWO_3$ electrode. Any factor influencing either the rate of $Na_xWO_3$ oxidation or the rate of $O_2$ reduction reactions as a function of potential (polarization curves) will subsequently alter the mixed-potential response of the electrode.

The enhanced response to dissolved oxygen in the presence of trace Ag(I) (Figure 15) can be explained if the minute quantity of Ag metal depositing on the bronze electrode acts as a catalyst for the oxygen reduction reaction. A number of metals, including Ag, have been shown to catalyze the reduction of dissolved oxygen at a $Na_xWO_3$ electrode when present in the bronze as impurities (70). Such catalysis would shift the cathodic oxygen waves (Figure 37) to more positive potential and result in a larger mixed-potential response to dissolved oxygen.

The poor oxygen response for low x $Na_xWO_3$ electrodes in LiOH (Figure 10) may be rationalized on the basis of a change in the $Na_xWO_3$ anodic wave. The negative charge on the electrode and the small ionic size of the $Li^+$ ion suggests the possibility of lithium diffusing into the $Na_xWO_3$ crystal lattice forming a $Li_xWO_3$ or mixed $Li_xWO_3$-$Na_xWO_3$ layer at the electrode surface. This would be most apt to happen with low x value bronzes which have a greater number of available vacant lattice sites. Lithium tungsten bronzes and mixed sodium-lithium tungsten bronzes are known to be much more resistant to oxidation in basic solution than the

pure sodium bronzes (12,13,54). Under these circumstances the anodic wave for the bronze oxidation could be shifted far enough toward positive potentials to render the mixed-potential response to oxygen inoperative.

The day-to-day variations in electrode response and the dependence of the potential on stirring rate can also be understood in terms of the mixed-potential mechanism. Changes in the electrode surface will result from the slow dissolution of the electrode in oxygenated basic solution. If the bronze is not perfectly homogeneous preferential attack of the more active sites will occur. Such surface changes are certain to alter both the anodic and cathodic polarization curves and result in a change in the oxygen response. The rate of stirring will primarily affect the polarization curve for the diffusion controlled oxygen reduction. Increased stirring will result in a larger cathodic current for a given oxygen concentration and explain the shift of the mixed potential toward a more positive potential.

Voltammetric curves for several other highly conducting alkali metal tungsten bronze electrodes in 0.1M KOH-1mM EDTA are presented in Figures 40 to 43. Immediately apparent is the absence of any bronze oxidation wave at potentials between -0.5 and -1.0 V in deoxygenated ($N_2$ saturated) solution. The inability of these bronzes to undergo oxidation and establish a mixed potential with the oxygen or Cu(II) reduction couples is consistent with their poor performance in responding to dissolved oxygen and in detecting the equivalence point in chelometric titrations.

A number of these electrodes however, did exhibit some potentiometric response to dissolved oxygen in 0.1M KOH-1mM EDTA (Figure 17) and a 30-40 mV/decade response to Cu (II) in 1M $NH_4OH$ (Figure 30). Other mixed-

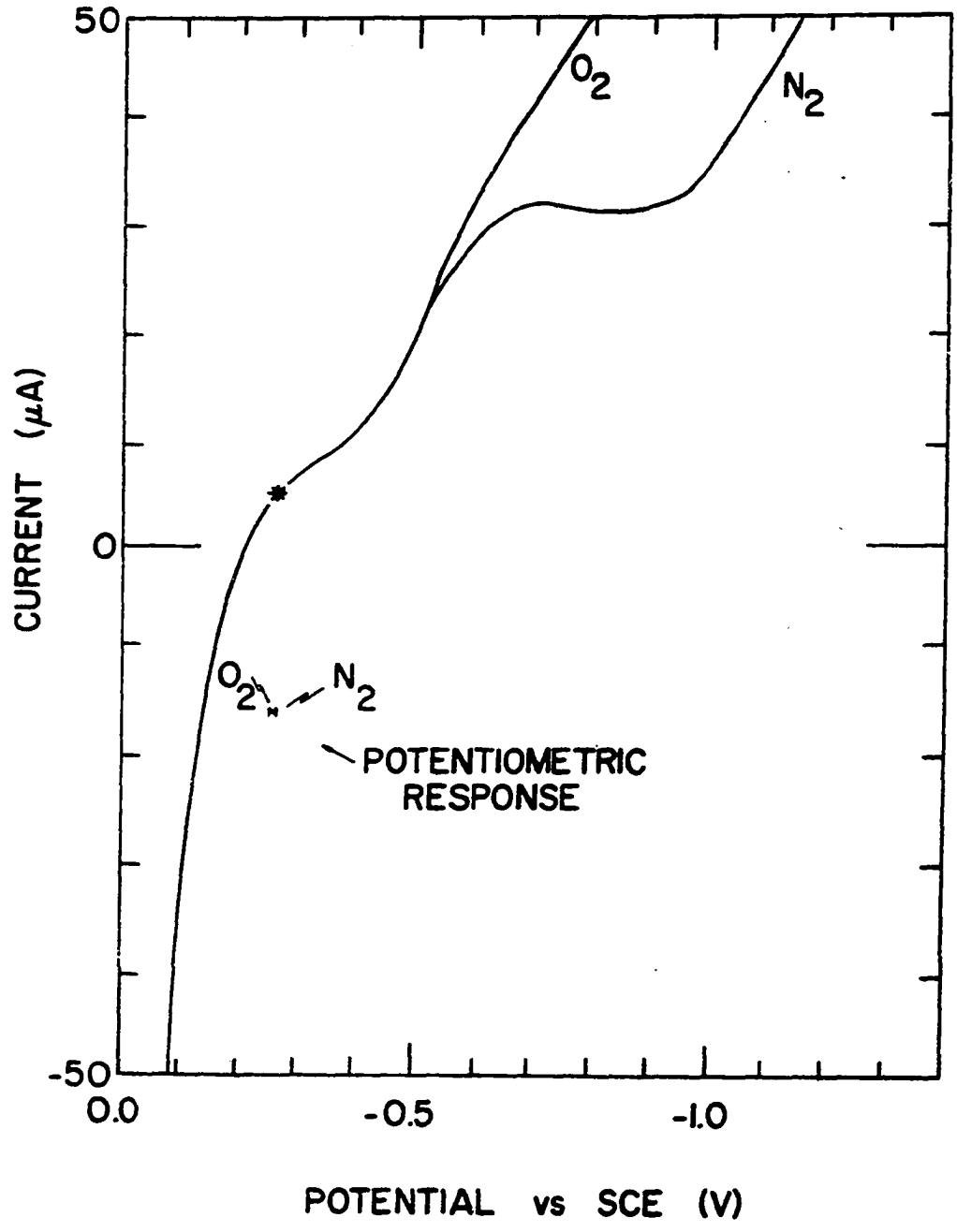


Figure 40. Voltammetric curves of hexagonal $K_{0.3}WO_3$ electrode in oxygen and nitrogen-saturated 0.1M KOH-1mM EDTA solutions
(*) Open circuit potential in $N_2$-saturated solution

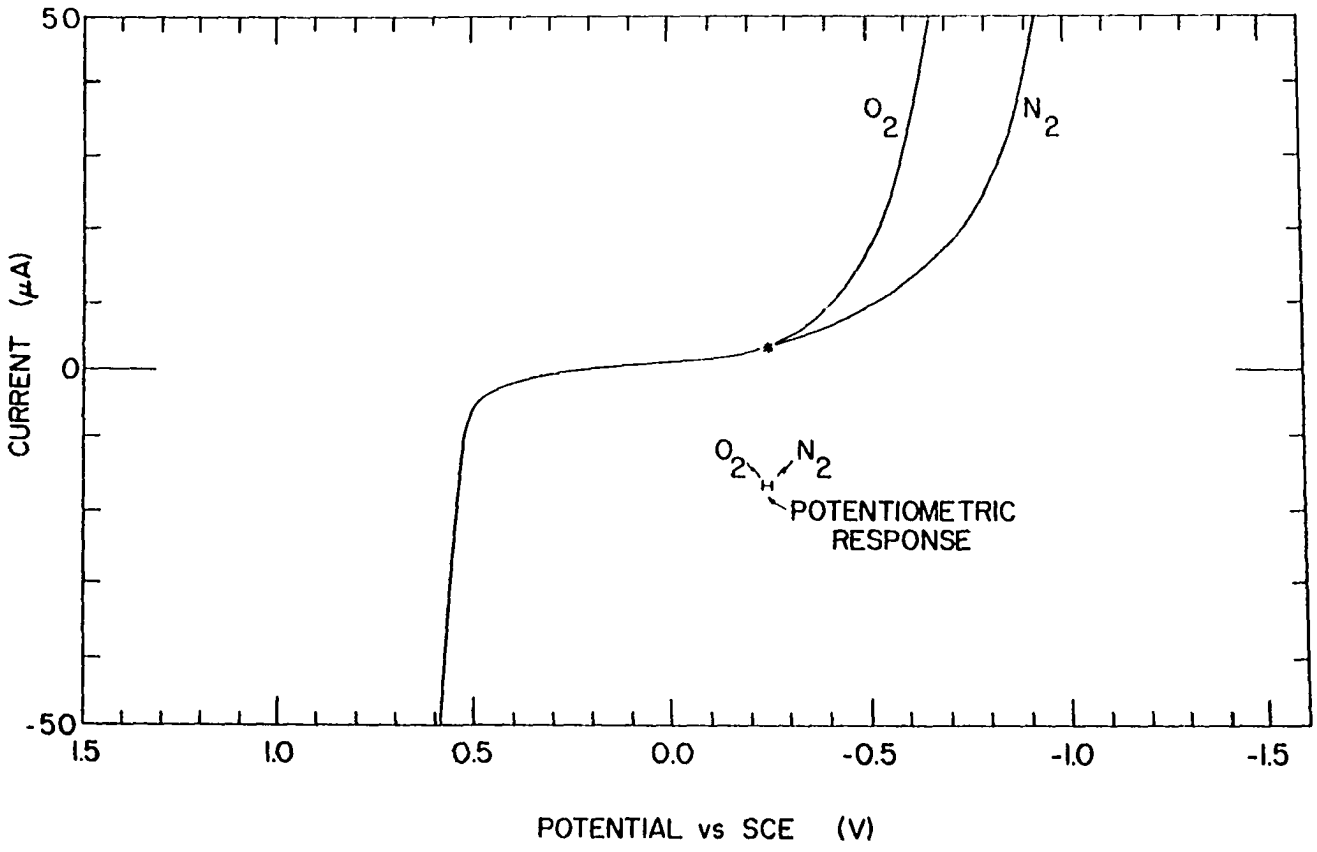


Figure 41. Voltammetric curves of hexagonal $Rb_{0.3}WO_3$ electrode in oxygen and nitrogen-saturated 0.1M KOH-1mM EDTA solutions

(*) Open circuit potential in $N_2$-saturated solution

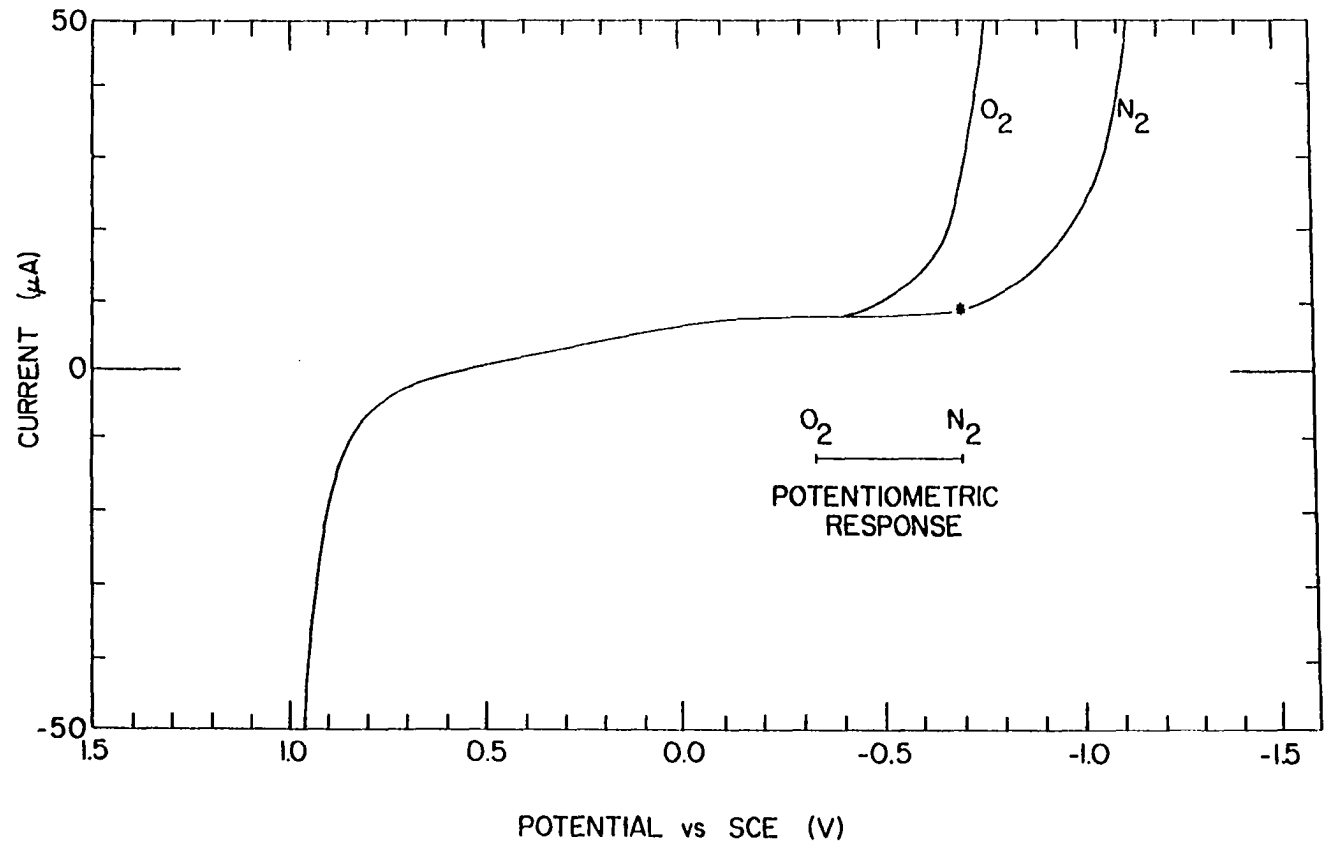


Figure 42. Voltammetric curves of hexagonal $Cs_{0.3}WO_3$ electrode in oxygen and nitrogen-saturated 0.1M KOH-1mM EDTA solutions

(*) Open circuit potential in $N_2$-saturated solution

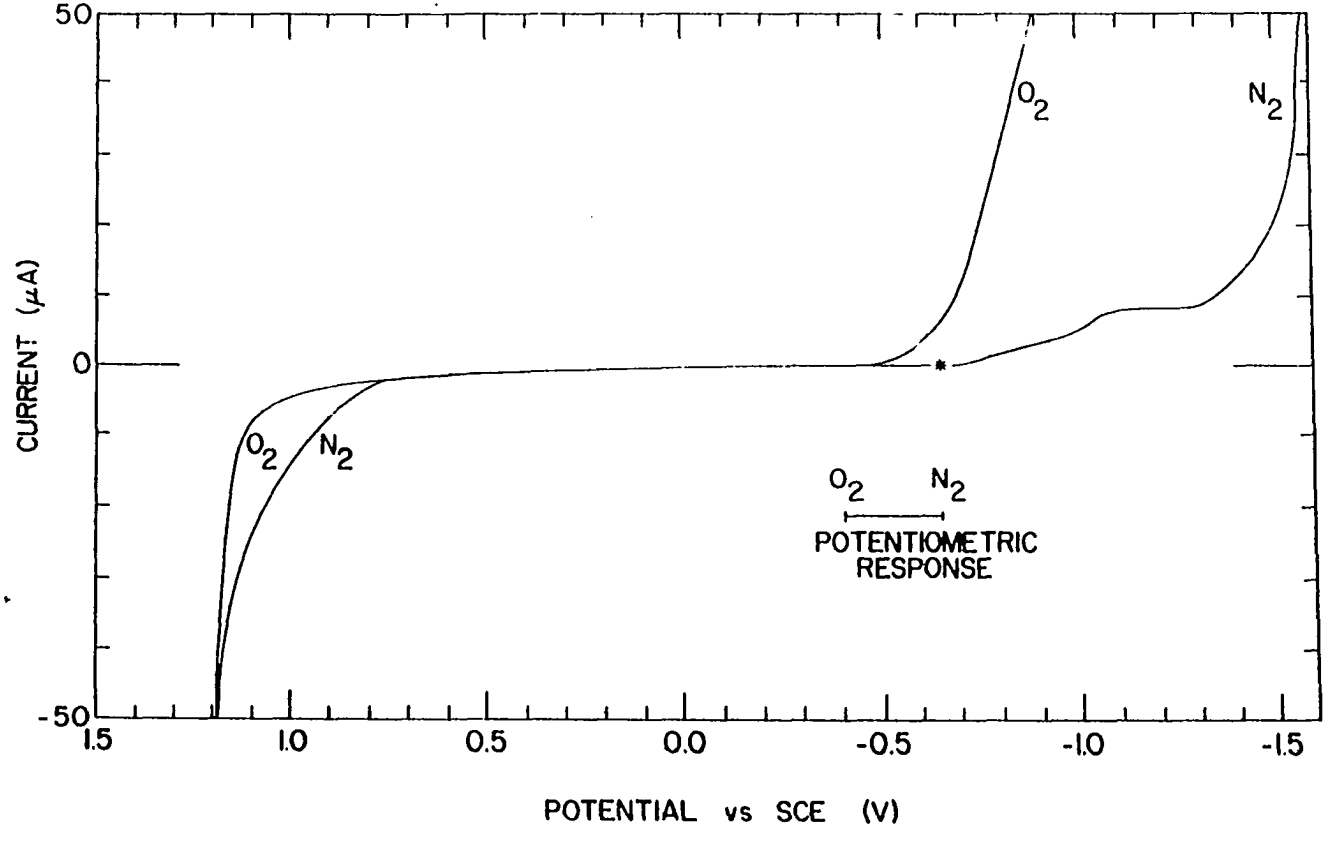


Figure 43. Voltammetric curves of cubic $Li_{0.35}WO_3$ electrode in oxygen and nitrogen-saturated 0.1M KOH-1mM EDTA solutions

(*) Open circuit potential in $N_2$-saturated solution

potential phenomena are suspected as the cause of these observations. The oxidation partial current here may involve the formation of an oxide layer at the electrode surface or the oxidation of water to $O_2$ or $H_2O_2$. The fact that the hexagonal $K_{0.3}WO_3$ and $Rb_{0.3}WO_3$ exhibited no response whatsoever to dissolved oxygen is an extremely strong argument for the mixed-potential response mechanism. The voltammetric curves for these electrodes (Figures 40 and 41) show that the $O_2$ reduction wave begins at more negative potentials than the open circuit potential in deoxygenated solution. In these instances, dissolved oxygen is not a strong enough oxidizing agent to participate in establishing a mixed potential.

The substantial shift in the potential of the $Na_xWO_3$ electrode in chelometric titrations of nonelectroactive species can also be explained by the mixed-potential mechanism. Copper or some other oxidizing agent complexed by EDTA would indeed act as a potentiometric indicator if it was present in the titration solution. The voltammetric curves for the $Na_{0.65}WO_3$ electrode in 1M $NH_4OH$ (Figure 37) clearly demonstrate a negative shift in the mixed potential with decreasing Cu(II) concentration. A similar shift would be expected if a given amount of Cu(II) was complexed with excess EDTA making it more difficult to undergo reduction. In practice however, there does not appear to be enough Cu(II) or other EDTA-complexable oxidizing agent present to cause this effect, especially in view of the large amount of reducible oxygen present during these titrations.

The shift in the mixed potential at the equivalence point is due to the presence of the EDTA itself instead of the effect of complexing a trace potentiometric indicator. Figure 44 presents voltammetric curves

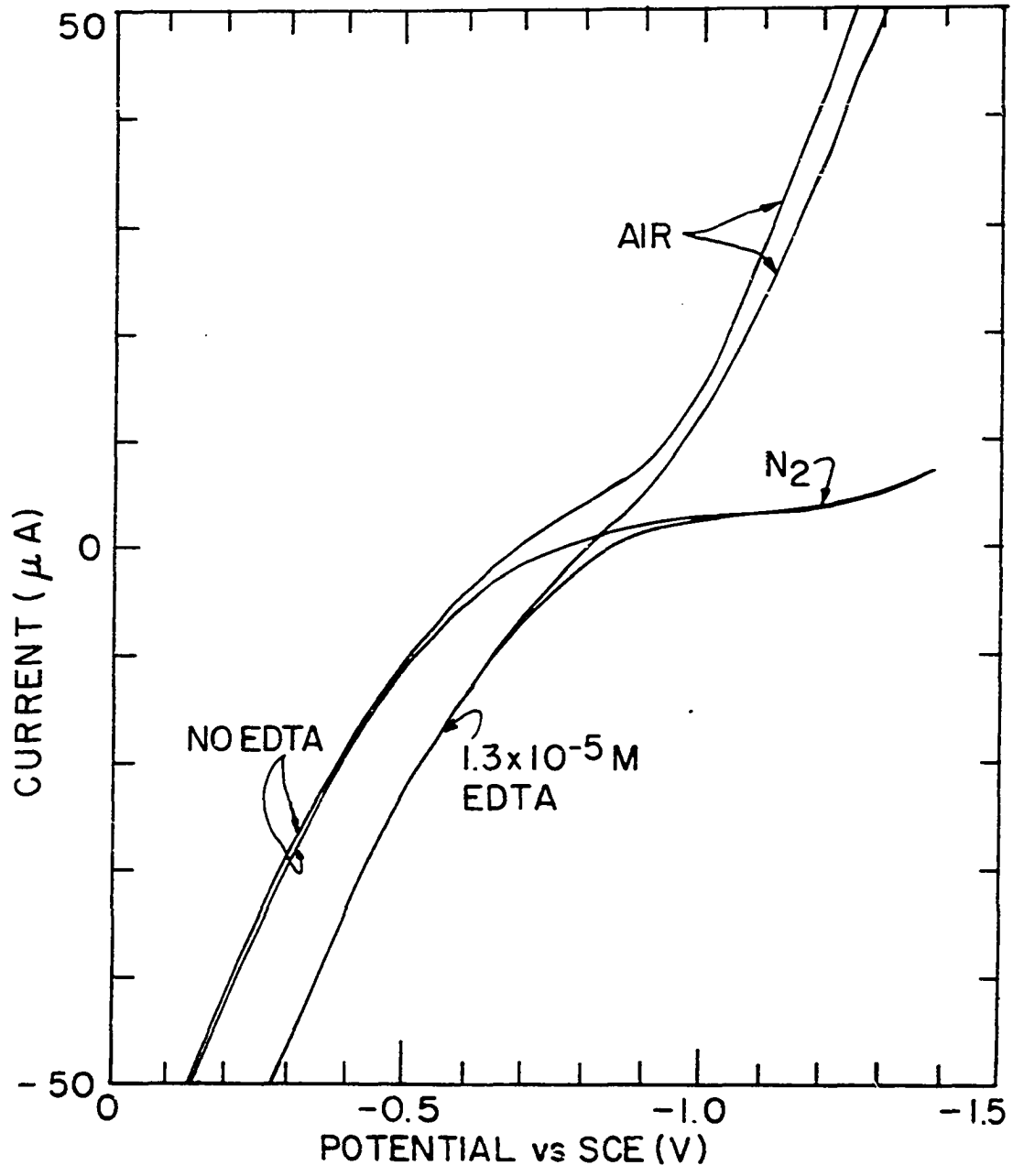


Figure 44. Voltammetric curves for the $Na_{0.65}WO_3$ electrode in 1M $NH_4OH$ showing the effect of trace EDTA

for the $Na_{0.65}WO_3$ electrode in nitrogen and air-saturated 1M $NH_4OH$ solution showing the effect of EDTA at a concentration of $1.3 \times 10^{-5}$M. The presence of trace EDTA was found to shift the anodic polarization wave for the oxidation of the $Na_{0.65}WO_3$ electrode to more negative potentials by 120-140 mV. This oxidation at more negative potential may result from the EDTA complexing tungsten and driving the following reaction to the right.

$$Na_xWO_3 + 2OH^- \text{ --------> } xNa^+ + WO_4^{2-} + H_2O + xe^- \qquad (8)$$

The EDTA also appears to affect the cathodic polarization wave for the reduction of oxygen at the $Na_xWO_3$ electrode. The negative 20-30 mV. potential shift in this wave may be the result of the EDTA hindering the oxygen reduction reaction. If this shift in the cathodic wave is also characteristic of other metallic electrodes the 20-30 mV shift observed in chelometric titrations using the other tungsten bronze electrodes (Figure 29) and the Pt, Cu and W electrodes (Figure 31) can be explained.

# CONCLUSION

The sodium tungsten bronzes have been shown to be highly useful potentiometric-indicating electrodes for determining dissolved oxygen in aqueous solution and for indicating the equivalence point in metal-EDTA titrations.

The response to dissolved oxygen differs from that of conventional polarographic, voltammetric and galvanic electrochemical methods (81) in that a potential rather than a current is indicative of the oxygen concentration. Although the analytical applicability of the $Na_xWO_3$ electrode was only demonstrated at dissolved oxygen concentrations above 0.04 ppm ($P_{O_2}$ = 0.001 atm), there is an additional 150-200 mV potential region available to perhaps extend the range of analysis another order of magnitude lower. The logarithmic potential response has in theory a distinct advantage over the linear current response of the conventional methods when working at extremely low concentrations. It becomes increasingly more difficult to instrumentally measure the smaller and smaller currents involved but no more difficult to measure a more negative potential.

The high degree of sensitivity and the magnitude of the potential change per unit change of oxygen concentration (120 mV/decade) demonstrate the utility of the $Na_xWO_3$ electrode for dissolved oxygen determinations. The simplicity and low cost of the electrode and the relative ease with which potential measurements can be made are additional advantages. The ability to incorporate the electrode into a flow-through system or perhaps a recirculating system suggests applicability for field measurements of

dissolved oxygen in river and lake waters. The major disadvantage however, is that the response is limited to basic solution and a deaerated reagent would have to be introduced into the sample. The membrane voltammetric and galvanic electrodes on the other hand, will operate over an extended pH range and in organic liquids (81).

An extremely useful application of the $Na_xWO_3$ electrode is the potentiometric detection of equivalence points in metal-EDTA titrations. As little as 0.01 millimole of metal can be easily measured in these titrations and the method is applicable for the determination of nonelectroactive as well as electro-active metals. Similar chelometric titrations have been demonstrated using a mercury electrode (78,94) and copper ion-selective electrodes (95,96) but these require the presence of an indicator ion for successful titrations. Equivalence-point detection with the $Na_xWO_3$ electrode appears to be a result of the electrode's direct response to the EDTA itself. The absence of any indicator is a distinct advantage when titrating for minute quantities of metal because corrections for the indicator blank are unnecessary. As in the case of the $Na_xWO_3$ oxygen electrode, the simple design and low cost of the electrode are additional advantages.

The potentiometric response of the $Na_xWO_3$ electrode in basic solution is attributed to a mixed potential established from the spontaneous oxidation of the electrode surface by dissolved oxygen. The simultaneous reduction of dissolved oxygen and oxidation of the $Na_xWO_3$ electrode over the same general potential range as the potentiometric response was demonstrated by voltammetry. A mixed potential mechanism explains the response to dissolved oxygen and the response in chelometric titrations.

Also explained by the mixed-potential mechanism are the many idiosyncrasies connected with the response of the $Na_xWO_3$ electrode. These include the variability in electrode response, the effect of stirring, the loss of $O_2$ response in LiOH and the enhancement of $O_2$ response in the presence of trace Ag(I), and the uniqueness of the cubic $Na_xWO_3$ electrode in responding to dissolved oxygen and the equivalence point in chelometric titrations.

## Future Studies

Although the $Na_xWO_3$ electrode has been demonstrated to be very useful in dissolved oxygen determinations, there are two disadvantages to be overcome in order to improve results. These are the slow response at low oxygen concentrations and the variability in electrode response over a period of time. The response characteristics may possibly be improved by changing the composition of the $Na_xWO_3$ electrode. Incorporation of $Li_xWO_3$ into $Na_xWO_3$ for example, will increase resistance toward oxidation and minimize deterioration of the electrode surface. This may result in a more stable response without too much sacrifice in response slope and sensitivity. Incorporation of trace platinum in $Na_xWO_3$ electrodes is known to catalyze the reduction of oxygen. This may result in a more rapid response of the electrode to dissolved oxygen.

In this study, the application of the $Na_xWO_3$ electrode in chelometric titrations was demonstrated only for EDTA. Additional studies are warranted to determine if other complexing agents would cause a similar mixed potential shift and be useful as titrants. Studies involving the use of masking agents in conjunction with EDTA for selectively determining

metals in mixtures may also prove to be useful.

The voltammetric studies presented here have shown the cubic sodium tungsten bronzes to undergo oxidation in basic solution much more easily than the other alkali metal tungsten bronzes. Also demonstrated by voltammetry is the extremely interesting series of observations concerning oxidation at the hexagonal tungsten bronze electrode in basic solution. Oxidation occurs most readily at the $K_xWO_3$ electrode and least readily at the $Cs_xWO_3$ electrode with $Rb_xWO_3$ in between. Correlation of these observations with other properties of the tungsten bronzes would make a most interesting study.

## LITERATURE CITED


1. P. G. Dickens and M. S. Whittingham, Quart. Rev. (London) 22(1), 30 (1968).

2. P. Hagenmueller, "Les Bronzes Oxygenes," Progress in Solid State Chemistry, Vol. 5, H. Reiss, Ed., Pergamon Press, Oxford, England, 1971, pp 71-144.

3. E. Banks and A. Wold, Prep. Inorg. React., 4, 237 (1968).

4. E. Schwarzmann and R. Birkenberg, Z. Naturforsch., B, 26(10), 1069 (1971).

5. P. G. Dickens, A. C. Halliwell, D. J. Murphy and M. S. Whittingham, Trans. Faraday Soc., 67(Part 3), 794 (1971).

6. F. Wöhler, Ann. Chim. Phys., 43(2), 29 (1823).

7. A. Laurent, Ann. Chim. Phys., 67, 215 (1838).

8. L. A. Hallopeau, Ann. Chim. Phys., 19, 117 (1900).

9. O. Brunner, Ph.D. Thesis, University of Zurich, Zurich, Switzerland, 1903.

10. E. Schaefer, Z. Anorg. Allg. Chem., 38, 158 (1904).

11. M. J. Sienko, J. Amer. Chem. Soc., 81, 5556 (1959).

12. M. E. Straumanis and S. S. Hsu, J. Amer. Chem. Soc., 72, 4027 (1950).

13. M. E. Straumanis, J. Amer. Chem. Soc., 71, 679 (1949).

14. E. O. Brimm, J. C. Brantley, J. H. Lorenz and M. H. Jellinek, J. Amer. Chem. Soc., 73, 5427 (1951).

15. W. McNeill, Ph.D. Thesis, Temple University, Philadelphia, Pa., 1961; Diss. Abstr. Int. B, 22, 60 (1961).

16. W. McNeill and L. E. Conroy, J. Chem. Phys., 36, 87 (1962).

17. W. Ostertag, Inorg. Chem., 5, 758 (1966).

18. B. Broyde, Inorg. Chem., 6, 1588 (1967).

19. A. Magneli and B. Blomberg, Acta Chem. Scand., 5, 372 (1951).

20. R. A. Bernoff and L. E. Conroy, J. Amer. Chem. Soc., 82, 6261 (1960).

21. L. E. Conroy and G. Podolsky, Inorg. Chem., 7, 614 (1968).

22. A. Magneli, Ark. Kemi, 1, 213 (1949).

23. D. Van Duyn, Rec. Trav. Chim. Pays-Bas, 61, 669 (1942).

24. B. L. Chamberland, Inorg. Chem., 8, 1183 (1969).

25. L. D. Ellerbeck, H. R. Shanks, P. H. Sidles and G. C. Danielson, J. Chem. Phys., 35, 298 (1961).

26. H. R. Shanks and G. C. Danielson, J. Appl. Phys., 38, 4923 (1967).

27. H. R. Shanks, J. Crystal Growth, 13-14, 433 (1972).

28. C. T. Hauck, A. Wold and E. Banks, Inorg. Syn., 12, 153 (1970).

29. A. Magneli and R. Nilsson, Acta Chem. Scand., 4, 398 (1950).

30. M. J. Sienko and T. B. N. Truong, J. Amer. Chem. Soc., 83, 3939 (1961).

31. R. A. Fredlein and A. Damjanovic, J. Solid State Chem., 4, 94 (1972).

32. L. Meites, E. Banks and C. E. Fleischmann, Anal. Chem., 44, 1133 (1972).

33. M. S. Whittingham and R. A. Huggins, National Bureau of Standards Special Publication N. 364, U. S. Government Printing Office, Washington, D. C., 1972, pp 51-62.

34. W. F. de Jong and H. J. Stek, A. Kristallogr., 83, 496 (1932).

35. W. F. de Jong, Z. Kristallogr., 81, 314 (1932).

36. G. Hagg, Nature, 135, 874 (1935).

37. G. Hagg, Z. Physik. Chem., B29, 192 (1935).

38. B. W. Brown and E. J. Banks, J. Amer. Chem. Soc., 76, 963 (1954).

39. R. J. Reuland and A. F. Voigt, Anal. Chem., 35, 1263 (1963).

40. A. Magneli, Acta Chem. Scand., 5, 670 (1951).

41. A. S. Ribnik, B. Post and E. Banks, "Phase Transitions in Sodium Tungsten Bronze," Advances in Chemistry Series, No. 39, American Chemical Society, Washington, D. C., 1963, pp 246-253.

42. A. Magneli, Nature, 169, 791 (1952).

43. A. Magneli, Acta Chem. Scand., 7, 315 (1953).

44. M. J. Sienko, "Electric and Magnetic Properties of the Tungsten and Vanadium Bronzes," Advances in Chemistry Series, No. 39, American Chemical Society, Washington, D. C., 1963, pp 224-236.

45. H. R. Shanks, P. H. Sidles and G. C. Danielson, "Electrical Properties of the Tungsten Bronzes," Advances in Chemistry Series, No. 39, American Chemical Society, Washington, D. C., 1963, pp 237-245.

46. L. D. Muhlestein and G. C. Danielson, Phys. Rev., 158, 825 (1967).

47. E. J. Huibregtse, Iowa State Coll. J. Sci., 26, 222 (1952).

48. J. D. Greiner, H. R. Shanks and D. C. Wallace, J. Chem. Phys., 36, 772 (1962).

49. A. R. Mackintosh, J. Chem. Phys., 38, 1991 (1963).

50. R. Fuchs, J. Chem. Phys., 42, 3781 (1965).

51. J. B. Goodenough, Bull. Soc. Chim. Fr., 1965, 1200 (1965).

52. A. Feretti, D. B. Rodgers and J. B. Goodenough, J. Phys. Chem. Solids, 26, 2007 (1965).

53. J. B. Goodenough, "Metallic Oxides," Progress in Solid State Chemistry, Vol. 5, H. Reiss, Ed., Pergamon Press, Oxford, England, 1971, pp 145-399.

54. M. E. Straumanis and G. F. Doctor, J. Amer. Chem. Soc., 73, 3492 (1951).

55. F. T. Jones, Ph.D. Thesis, Polytechnic Institute of Brooklyn, Brooklyn, N. Y., 1960; Diss. Abstr., Int. B, 21, 1390 (1960).

56. A. A. Balandin and N. P. Sokolova, Problemy Kinetiki i Kataliza, Akad. Nauk. S. S. S. R., No. 10, 363 (1960).

57. D. B. Sepa, D. S. Ovcin and M. V. Vojnovic, J. Electrochem. Soc., 119, 1285 (1972).

58. L. W. Niedrach and H. I. Zeliger, J. Electrochem. Soc., 116, 152 (1969).

59. D. B. Sepa, A. Damjanovic and J. O'M. Bockris, Electrochim. Acta, 12, 746 (1967).

60. A. Damjanovic, D. Sepa and J. O'M. Bockris, J. Res. Inst. Catal., Hokkaido Univ., 16, 1 (1968).

61. B. Barret, J. Catal., 10, 13 (1968).

62. J. H. Fishman, J. F. Henry and S. Tessore, Electrochim. Acta, 14, 1314 (1969).

63. J. O'M. Bockris, R. A. Fredlein and A. Damjanovic, U. S. Clearinghouse Fed. Sci. Tech. Inform., No. 706861, 1970, 37 pp.

64. R. A. Fredlein and J. McHardy, Power Sources Symp., Proc., 24, 175 (1970).

65. J. McHardy, K. L. Mittal, and J. O'M. Bockris, U. S. Nat. Tech. Inform. Serv., No. 747766, 1972, 92 pp.

66. J. McHardy, Ph.D. Thesis, University of Pennsylvania, Philadelphia, Pa., 1972; Diss. Abstr. Int. B, 33, 1484 (1972).

67. M. Voinor and H. Tannenberger in "From Electrocatalysis to Fuel Cells," G. Sandstede, Ed., Univ. Wash. Press, Seattle, Wash., 1972, pp 101-108.

68. J. McHardy and J. O'M. Bockris in "From Electrocatalysis to Fuel Cells," G. Sandstede, Ed., Univ. Wash. Press, Seattle, Wash., 1972, pp 109-112.

69. J. McHardy and J. O'M. Bockris, J. Electrochem. Soc., 120, 53 (1973).

70. J. O'M. Bockris and J. McHardy, J. Electrochem. Soc., 120, 61 (1973).

71. A. G. Koksharov and V. F. Ust-Kachkinsev, Uch. Zap. Perm. Gos. Univ., 111, 63 (1964); Chem. Abstr., 64, 1617g (1966).

72. A. G. Koksharov and V. F. Ust-Kachkinsev, Izv. Vyssh. Ucheb. Zaved. Khim. Khim. Tekhnol., 10, 243 (1967); Chem. Abstr., 67, 39512b (1967).

73. A. G. Koksharov and V. F. Ust-Kachkinsev, Uch. Zap. Perm. Gos. Univ., 178, 117 (1968); Chem. Abstr., 73, 61979e (1970).

74. M. A. Wechter, H. R. Shanks, G. Carter, G. M. Ebert, R. Guglielmino and A. F. Voigt, Anal. Chem., 44, 850 (1972).

75. A. Weser and E. Pungor, Acta Chim. Acad. Sci. Hung., 59, 319 (1969).

76. M. A. Wechter and A. F. Voigt, Anal. Chem., 38, 1681 (1966).

77. M. A. Wechter, H. R. Shanks and A. F. Voigt, Inorg. Chem., 7, 845 (1968).

78. A. I. Vogel, "Quantitative Inorganic Analysis," John Wiley and Sons, Inc., New York, N. Y., 1961.

79. R. C. Weast, S. M. Selby and C. D. Hodgman, Eds., "Handbook of Chemistry and Physics," 46th Ed., The Chemical Rubber Co., Cleveland, Ohio, 1964, 1965.

80. D. C. Johnson and S. Bruckenstein, Anal. Chem., 43, 1313 (1971).

81. J. P. Hoare, "The Electrochemistry of Oxygen," Interscience Publishers, New York, N. Y., 1968.

82. R. E. Davis, G. L. Horvath, and C. W. Tobias, Electrochim. Acta, 12, 287 (1967).

83. T. S. Light in "Ion Selective Electrodes, "R. A. Durst, Ed., National Bureau of Standards Special Publication 314, U. S. Government Printing Office, Washington, D. C., pp 354-355.

84. N. A. Lange and G. M. Forker, Eds., "Handbook of Chemistry," 10th ed, McGraw-Hill, New York, N. Y. 1967.

85. F. D. Snell and C. T. Snell, "Colorimetric Methods of Analysis," Vol. II A, D. Van Nostrand Co. Inc., Princeton, N. J., 1959, p 76.

86. G. Eisenman, Ed., "Glass Electrodes for Hydrogen and Other Cations," Marcel Dekker, Inc., New York, N. Y., 1967.

87. R. A. Durst, Ed., "Ion-Selective Electrodes," National Bureau of Standards Special Publication 314, U. S. Government Printing Office, Washington, D. C., 1969.

88. C. Wagner and W. Traud, Z. Electrochem., 44, 391 (1938).

89. P. Delahey, "Double Layer and Electrode Kinetics," Interscience Publishers, New York, N. Y., 1965, pp 172-173.

90. D. Gray and A. Cahill, J. Electrochem Soc., 116, 443 (1969).

91. I. M. Kolthoff, E. B. Sandell, E. J. Meehan and S. Bruckenstein, "Quantitative Chemical Analysis," 4th ed, Macmillan Co., London, England, 1969, pp 944-945.

92. J. Koryta, J. Dvorak and V. Bochackova, "Electrochemistry," Methuen and Co. Ltd., London, England, 1970, pp 318-321.

93. J. M. Herbelin, T. N. Andersen and H. Eyring, Electrochim. Acta, 15, 1455 (1970).

94. A. E. Martin and C. N. Reilley, Anal. Chem., 31, 992 (1959).

95. J. W. Ross, Jr. and M. S. Frant, Anal. Chem., 41, 1900 (1969).

96. E. W. Baumann and R. M. Wallace, Anal. Chem., 41, 2072 (1969).

ACKNOWLEDGMENTS

The author wishes to extend his gratitude to his major professor, Dr. Adolf F. Voigt, for his encouragement and assistance during the author's graduate study at Iowa State University.

Special thanks are also due to Dr. Margaret Wechter for her continued interest and support throughout this study.

The author would like to thank Dr. Dennis Johnson for his many helpful suggestions, and Mr. Howard Shanks for providing the tungsten bronze crystals used in this study.

The author wishes to express his appreciation to his wife, Pat, for an excellent job of editing and typing this dissertation.